

# NEW INSIGHTS INTO DRUG ABSORPTION FROM OIL DEPOTS

Nieuwe inzichten van geneesmiddelopname vanuit olie depots  
(met een samenvatting in het Nederlands)

## PROEFSCHRIFT

ter verkrijging van de graad van doctor aan de Universiteit Utrecht op gezag van de rector magnificus, prof.dr. G.J. van der Zwaan, ingevolge het besluit van het college voor promoties in het openbaar te verdedigen op woensdag 26 april 2017 des middags te 4.15 uur

door

Raween Wikesh Kalicharan

geboren op 8 januari 1987  
te Utrecht

Promotor: Prof.dr. H. Vromans

Copromotor: Dr. C. Oussoren

# Content

## CHAPTER 1

Introduction 11

## CHAPTER 2

Pharmacokinetics in elderly women of benzyl alcohol from an oil depot 31

## CHAPTER 3

Fundamental understanding of drug absorption from a parenteral oil depot 45

## CHAPTER 4

Spatial distribution of oil depots monitored in human muscle using MRI 63

## CHAPTER 5

The *in-vivo* fate of an oil depot in different tissues 81

## CHAPTER 6

Where does hydrolysis of nandrolone decanoate occur in the human body after release from an oil depot? 99

## CHAPTER 7

General discussion 117

## APPENDIX

References 130

Supplementary data Chapter 3 139

Summary 143

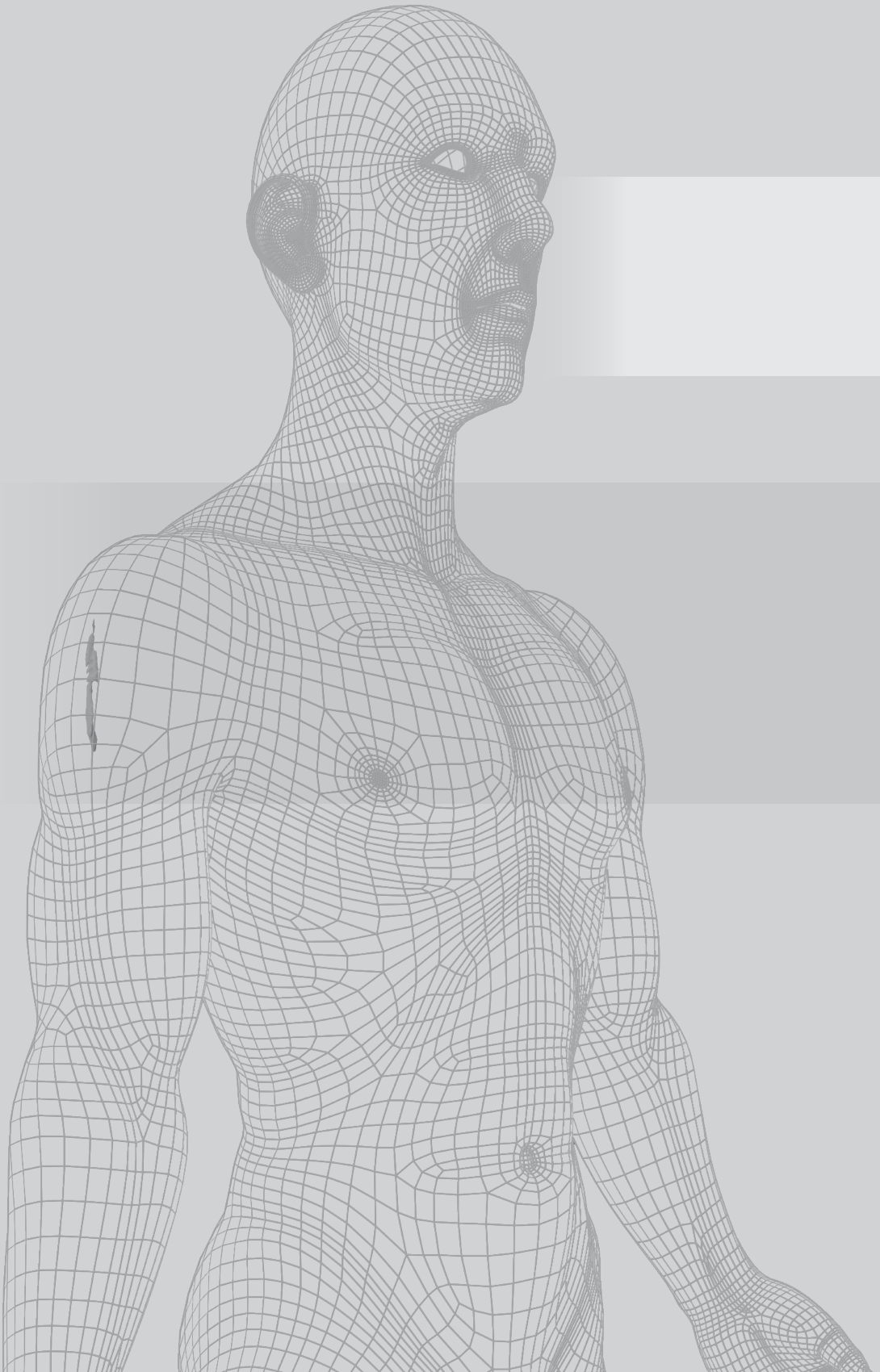
Samenvatting 149

List of coauthors 155

List of publications 157

Dankwoord 159

Curriculum Vitae 167



Chapter 1

**Introduction**



Sustained delivery of drugs has gained a significant place in the long-term drug treatment of several diseases, such as psychiatric and hormone-dependent disorders. A commonly used approach to deliver active substances for an extended period of time into the body is by using an oil depot. This type of parenteral drug formulation is administered either intramuscularly (i.m.) or subcutaneously (s.c.) and is composed of a solution of the lipophilic molecules in a lipid oil.

In 1935, the male hormone testosterone was discovered by prof. Laqueur in Amsterdam (the Netherlands) (1). The first testosterone oil depot was launched in 1939 by Roche-Organon (1). This depot contained testosterone as such and was meant as a rejuvenation for old men. It was advertised that it helped regain muscle strength which would therefore also attract young ladies. In these days, the formulation was a result of trial and error. It became clear however that testosterone exhibits two effects: the anabolic and androgenic effect. The anabolic effect is expressed in the building up of e.g. bone and muscle while the androgenic effect is responsible for the stimulation and maintenance of sexual functions (2). The undesired androgenic effect was less pronounced for 19-nortestosterone (nandrolone, discovered in 1942), which appeared to have a predominant anabolic mode of action. Upjohn Company patented this molecule in 1953, which had a “twice as strong anabolic effect and only one fifth of the androgen effect compared to testosterone” (1). In 1955, Organon patented an oil depot with nandrolone phenylpropionate, which is an esterified form of nandrolone. In an animal study by *Overbeek* and *De Visser* in 1957, it became clear that this esterified form ensures a stable nandrolone concentration in blood, due to the sustained release from the oil depot (3). This drug product is known as *Durabolin*. There was however room for improvement: In 1965, *Van der Vies* published a paper which compared nandrolone phenylpropionate with nandrolone decanoate (4). Here, it became clear that the anabolic duration of nandrolone was longer with the decanoate acid compared to the phenylpropionate acid due to a longer residence time at the site of injection (1,4).

### PHARMACOLOGICAL EFFECTS OF NANDROLONE

In this dissertation nandrolone decanoate is used as a model compound which is representative for the majority of compounds that are formulated in oil depots. Nandrolone is a synthetic analogue of testosterone (5). The physical testosterone concentrations in normal adult males range between 10-35 nmol/L, whereas in children and in females it is below 2 nmol/L (Figure 1.1) (6).

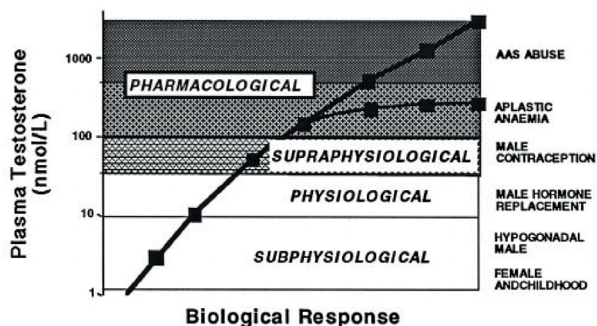


Figure 1.1: Concentration–response relation of biological responses to increasing concentrations of circulating testosterone characteristic of various clinical situations and therapeutic indications. Figure is obtained from (6).

Nandrolone exposes a more anabolic profile than an androgenic one (7). This is a reason for off label use: Unfortunately, directly after the introduction in the 1950s, the rate of nandrolone abuse was between 1-7% of the gym population in the United States of America (USA) (2). In 2005, the National Institute on Drug Abuse in the USA reported a steroid abuse of 1.5-2.5% of the gym population. In the Netherlands, this was 0.4% of the gym population in 2009 (8).

#### PARENTERAL VS ORAL MEDICATION

The sustained release of lipophilic molecules from oil depots covers a much longer therapeutic period than can be achieved with oral administration. Where oral medication requires (at least) a daily intake to maintain therapeutic blood levels, oil depots only require one injection every 2-4 weeks. For instance, therapeutic blood levels of 10-35 nmol/L testosterone (6) can either be achieved by oral or buccal administration of 40-120 mg testosterone undecanoate daily (9-12), or with one injection of 750-1000 mg testosterone undecanoate every 10-14 weeks (13,14). Another advantage of the sustained release is that a stable concentration in blood can be achieved. This prevents fluctuating drug levels in blood, as can be expected with daily use of oral medication with active substances having a short half-life. As generally known, high peak levels are more likely to cause side effects. This implies that less side effects occur when using oil depots instead of oral medication.

#### OIL DEPOTS FOR CLINICAL USE ON THE MARKET

In the Netherlands, a number of oil depots are registered for therapeutic use (Table 1.1). Most active substances processed in oil depots are antipsychotic agents (fluphenazin (15), haloperidol (16), bromperidol (17), zuclopentixol (18), flupentixol (19)) or agents for hormone therapy (nandrolone (20), fulvestrant (21), cyproterone (22) and testosterone (multiple ester moieties) (23,24)). Artemotil (Artecef® (25)) is registered for severe malaria by *Plasmodium falciparum*.

Table 1.1: An overview of oil depots registered for therapeutic use in the Netherlands.

Product name	Active compound (ester moiety)		Excipients		Type	Dose (mg) and interval (weeks)	Route
	Oil type	BOH (%)	EtOH (%)	BBA (%)			
Anatenzol (15)	Fluphenazin (decanoate)	S	1.5	-	Antipsychotic	12.5-100; 3-4	i.m.: gluteal
Haldol decanoas (16)	Haloperidol (decanoate)	S	1.5 (14)	-	Antipsychotic	50-150; 4	i.m.: gluteal
Imprommen decanoas (17)	Bromperidol (decanoate)	S	1.5 (14)	-	Antipsychotic	50-150; 4	i.m.: gluteal
Cisordinol Depot (18)	Zuclopentixol (decanoate)	CO	-	-	Antipsychotic	200-400; 2-4	i.m.: gluteal
Fluanxol (19)	Flupentixol (decanoate)	CO	-	-	Antipsychotic	20-40; 2-4	i.m.: gluteal
Deca-Durabolin (20)	Nandrolone (decanoate)	A	10	-	Androgen	50-200; 1-4	deep i.m.
Nebido (23)	Testosterone (undecanoate)	CA	-	-	Androgen	1000; 10-14	i.m.
Sustanon (24)	30 mg testosterone (propionate) 60 mg testosterone (phenylpropionate)	A	10 (14)	-	Androgen	250; 3	deep i.m.
Faslodex (21)	60 mg testosterone (isocaproate) 100 mg testosterone (decanoate)	CA	10	10	Antioestrogen	500; 2-4	i.m.: gluteal
Androcur Depot (22)	Cyproterone (acetate)	CA	-	-	Progestogen	250; 1-2	deep i.m.
Artecef (25)	Artemotil (-)	S	-	-	Antimalarial	Based on body weight (25)	i.m.: vastus lateralis

Type of oil: S = sesame oil; CO = coconut oil; A = arachis oil; CA = castor/ricinus oil. BOH = benzyl alcohol. EtOH = ethanol. BBA = benzyl benzoate. Percentages are given as weight/volume. ? = undefined; - = not used in product. i.m. = intramuscular. NOTE: dose is indicated for adults

## CHARACTERISTICS OF OIL DEPOTS

### Active pharmaceutical ingredient

Most often, a prodrug is used in the formulation of an oil depot. Prodrugs are pharmacologically inactive compounds, that become active after a metabolic conversion. In these oil depots, the prodrug is always a carboxyl ester of a fatty acid which is attached to a hydroxyl-group of the active pharmaceutical ingredient (API). Here, the prodrug becomes active after (enzymatic) hydrolysis of the ester bond. An example is given below in Figure 1.2, where nandrolone decanoate is the esterified prodrug and nandrolone the active substance.

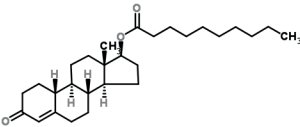
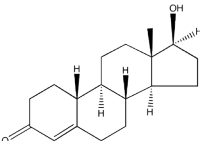
	Compound	Molecular structure	Molecular weight (g/mole)	Log P (o/w)
Prodrug	Nandrolone decanoate		428.6	8.1
Active substance	Nandrolone		274.4	3.0

Figure 1.2: Differences in molecular structure, molecular weight and partition coefficient (log P) between prodrug and active substance of nandrolone. All data is obtained from <http://www.chemspider.com/>, 2016.

As can be seen in Figure 1.2 both the prodrug nandrolone decanoate and active substance nandrolone are lipophilic molecules, as the partition coefficient (log P) is in both cases above 1. Until now, it is unknown where the ester prodrug is hydrolysed once released from the oil depot: near the site of injection, in the (systemic) central circulation or in the liver.

### Excipients

The vehiculum in oil depots is of course the oil. There are several types of oil that can be processed: sesame oil, arachis oil, castor oil and coconut oil (also known as medium-chain triglycerides (MCT)) (Table 1.2). All oils are derived from a mixture of saturated fatty acids. The viscosity of the oil is relevant during administration because high viscous liquids cause difficulties to pass through a needle. Furthermore, it is a parameter that influences the diffusion coefficient, which will be explained in the next paragraph.

Table 1.2: An overview of types of oil processed in oil depots.

Type of oil	Dynamic viscosity (mPa.s)	Origin
Sesame oil	43 (unknown temperature)	Ripe seeds from cultivated varieties of <i>Sesamum indicum</i> (Fam. Pedaliaceae).
Arachis oil (peanut oil)	35.2 at 37 °C	Seeds of <i>Arachis hypogaea</i> (Fam. Leguminosae).
Castor oil (ricinus oil)	200-1000 between 20-40 °C	Seeds of <i>Ricinus communis</i> (Fam. Euphorbiaceae).
Coconut oil	27-32 at 20 °C	Fixed oil extracted from the hard, dried fraction of the endosperm of <i>Cocos nucifera</i> .

All data was obtained from the Handbook of Pharmaceutical Excipients (26).

Besides the oil component, an additional excipient in oil depots is benzyl alcohol (BOH) (see Table 1.1). The main function in oil depots is that it enhances the solubility of the processed lipophilic prodrugs (Table 1.3). The second function of BOH is to ease the administration because of its viscosity reducing effect. The last function of BOH is that it acts as a local anaesthetic.

Other frequently used excipients are benzyl benzoate (BBA) and ethanol (EtOH). An overview is given in Table 1.3 below.

Table 1.3: An overview of other frequently used excipients in oil depots.

Excipient	Function(s) in oil depots	% in oil depots (mass/volume)	Log P (o/w)
Benzyl alcohol	<ul style="list-style-type: none"> <li>• Solubility enhancer</li> <li>• Oil viscosity reducer</li> <li>• Local anaesthetic</li> </ul>	1-10	1.1
Benzyl benzoate	<ul style="list-style-type: none"> <li>• Solubility enhancer</li> <li>• Solvent</li> </ul>	15	4.0
Ethanol	Solvent	5-10	-0.31*

All data was obtained from the Handbook of Pharmaceutical Excipients (26), unless otherwise specified. \* via drugbank.ca, visited on November 9<sup>th</sup>, 2016

### Routes of administration

Oil depots are either administered in the muscular or subcutaneous (adipose) tissue. In these tissues, the volume that can be administered is limited. For the deltoid and vastus lateralis the maximum reported injection volume is respectively 2 and 5 mL (27). The maximum volume for i.m. gluteal injections is assumed to be around the 4 mL (27). Figure 1.3 illustrates the mentioned muscular injection sites.

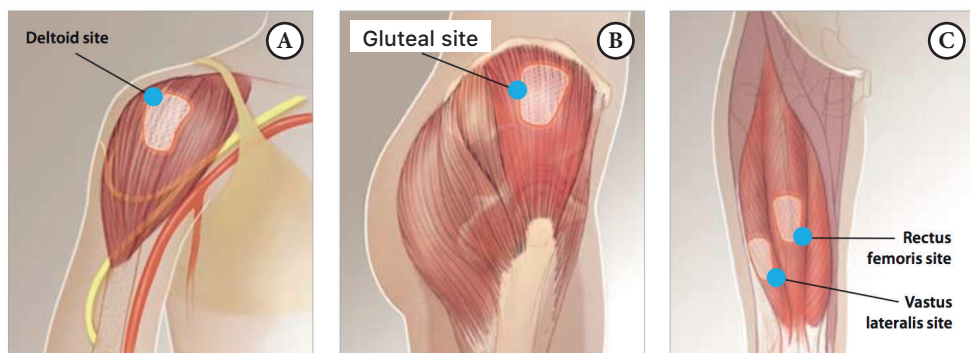


Figure 1.3: Injection sites where oil depots can be administered: the deltoid (A), gluteal (B) or vastus lateralis site (C). Figures are adapted from *Rodger et al.* (27).

It is believed that the maximum tolerated subcutaneous injection is 1.5-2.5 mL. Volumes >2.5 mL are associated with leakage and injection pain at the injection site (28).

The volume of an injection may have an effect on the drug absorption characteristics. A slight positive correlation between either area under the curve ( $AUC$ ), or rate of drug absorption from the injection site ( $k_a$ ) and the injection volume on the other hand was established in a rat study with aqueous solution injections (Figure 1.4) (29). In a study with oil depots in humans, there were no significant  $AUC$  differences seen after injection with a higher injection volume of oil (Figure 1.5 and Table 1.4) (30). In these two studies, the drug load administered was kept constant.

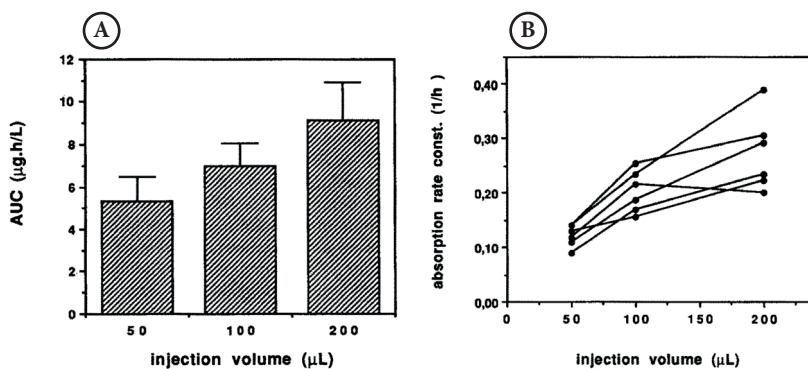


Figure 1.4: A) Mean AUC values following intramuscular injection of 3 mg propranolol HCl in an aqueous solution: 50, 100 and 200 µL, respectively. Bars indicate standard deviation (n = 6). B) Individual absorption rate constants after the same injections. Lines connect individual values for the same rat. Figures are obtained from (29).

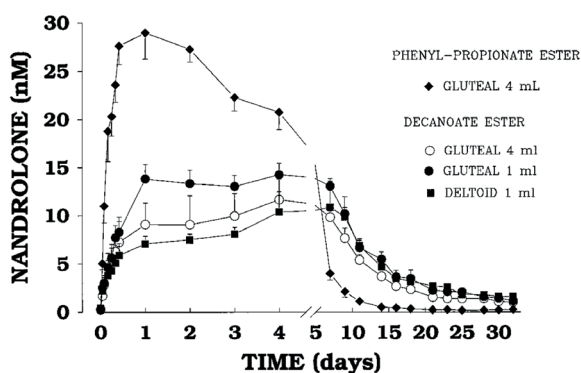


Figure 1.5: Time course of plasma nandrolone concentrations in 23 healthy men over 32 days after i.m. injection of 100 mg of nandrolone phenylpropionate in 4 mL of arachis oil vehicle into the gluteal muscle (group 1) (♦) or injection of 100 mg of nandrolone decanoate into the gluteal muscle in 4 mL of arachis oil vehicle (group 2) (○), into the gluteal muscle in 1 mL of arachis oil vehicle (group 3) (●) or into the deltoid muscle in 1 mL of arachis oil vehicle (group 4) (■). Results are expressed as mean and S.E.M., unless the S.E. is smaller than symbol. Figure is obtained from (30).

Table 1.4: Nandrolone AUC after 1 or 4 mL oil depot injection of nandrolone decanoate in the gluteal and deltoid muscle.

	Gluteal	Gluteal	Deltoid
Injection volume	1	4	1
Dose nandrolone decanoate (mg)	100	100	100
Area under the curve (nmol*day/liter)	193 ± 29	144 ± 30	162 ± 34

Results are expressed as mean and S.D. Table is obtained from (30).

## THE BIOPHARMACEUTICAL ASPECTS OF DRUG ABSORPTION FROM OIL DEPOTS

Since 1968, the biopharmaceutical aspects of solution injections have been studied (31). *In vitro* models examined the characteristics of the drug release from different oil depots, while other studies focussed mainly on the final result of both release and absorption of the compounds, i.e. the pharmacokinetic profiles (30,32,33). What happens between the moment the prodrug is released from the oil and the appearance of the parent compound in the central circulation has remained relatively unexplored however.

### Release from the oil depot

After injection in either the muscular or subcutaneous tissue, the oil depot is not only surrounded by tissue cells, but also by tissue fluid (*interstitial fluid*). This fluid is the residue of blood plasma (34), which may contain proteins. Due to the polar characteristics, water molecules attract each other in contrast to the oil molecules. Consequently, the oil and the tissue fluid do not mix with each other which results in separated fluids.

It was suggested by *Ballard* in 1968 (31) that drug absorption from solution injections takes place passively by diffusion through tissues at the injection site, which can be described by Fick's Law:

$$\frac{dN}{dt} = \frac{D * A * K}{\delta} (C_{donor} - C_{acceptor}) \quad \text{[Equation 1.1]}$$

where  $dN/dt$  is the penetration rate that can be used to estimate drug absorption from solution injections. Here,  $N$  is the amount of drug particles penetrating the tissue,  $t$  is the time and ( $D$ ) the diffusion coefficient of the drug in the membrane with surface area ( $A$ ). ( $K$ ) is the distribution coefficient between the membrane lipids and aqueous phases around the injection site, while the concentration gradient between the oil depot ( $C_{donor}$ ) and aqueous phase around the injection site ( $C_{acceptor}$ ) is the driving force for drug absorption. The rate-controlling diffusion path ( $\delta$ ) is assumed to be constant for each animal and site.

The concept suggested by *Ballard* was taken over by *Larsen et al.* in various studies (35–38). The influence of the diffusion coefficient was estimated using *in vitro* models: An example of such *in vitro* model for testing drug release from oil solutions intended for oil depots was evaluated in a publication by *Thing et al.* (36). This evaluation included an oil and aqueous phase for respectively the donor and acceptor compartment (Figure 1.6).

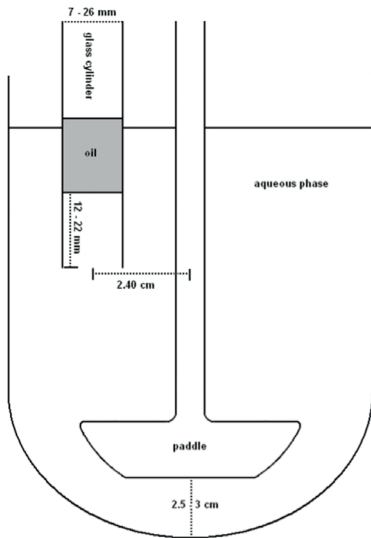


Figure 1.6: Schematic representation of the in vitro model consisting of the paddle apparatus equipped with a glass cylinder used by *Thing et al.* (36). The oil compartment is obviously the representation of the oil depot. The small compartment underneath it is the aqueous diffusion layer ( $\delta$  in Eq. 1.1) as intended by *Ballard* in its paper (31).

The oil contained naproxen dissolved in either coconut oil (viscosity = 12 mPa.s) or castor oil (viscosity = 283 mPa.s). All other parameters (naproxen concentration in the oil depot, pH and volume in the acceptor compartment, surface area between oil depot and acceptor compartment and diffusion length) that affect the release rate were kept constant. The partition coefficient between naproxen in coconut oil ( $P = 0.44$ ) and castor oil ( $P = 0.46$ ) were comparable, and therefore identical conditions were achieved.

It was shown that the drug release rate depended on the drug diffusivity in the oil and the degree of agitation generated in the oil vehicle (Figure 1.7). One should note here that this is in contrast to *Ballard's* suggestion, because *Ballard* assumes diffusion through the aqueous layer instead of through the oil. This aqueous layer is the compartment underneath the oil compartment in Figure 1.6.

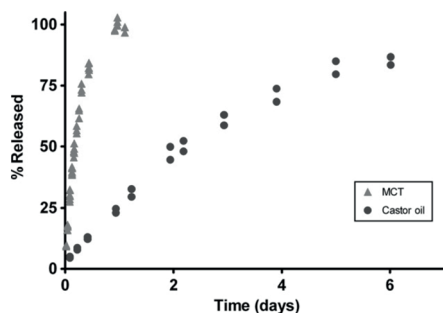


Figure 1.7: Release profiles of naproxen from coconut oil and castor oil. Naproxen released from coconut oil ( $t_{50\%} = 4.2$  h) was much higher than from castor oil ( $t_{50\%} = 48$  h). Figure is obtained from (36).

The authors claim that a more viscous oil depot releases its compounds slower compared to a less viscous oil depot, which is explained by the diffusion coefficient (Stokes Einstein) equation:

$$D = \frac{k * T}{6 * \pi * \eta * r} \quad [\text{Equation 1.2}]$$

An increase in the solvent dynamic viscosity ( $\eta$ ) results in a decreased diffusion coefficient ( $D$ ), whereby the other parameters remain constant. The other parameters are the Boltzmann constant ( $k$ ), the absolute temperature ( $T$ ) and the radius ( $r$ ) of the molecule dissolved in the solute. A decreased diffusion coefficient results in a lower penetration rate (see Equation 1.1). This means that particles/molecules diffuse slower to the interfacial surface. Unfortunately, the authors fail to state that there is a diffusion layer in the oil phase that dominates the release process.

The partitioning of the drug between the oil vehicle and the aqueous phase was found to influence the release rate (36,37,39,40). *Larsen et al.* reported that the overall rate constant towards the aqueous phase decreased when the lipophilicity of dissolved molecules in oil depots increased (37). Thus, the partition coefficient determines the mass transfer between two immiscible liquids. In fact, Equation 1.1 apparently needs to be extended with the partition coefficient between the oil formulation and the tissue liquid.

### Surface area

It is clear that according to Equation 1.1, the surface area is of importance for drug release from oil depots. This seems to be confirmed in the *in vitro* study with naproxen depots by *Thing et al.* (36), where the surface area was varied. It was established *in vitro* that a larger surface area yielded a higher amount of naproxen (Figure 1.8).

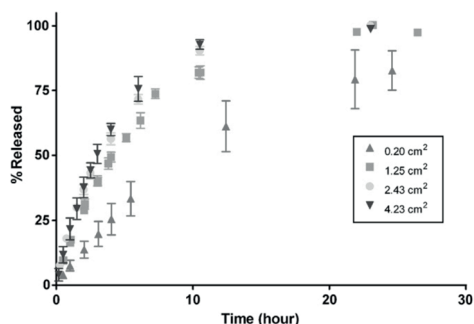


Figure 1.8: Release of naproxen from coconut oil using cylinders with varying areas at a constant oil volume/area ratio of 8 mm. Bars represent standard deviations,  $n = 3$ . Figure is obtained from (36).

In this respect, it is of importance to know the surface area of an oil depot in the tissue. In 1929, the oil depots were reported to be spherically-shaped when injected in human gluteal muscle (41). However, the *in situ* surface area of injected oil depots has not been published yet.

#### Tissues around injection site

Once released in the acceptor phase, there are several pathways suggested for drug absorption into the central compartment: small molecules (< 5 kDa) can directly be absorbed into the central compartment, whereas larger molecules (> 16 kDa) are absorbed via the lymphatic system. The rate at which small molecules permeate through tissue is reported to be dependent upon the lipophilicity (31,42,43). This has also been shown in a study with aqueous solutions administered to pigs. Lipophilic molecules were absorbed slower than hydrophilic molecules (Figure 1.9) (44).

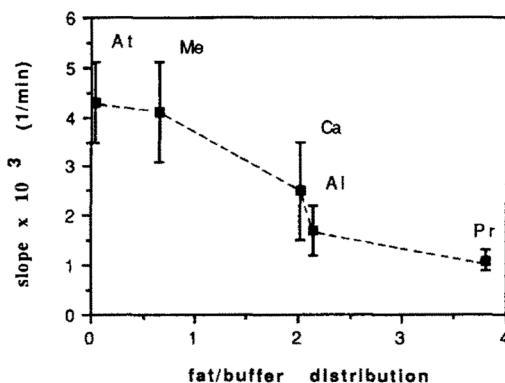


Figure 1.9: Correlation between the fat-buffer distribution constants and release rates (reflected by the slope) on intra-adipose administration of atenolol (At), metoprolol (Me), carazolol (Ca), alprenolol (Al), propranolol (Pr). The fat-buffer distribution constants can be interpreted as a translation of the partition coefficient. Figure is obtained from (44).

From the studies published until now it is not clear if it is the prodrug that is absorbed in the central compartment or if the prodrug is first hydrolysed at the site of injection. This is relevant as it is clear that the parent compound will permeate much faster through the tissue than the prodrug.

#### Activation of the parent compound by hydrolysis of prodrugs

An important process during drug absorption is the activation of the active substance via hydrolysis of the prodrug. This hydrolysis may occur in the interstitial fluid, tissue cells, lymph nodes or in intravascular fluids. *Wijnand et al.* suggested that this hydrolysis for the

prodrug nandrolone decanoate (ND) may occur in human serum (32). It was suggested that ND should hydrolyse within 10 minutes in human serum, based on ND hydrolysis studies in rat plasma conducted by *Van der Vies* (4). Until now, there is no published data that clearly demonstrates hydrolysis of ND in human serum, nor in other fluids or tissues.

### Pharmacokinetic studies

*Wijnand et al.* (32) studied the pharmacokinetic profiles of nandrolone after injection in the vastus lateralis muscle of females and males (respectively Figure 1.10A and 1.10B). Volunteers in both groups received respectively a dose of 100 mg (1 mL) and 200 mg (2 mL) nandrolone decanoate. Notice the almost equal maximum concentrations of nandrolone in Figure 1.10, whereas a higher concentration of nandrolone in the male group was expected due to the higher administered dose of nandrolone decanoate. It was argued by the authors that the serum clearance of nandrolone was higher in the male group compared to the female group, which lowered the nandrolone concentration (32)

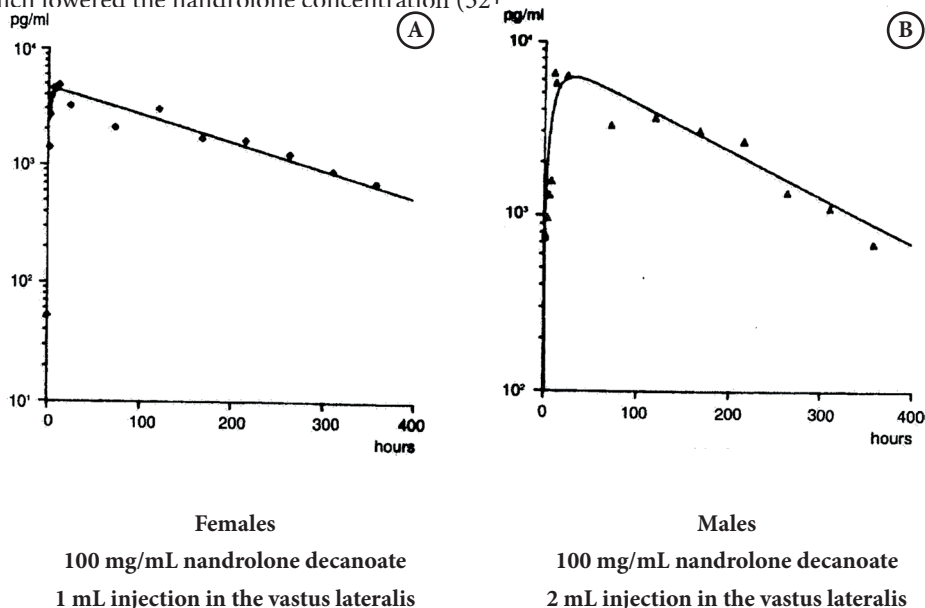


Figure 1.10: Nandrolone levels in serum (Y-axis) after intramuscular injection of A) 100 mg in females or B) 200 mg in males of nandrolone decanoate (100 mg/mL). The scale on the y-axis is not the same in A and B, resulting in a biased pharmacokinetic profile may arise between the two curves after plasma  $C_{max}$ . Figures are obtained from *Wijnand et al.* (32)

*Minto et al.* (30) studied the injection sites deltoid and gluteal muscle and various injection volumes (Figure 1.5 and Table 1.4). This paper showed that the  $AUC$ ,  $C_{max}$  and  $T_{max}$  were not significantly different between the injection sites and volumes.

*Bagchus et al.* (33) reported the pharmacokinetic profiles after injection with various

nandrolone decanoate concentrations: there was no linear increase in nandrolone  $C_{max}$  although the concentration of nandrolone decanoate tripled (Figure 1.11).

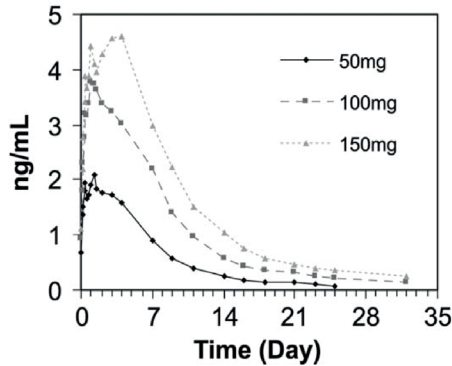


Figure 1.11: Mean serum concentration profiles for nandrolone after single 1 mL i.m. injection of 50, 100, or 150 mg nandrolone decanoate in healthy men. Figure is obtained from (33).

It is assumed by *Garret et al.* and *Rowland et al.* that, once released from sustained release drug products, drugs follow first-order kinetics in a one-compartment body model (45,46). The Bateman function (Equation 1.3) is used to characterise the filling and draining of one compartment in time ( $t$ ). A fraction ( $F$ ) of a predetermined amount of drug ( $D$ ) is distributed over an apparent volume ( $V_d$ ) with a first-order constant of absorption ( $k_a$ ) and removed with a first-order rate constant of elimination ( $k_e$ ) (45).

$$C_t = \frac{D * F}{V_d} * \frac{k_a}{(k_a - k_e)} * (e^{-k_e * t} - e^{-k_a * t}) \quad [\text{Equation 1.3}]$$

The concentration of the drug in the central compartment at a certain time point is  $C_t$  here. The absorption rate constant,  $k_a$ , is actually the sum of rate constants of all invading prodrug particles towards the central compartment (45).

Usually the absorption rate outreaches elimination rate, which results in a quick increase in the drug concentration and a first-order decline of the blood levels in the central compartment (45). An uncommon phenomenon occurs when the elimination rate dominates the absorption rate significantly ( $3 * k_e > k_a$ ) (45). In these circumstances the component  $e^{-k_e * t}$  can be neglected, because of the very low contribution to the whole equation (Equation 1.3). This phenomenon is called *flip-flop* kinetics and occurs often when a sustained release formulation is applied. Furthermore, the drug absorption after release can be hampered by adhesion to cell membranes at the injection site (47). This causes a very low drug absorption rate, which is in these cases much lower than the elimination rate.

### Contribution benzyl alcohol on drug absorption

Interestingly, almost all oil depots contain the excipient benzyl alcohol (BOH). One of the functions of BOH is to enhance the solubility of the lipophilic prodrug in the oil. Furthermore, as already suggested, it can be expected that BOH lowers the viscosity of the oil and therefore increase the diffusion coefficient (Equation 1.2). As a result, both the influenced partition coefficient and diffusion coefficient of the prodrugs may cause an increased release rate from the oil depot. Until now, no paper describes the influence of BOH on the drug release or absorption from oil depots.

### MECHANISM OF DRUG ABSORPTION FROM OIL DEPOTS

The amount released from the oil depot follows first-order absorption into the central compartment ( $k_a$ ), whereas first-order elimination ( $k_e$ ) represents the removal from this compartment. An outline of the compound flow is seen below in Figure 1.12, where nandrolone decanoate is used as a model compound.

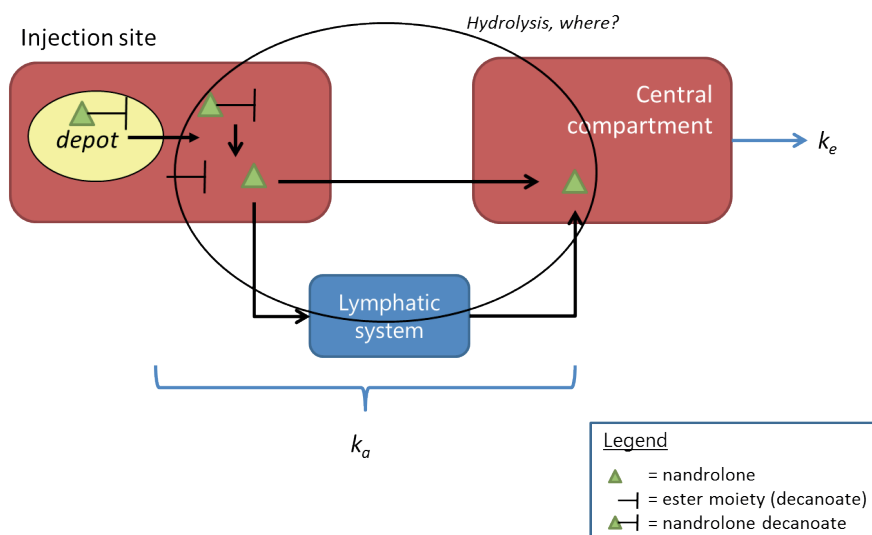


Figure 1.12: Schematic overview of the mechanism of drug absorption from oil depots until now. After release from the oil depot (yellow circle at the injection site), it is assumed that the prodrug is hydrolysed in serum. If this occurs locally, the active substance can be absorbed directly into the central compartment. Otherwise, the prodrug can be hydrolysed in the lymphatic system or at the end of the pathway in the central compartment. These pathways were already suggested by *Larsen et al.* (48).  $k_a$  = absorption rate constant;  $k_e$  = elimination rate constant.

Until now, it is assumed by *Tanaka et al.* that the prodrug (nandrolone decanoate is used as a model compound in Figure 1.12) is released from the oil depot locally (40). A rat study where i.m. oil depots were injected showed that the prodrug haloperidol decanoate and parent compound haloperidol were recovered in both lymph nodes and the central compartment (49). This suggests that a fraction of prodrug is transported via the lymphatic system towards

the central compartment. This pathway is also suggested by *Larsen et al.* for prodrug transport after oil depot administration in humans (48). Although the actual location is yet unknown, this prodrug is hydrolysed in human serum, as suggested by *Wijnand et al.* (32).

## OBJECTIVES OF THIS RESEARCH AND OUTLINE OF THIS DISSERTATION

As stated in this introduction, some critical parameters influence drug absorption from oil depots. According to *De Haan et al.* (39) and *Larsen et al.* (37), at least the partition coefficient of the prodrug between the oil and aqueous phase and the surface area of the oil determine the drug release from the oil depot.

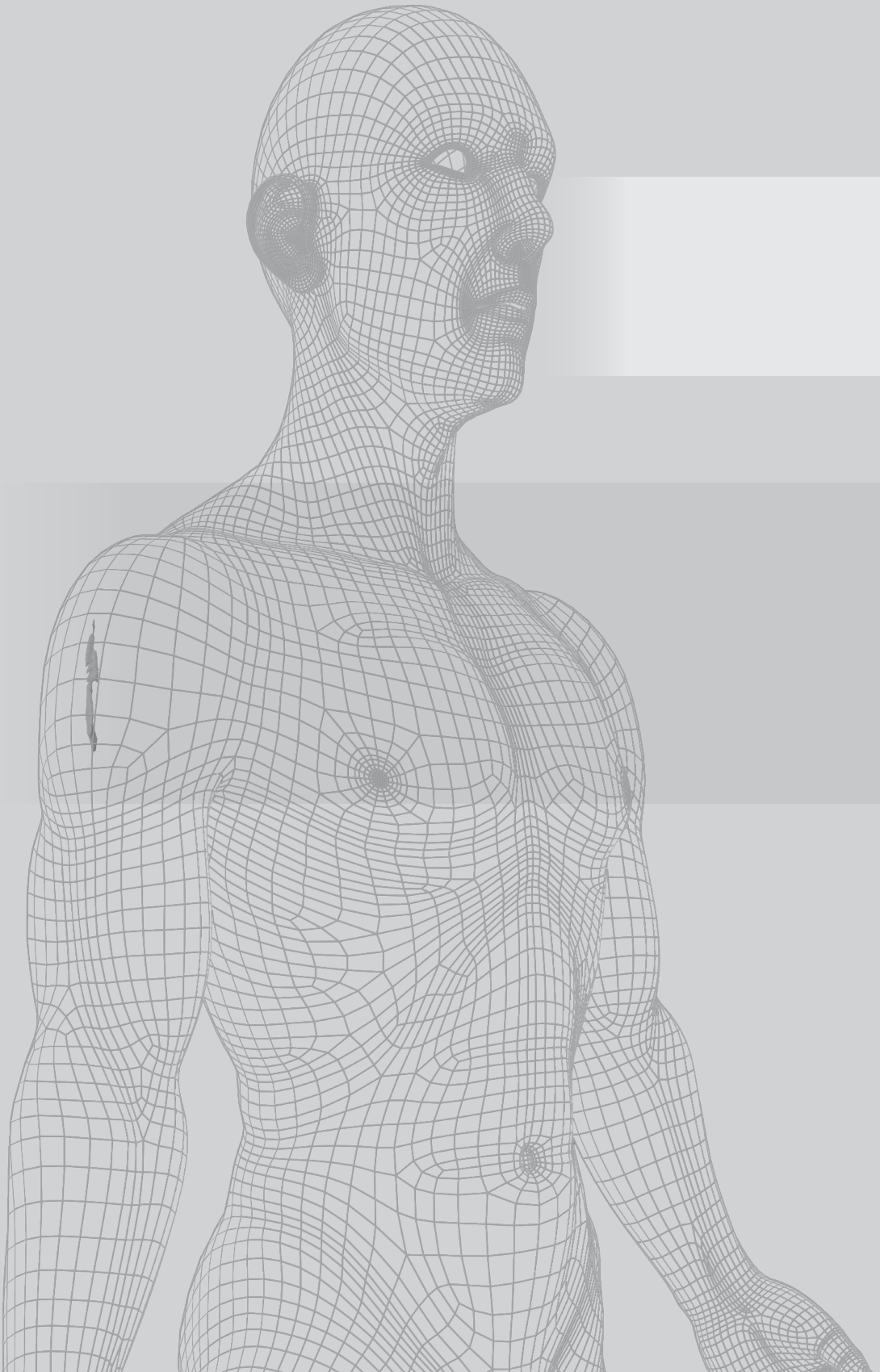
Although some excipients used in oil depots may influence this partition coefficient, no studies were conducted to examine the influence of oil depot excipients on the absorption kinetics of the active substance. Especially, the effect of benzyl alcohol is of interest, because it is processed in almost every oil depot (Table 1.1).

The shape and surface area of oil depots after injection is often regarded as a sphere (41). Although this seems acceptable, this assumption has never been confirmed. Furthermore, neither the *in situ* surface area, nor the disappearance rate of the oil depot has been determined.

In this dissertation, one of the oldest prodrugs processed in oil depots, nandrolone decanoate, is used as a model compound. Until now, the rate of hydrolysis of nandrolone decanoate is unknown in human serum, or even in human blood. This is relevant because when this rate is too low, a postponed or delayed therapeutic effect may be noticeable. Obviously, this is not only relevant for nandrolone decanoate hydrolysis, but for all esterified prodrugs processed in oil depots.

The aim of this dissertation is therefore to assess the fundamental parameters that influence drug absorption from oil depots. The parameters described above will be examined in the following chapters:

- Before the influence of the commonly used excipient in oil depots (benzyl alcohol) on the absorption of nandrolone can be examined, the bioassay to examine benzyl alcohol and its metabolites in human serum must be developed. This bioassay and subsequently the application to samples obtained from a clinical study are described in detail in *Chapter 2*.
- The influence of the critical factors on drug absorption from oil depots are described in *Chapter 3*.
- *Chapter 4* describes a method to visualise the spatial distribution of the oil depot after injection. With this method, the surface area and volume of an oil depot administered in the upper arm were examined over a period of 2 weeks in healthy volunteers.
- *Chapter 5* continues the experiments of the previous chapter: the surface area and volume of oil depots injected in two other muscles were followed over time in healthy volunteers. These two muscles were chosen based on interpreted results originating from Chapter 3.
- *Chapter 6* describes the hydrolysis of a nandrolone decanoate in blood and in tissues near the injection site.
- Finally, *Chapter 7* discusses the important findings in the general discussion. This chapter also provides the perspectives for future research and, in the end, a conclusion is drawn.



## Chapter 2

# Pharmacokinetics in elderly women of benzyl alcohol from an oil depot

R.W. Kalicharan

M. El Amrani

P. Schot

H. Vromans

*Journal of Pharmaceutical Sciences* 105 (2016) 1519-1525

### ABSTRACT

Pharmaceutical oil depots are meant to release active substances at a sustained rate. Most of these depots contain benzyl alcohol to facilitate the production and administration. Since benzyl alcohol changes the solubility of components in both the body fluid and the oil formulation, it is relevant to know the change in the benzyl alcohol concentration in the oil over time. In this study, volunteers were subcutaneously injected with an oil depot that contained 10% benzyl alcohol, nandrolone decanoate and cholecalciferol. The aim of this study was to determine the pharmacokinetic profiles of benzyl alcohol and its metabolites benzoic acid and hippuric acid simultaneously in serum to estimate the benzyl alcohol release out of the depot. For this, an HPLC bioassay was developed and adequately validated. Hereafter, the bioassay was applied to serum samples obtained at several time points between 0 and 35 days. Benzyl alcohol appeared immediately in serum after injection. The pharmacokinetic profile revealed that all benzyl alcohol was depleted from the depot within 52 hours after injection. Thus, the partition coefficient of active substances between the oil formulation and the body tissue changes rapidly in the first days after injection but will remain constant hereafter.

## INTRODUCTION

Benzyl alcohol (BOH) is a commonly used excipient in oil depots in a concentration range of 1.5-10% v/v (30,32,33,50). It is used as co-solvent, local anesthetic and as viscosity reducer in oil depots (26). In other parenteral pharmaceutical products and in cosmetics, it is used as an antimicrobial preservative in concentrations varying from 1-10% v/v (26,51,52). Oil depots are meant to exhibit extended release of (active) substances.

Usually, these depots are administered in muscular or subcutaneous tissue. Both tissues contain aqueous interstitial fluid in which the active substance and BOH are released. Although BOH is nearly always used in oil depots, there are no publications available on the release of this excipient from these formulations, or on the effect of this toward the release of the drug. In *Chapter 3*, we show that the absorption of (active) substances from depots is determined by the partition coefficient. Since BOH changes solubility of components in both the oil and the body fluid, the distribution of (active) substances between the oil and body fluid may alter during BOH release. As a result, the absorption of these substances can be influenced during BOH release and is therefore clinically relevant.

When benzyl alcohol is released from the depot, it is metabolized into benzoic acid (BA) (53). In the liver, benzoic acid is subsequently conjugated with glycine to form hippuric acid (HA) (54,55). Table 2.1 gives a summary of the mentioned substances.

It is important to realize that BA is also processed as such as a preservative in pharmaceutical products (26) and in food (56,57). As there may be another source of BA than the BOH released out of the depot, it is therefore meaningful to measure the levels of BOH and its metabolites simultaneously. Until now, no analytical methods are available to separate these compounds in human serum. The HPLC method published by *Tan et al.* (58) to determine BOH, BA and HA simultaneously in dog plasma was not applicable for human serum, based on our own research. This was the reason to start the development of a bioassay to determine the components of interest in human serum.

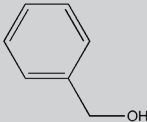
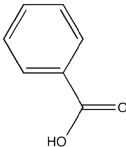
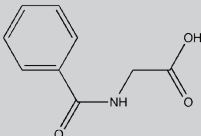
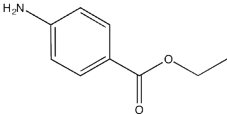
The aim of this study was to determine the pharmacokinetic profiles of benzyl alcohol and its metabolites benzoic acid and hippuric acid in serum to estimate the benzyl alcohol release out of the depot. This was achieved with an appropriate analytical method that enables determination of the parent and its metabolites simultaneously.

## MATERIALS AND METHODS

### Chemicals and reagents

Benzyl alcohol, benzoic acid, hippuric acid, benzocaine (internal standard, IS) and 1 M triethylammonium phosphate (TEAP; pH 3.0) buffer solution were purchased from Sigma-Aldrich (Missouri, United States of America (USA)). HPLC-grade methanol, acetonitrile and perchloric acid were obtained from Merck (Darmstadt, Germany). Newborn calf serum was purchased from Life Technologies (California, USA).

Table 2.1: Summary of components used in this assay and their molecular properties.

Component name	Molecular formula	Molecular structure	Molecular weight (g/mole)
Benzyl alcohol	$C_7H_8O$		108.1
Benzoic acid	$C_7H_6O_2$		122.1
Hippuric acid	$C_9H_9NO_3$		179.2
Benzocaine (IS)	$C_9H_{11}NO_2$		165.2

IS = internal standard. Source: [www.chemspider.com](http://www.chemspider.com), visited at November 13, 2015.

### High-performance liquid chromatography equipment and conditions

The separation of the analytes and IS was carried out with an isocratic HPLC method. Based on a published method by *Tan et al*, benzocaine (Table 2.1) was selected as an internal standard (58). The liquid chromatography system was from Agilent Technologies 1290 Infinity series with a diode array detector (DAD) type G4212. The autosampler kept the samples at 4°C and the injection volume was 25.0 µL. Separation was carried out on an Agilent Poroshell 120 EC-C18 (100 x 4.6 mm ID, 2.7 µm particle size) column, kept at 30°C during analysis. A phenomenex guard column (C18, 4 x 2 mm ID, 5.0 µm particle size) was used to filter out contaminants from each injection. Mobile phase composed of 40 mM TEAP-buffer (pH 3.0), methanol and acetonitrile (75:12.5:12.5, v/v/v) and the flow rate was set at 1.0 mL/min.

A full UV spectrum analysis from 190.0 – 400.0 nm was carried out for each component (benzyl alcohol, benzoic acid, hippuric acid and benzocaine) to determine the maximal absorption ( $\lambda_{max}$ ) and applied to the detection method (Figure 2.1). Software used for equipment control and data acquisition was Chromeleon, version 7.1.3.2425 from Thermofisher Scientific (Massachusetts, USA).

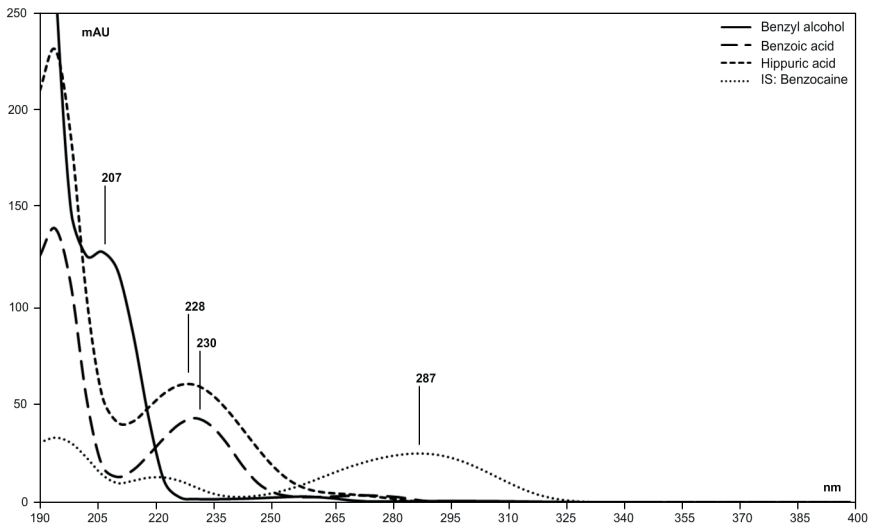


Figure 2.1 Full UV spectrum of benzyl alcohol, benzoic acid, hippuric acid and internal standard (IS) benzocaine was obtained at range 190.0 – 400.0 nm. Characteristic peak heights for benzyl alcohol, benzoic acid, hippuric acid and IS were 207, 230, 228 and 287 nm respectively.

### Benzyl alcohol, benzoic acid, hippuric acid and benzocaine standards

A mixed stock solution of BOH, BA and HA was prepared at a final concentration of 1 mg/mL solution in 100% methanol and further diluted in newborn calf serum to obtain working solutions of 0.1, 0.5, 1, 2.5, 5 and 10  $\mu\text{g}/\text{mL}$ . Internal standard benzocaine was freshly prepared as a 10  $\mu\text{g}/\text{mL}$  solution in a mixture (1:1, v/v) of acetonitrile and methanol. All standards were stored at  $-70^\circ\text{C}$ .

### Sample preparation

Two hundred-microliter serum (obtained from test subjects, see section *Test subjects*) or 200  $\mu\text{L}$  working standard solutions were pipetted in 1.5 mL mixing tubes (Eppendorf, Hamburg, Germany), followed by 100  $\mu\text{L}$  IS. Hereafter, 100  $\mu\text{L}$  perchloric acid (10%) was added while vortexing to precipitate serum proteins. Then, samples were centrifuged for 5 minutes at 14,000 rpm. Supernatant was analyzed using HPLC-DAD.

### Method validation

Identification was performed by comparing the full UV spectrum (190.0 – 400.0 nm) of the peaks found against a reference library (created in house). Furthermore, the software also performs peak purity test which gives an indication to the homogeneity of the peak. For both parameters, a match factor greater than 85% was considered satisfactory.

Specificity was performed using blank human serum from five different individuals and one newborn calf serum sample. These samples were tested for the presence of endogenous

substances co-eluting with BOH, BA, HA or IS. The observed chromatographic retention times of these six injections together with their full UV spectra were compared against a working standard injection in order to determine identity and to calculate the concentration.

Limit of quantitation (LoQ) was defined as lowest detectable concentration (0.1 µg/mL) with a signal to noise ratio of 10:1 (n=6). Carry-over effect was assessed by injecting a blank newborn calf serum sample after the highest quality control sample (8.0 µg/mL). Carry over in the newborn calf serum sample following the highest quality control sample should not be greater than 20% of the lower limit of quantitation.

Intra-day accuracy and precision of the assay were evaluated together within one run (also known as repeatability (59)). Inter-day accuracy and precision of the assay were evaluated together on five different days. Newborn calf serum was spiked with BOH, BA and HA at four quality control (QC) samples: 0.1, 0.5, 2.0 and 8.0 µg/mL. These concentrations were prepared in six folds and corresponded with LoQ, quality control low (QC\_L), quality control medium (QC\_M) and quality control high (QC\_H), respectively. The overall bias and the coefficient of variation (CV) were calculated to evaluate the accuracy and precision of the assay.

The intra- and inter-day accuracy and precision for all analytes were considered acceptable for all QC samples as indicated by the overall bias (accuracy; within ±15%) and CVs (precision; <15%), respectively (60). For LoQ, the acceptance value for the overall bias and CV was set at ±20% range and <20%, respectively (60). A one-way ANOVA test was used for the calculations.

Recovery validation was performed using newborn calf serum and distilled water. These liquids were spiked with the mixed stock solution of BOH, BA and HA (5 µg/mL) and IS. The recovery was calculated by dividing the peak heights of the analyte from the spiked serum by its respective counterparts from the spiked water solution (n=4 per analyte). Recoveries of 85% or higher were considered acceptable.

Linearity validation was performed using a six point calibration (0.1, 0.5, 1, 2.5, 5 and 10 µg/mL) (n=3 per concentration/analyte on three different days). Regression analysis of slope, intercept and correlation coefficients ( $R^2$ ) were calculated by Microsoft Excel 2010 using Data Analysis, Regression.

Long-term stability studies of BOH, BA and HA in newborn calf serum were evaluated at QC low and high concentrations (n=3 per concentration/analyte). Samples were stored at -20°C for 11 months.

Freeze and thaw stability studies of the analytes were evaluated during inter-day accuracy tests. Freeze-thaw cycles from -70°C to ambient temperature in serum were performed four times, whereby samples stored 4 hours at ambient temperature. Mean concentration of each analyte at each level within ±15% of the nominal concentration were considered acceptable.

### Test subjects

Fourteen healthy female Caucasian volunteers were enrolled in Groningen (the Netherlands) in a pharmacokinetic study. The demographic characteristics were (mean  $\pm$  standard deviation): Age =  $70.7 \pm 4.3$  year, length =  $1.65 \pm 0.1$  meter, weight =  $68.0 \pm 9.0$  kilogram and BMI =  $24.8 \pm 2.3$  kg/m<sup>2</sup>. These volunteers were initially enrolled to determine nandrolone decanoate and cholecalciferol in serum (see below for more information about the oil depot formulation and study). Residual serum samples from the same volunteers were used in present study.

There was no loss to follow-up and no adverse reactions were reported during this study. Ethics approval for the study was obtained from the Central Committee on Research Involving Human Subjects in the Netherlands. All volunteers signed the informed consent to participate in the study. Serum samples were collected at QPS Netherlands B.V. (Groningen, the Netherlands). All volunteers received a 0.5 mL oil depot, subcutaneously injected in the upper arm. This oil depot was manufactured under current Good Manufacturing Practice conditions in the hospital pharmacy at the University Medical Center Utrecht, the Netherlands. It contained 0.93 mmol/mL (=100 mg/mL) BOH, 50 mg/mL nandrolone decanoate and 28,000 IU/mL cholecalciferol in sesame oil. The sustained release of nandrolone decanoate and cholecalciferol were studied in a phase 1 clinical trial. The influence of BOH on the absorption of nandrolone is published in *Chapter 3*.

Samples were taken directly after injection (0 hour) and at 2, 4, 8, 12, 15, 22, 24, 36, 48, 72, 96, 168, 216, 264, 360, 456, 552, 648 and 840 hours after injection. Samples were stored at  $-70^{\circ}\text{C}$  until they were analyzed for BOH, BA and HA at the Clinical Pharmacy, University Medical Center Utrecht, the Netherlands.

### Data analysis of pharmacokinetic study

Data will be depicted as concentration-time curves (mean  $\pm$  SEM). Area under the curve (AUC) was calculated using the trapezoidal rule. The maximum serum concentration ( $C_{max}$ ) and the time to reach maximum serum concentration ( $T_{max}$ ) were obtained directly from the concentration-time curve.

## RESULTS AND DISCUSSION

This study was initiated to develop and validate a bioassay for benzyl alcohol, benzoic acid and hippuric acid in human serum by HPLC. Hereafter, this assay was applied to serum samples from healthy volunteers to study the pharmacokinetic profiles of benzyl alcohol and its metabolites.

### Analytical method development

A previously published LC-MS/MS method by *Penner et al.* for BA and HA analysis in urine was examined (61). This method, using an alkaline buffer, provides stable ions for BA and HA.

It was checked whether this method is applicable for BOH analysis. Unfortunately, neither positive nor negative benzyl alcohol-ions were formed with an acidic or with an alkaline mobile phase. In addition, formation of positive or negative adducts of benzyl alcohol with ammonium formate or LiCl did not result in a successful analytical method either.

Three other published GC methods(62–64) turned out to be inadequate as well: Without derivatization, BA appeared to be difficult to separate due to excessive peak tailing. Finally, several HPLC methods (58,65,66) were published for BOH, but unfortunately none were applicable for serum analysis of all components simultaneously. *Tan et al.* published an HPLC method to determine all three components in dog plasma (58). Unfortunately, our own research showed an undesirable resolution of the three components spiked in calf and human serum. HPLC methods published by *Sudareva et al.* (65) and *Pérez-Lozano et al.* (66) did not include hippuric acid, which was required to meet our aim.

The here developed method exhibits the benefit of having a fast and simple sample clean-up which was able to measure the levels of BOH and its metabolites in human serum simultaneously.

### Method validation

The developed analytical method was validated by evaluating specificity, identification, accuracy, precision, LoQ, recovery, carry-over effect, linearity and stability. This assay was validated in accordance to the latest criteria found in the ICH Q2(R1) guideline, the EMA Guideline for bioanalytical method validations and literature (59,60,67). All studied validation parameters met the predefined acceptance criteria.

The five blank human serum samples and the newborn calf serum samples were tested for specificity. BOH concentrations in all blank serum samples were below LoQ (See supplementary data file). All blank samples contained HA and BA. HA and BA concentrations (mean  $\pm$  SEM) found in the blank human samples were 0.8 ( $\pm$  0.5) and 0.05 ( $\pm$  0.01)  $\mu\text{g/mL}$ , respectively. Newborn calf serum contained 0.24 ( $\pm$  0.01) and 0.06 ( $\pm$  0.01)  $\mu\text{g/mL}$  HA and BA, respectively. Therefore, newborn calf serum was preferred as matrix for our standard solutions, because of the lower amounts of HA.

No interference peaks for BOH and BA were found in the chromatogram originating from the calf serum used (Figure 2.2 and supplementary data files). The analysis was adequate for all HA concentrations, except for the LoQ concentration (= 0.1  $\mu\text{g/mL}$ ) in the calibration curve (see supplementary data). However, all HA concentrations in the conducted clinical study were accepted, because they were all above 0.5  $\mu\text{g/mL}$ . Spectral match and peak purity data from the samples used in the pharmacokinetic study were above 85% for all analytes (Table 2.2).

Table 2.2: Overview of intra- and inter-day precision, accuracy and stability of benzyl alcohol, benzoic acid and hippuric acid.

	Nominal concentration (µg/mL)	Peak purity (%)	Intra-day (n=6) CV (%)	Inter-day (n=5) CV (%)	Overall CV (%)	Overall Bias (%)	Stability (%)
BOH	LoQ (0.1)	71.0	2.3	18.3	18.4	9.1	-
	QC_L (0.5)	98.1	1.9	3.5	4.0	-2.4	-8.6
	QC_M (2.0)	99.9	1.1	0.8	1.4	3.2	-
	QC_H (8.0)	100.0	0.5	2.2	2.2	-0.3	-1.0
BA	LoQ (0.1)	99.7	17.7	0.0	17.7	3.6	-
	QC_L (0.5)	100.0	7.6	0.0	7.6	3.3	-3.9
	QC_M (2.0)	100.0	0.7	1.2	1.4	4.2	-
	QC_H (8.0)	100.0	0.6	1.5	1.6	-0.8	-1.3
HA	LoQ (0.1)	99.3	1.6	5.0	5.2	8.9	-
	QC_L (0.5)	99.8	1.1	2.0	2.3	0.9	2.5
	QC_M (2.0)	100.0	9.8	0.0	9.8	5.9	-
	QC_H (8.0)	100.0	1.1	1.7	2.1	-1.1	-2.7

Abbreviations: BOH = benzyl alcohol; BA = Benzoic acid; HA = hippuric acid; CV = Coefficient of variation; LoQ = limit of quantitation; QC\_L = quality control low concentration; QC\_M = quality control medium concentration and QC\_H = quality control high concentration.

Peak purity of BOH at LoQ concentration (= 0.1 µg/mL) was 71.0%, however. As can be seen in the clinical study below, all BOH concentrations were above 0.5 µg/mL. Therefore, this peak purity was considered as clinically irrelevant for this study. IS peak purity for the nominal concentrations 0.1, 0.5, 2.0 and 8.0 µg/mL showed purities of 97.7, 97.3, 96.9 and 97.3%, respectively.

The results of the accuracy and precision for the three components are summarized in Table 2.2. The intra- and inter-day accuracy (overall bias) were determined by repeated analysis of six spiked newborn calf serum samples. The replicated analyses varied between -2.4% and +9.1%. The intra-day, inter-day and overall precision (% CV) were less than 9.8% for the QC samples and less than 18.4% for the LoQ spiked samples.

LoQs of all analytes in this assay were 0.1 µg/mL, which equals molar concentrations of 0.93, 0.82 and 0.56 nmol/mL for BOH, BA and HA, respectively. LoQ for the developed bioassay was comparable or superior to other methods (61,68). No carry-over effect in newborn calf serum from QC high was measured.

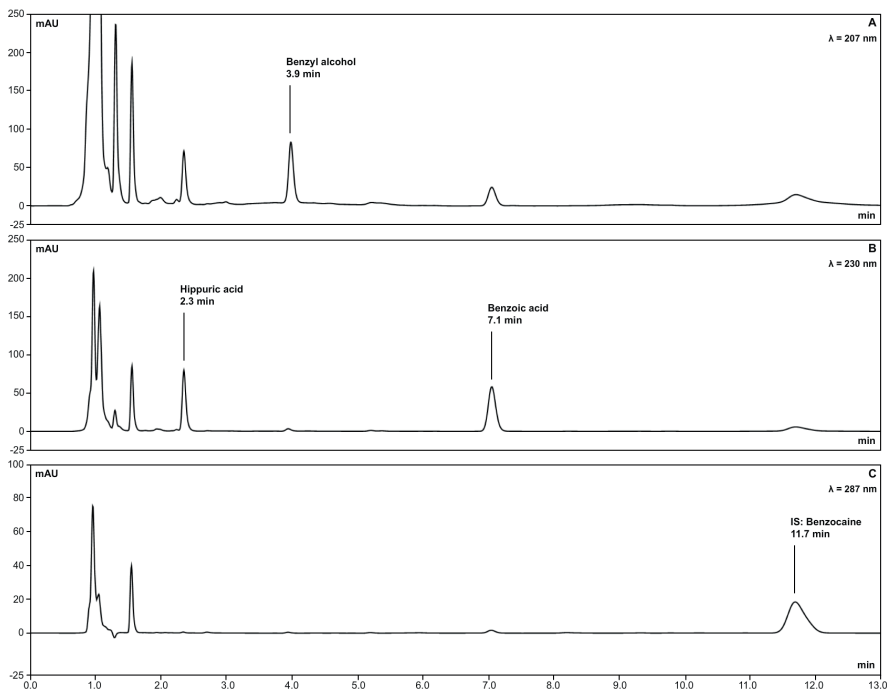


Figure 2.2: Three representative HPLC chromatograms obtained from one analytical run. Analyzed sample contained calf serum spiked with the four studied components (8.0  $\mu\text{g/mL}$ ): (A) benzyl alcohol with  $\lambda_{\text{max}}$  of 207 nm; (B) benzoic acid and hippuric acid with  $\lambda_{\text{max}}$  of 230 nm and (C) benzocaine was measured at 287 nm. All components were well separated from endogenous substances and from each other.

The recoveries of BOH, BA, HA and IS were (mean  $\pm$  RSD) 96.3% ( $\pm$  0.7), 87.5% ( $\pm$  0.6), 103% ( $\pm$  0.7) and 98% ( $\pm$  0.7) respectively, which is in line with literature data (58).

The linearity for the three analytes was evaluated over the range 0.1-10  $\mu\text{g/mL}$ . Regression coefficients were all  $\geq$  0.999.

All long-term stability (11 months at  $-20$   $^{\circ}\text{C}$ ) results were  $< \pm$  -8.6% (Table 2.2). Freeze-thaw stability was performed during inter-day accuracy and varied between -2.4% and +9.1% (Table 2.2).

#### Pharmacokinetic profiles of benzyl alcohol, benzoic acid and hippuric acid in serum

The here developed HPLC method was applied to analyze BOH, BA and HA in human serum samples. Figure 2.3 shows the mean serum concentration-time profiles of BOH and its metabolites for the entire study period. The pharmacokinetic parameters are summarized in Table 2.3.

Table 2.3: Pharmacokinetic parameters (mean  $\pm$  SEM) of BOH, BA and HA after subcutaneous administration of 0.46 mmol BOH in human (n=14).

	AUC <sub>0-840h</sub> (nmol/mL*h)	C <sub>max</sub> (nmol/mL)	T <sub>max</sub> (h)
BOH	397.3 $\pm$ 44.9	34.8 $\pm$ 1.5	3.3 $\pm$ 2.1
BA	417.4 $\pm$ 63.2	1.8 $\pm$ 0.4	36.3 $\pm$ 18.0
HA	7113.6 $\pm$ 1435.9	16.6 $\pm$ 2.7	374.6 $\pm$ 86.6

BOH = benzyl alcohol; BA = Benzoic acid; HA = hippuric acid;

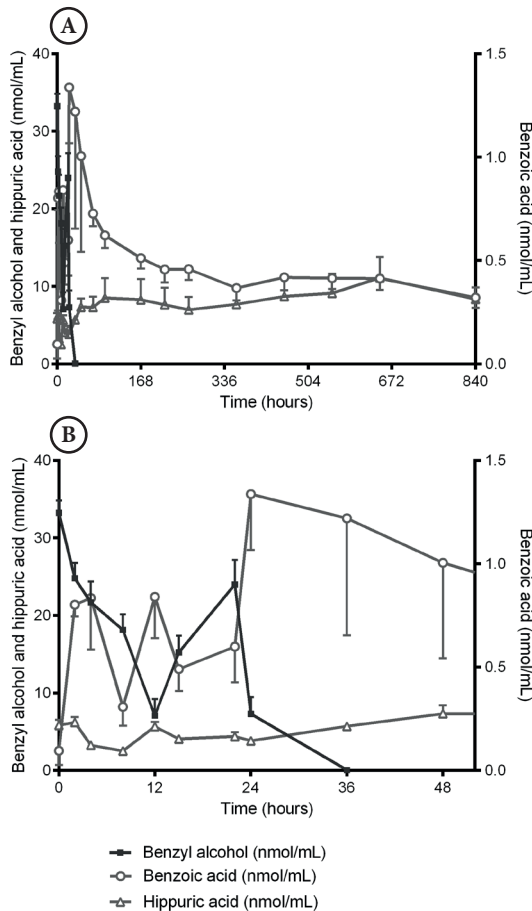


Figure 2.3: Pharmacokinetic profiles of benzyl alcohol (■), benzoic acid (○) and hippuric acid (△) in serum after injection, presented as mean  $\pm$  standard error. Healthy females (n=14) received subcutaneously 50 mg benzyl alcohol dissolved in an oil depot. Notice that the left y-axis shows the values for benzyl alcohol and hippuric acid and the right y-axis presents the values for benzoic acid. Upper figure (A) presents the entire study period (840 hours), while the first 52 hours after injection are illustrated at the bottom of this figure (B).

BOH levels appear directly in serum after subcutaneous injection, which shows that BOH is released immediately from the oil depot (Figure 2.3A). In general, the drug serum level is a net result of drug released from the oil depot and the drug elimination out of the central compartment. Here, the BOH serum concentrations decreased during the first 52 hours after

injection, except for the period of 12-24 hour after injection (Figure 2.3B). In this period a remarkable increase in BOH concentration was observed. To explain this phenomenon, one can speculate that the depot might exhibit a temporary higher release or that there is a temporary change in clearance. It should be noted that all volunteers received the injection between nine and eleven o'clock in the morning. It is likely that the volunteers slept in the period 12-24 hours after injection. It can be speculated that the mass transfer of the component out of the oil depot changes because of a certain body position, local pressure or even an increased body temperature. The latter, however, is not very likely; *Gillberg and Akerstedt* reported that body temperature does not increase during sleep, thus this parameter would not affect the mass flux of BOH in this study (69). A change in the elimination may occur, but there is no evidence for a changed enzyme activity of BOH oxidation during the night. Finally, enterohepatic circulation of BOH can be excluded, because its molecular weight is much lower than the threshold value of 500 for the biliary route of excretion (70).

Figure 2.3 shows that serum levels of BA increase when serum levels of BOH decline. This is what can be expected from the metabolism of benzyl alcohol. After conjugation with glycine, BA forms HA (71). HA is excreted from the body via the renal route (71,72). Although the reaction rates are unknown, it is possible that the conversion of BA to HA occurs faster than the oxidation process of BOH to BA. This could explain the more than 10-fold molar concentration differences between BOH and BA. AUCs<sub>0-840h</sub> of BOH were similar to those of BA with respective values of  $397.3 \pm 44.9$  nmol/mL\*h and  $417.4 \pm 63.2$  nmol/mL\*h. This indicates that all BOH was metabolized to BA and that apparently there is no other source of BA than the BOH.

The serum level of HA was 5.8 nmol/mL immediately after injection (Figure 2.3). As described above, HA is formed in the liver by conjugation of BA with a glycine molecule. Yet, no BA was determined at  $t = 0$ , implying this reaction has not taken place. Therefore, it is obvious that HA is present in the body as a metabolite of other (body/food) substances, as has been argued earlier (73-75). In contrast to BA, there is another source for HA other than BOH.

The major goal of the present study was to determine the pharmacokinetics of BOH from the oil depot. As shown in Figure 2.3, this excipient can only be measured in serum during only a few days. This means that the formulation that contains 10% of BOH at the moment of injection changes dramatically within this period. BOH acts as a co-solvent in oil, which means that the solubility of ingredients is positively affected by its presence. When the BOH is fully depleted, the partition coefficient of these ingredients between the oil formulation and the body fluids will be changed, which means that the driving force for diffusion (i.e. the rate of release) has altered. Whether this is directly related with a change in drug absorbance (i.e. the appearance in the central circulation) is not fully clear at this point because there are more variables of relevance in determining the drug absorption rate from the depot. The transfer

through the body tissue may also have a significant influence on the absorbance of the active substances. For this reason, it is of interest to monitor the absorption of active ingredients in the very first days of *in vivo* release. This is reported in a separate paper (*Chapter 3*).

#### Influence of other factors on serum levels on components of interest

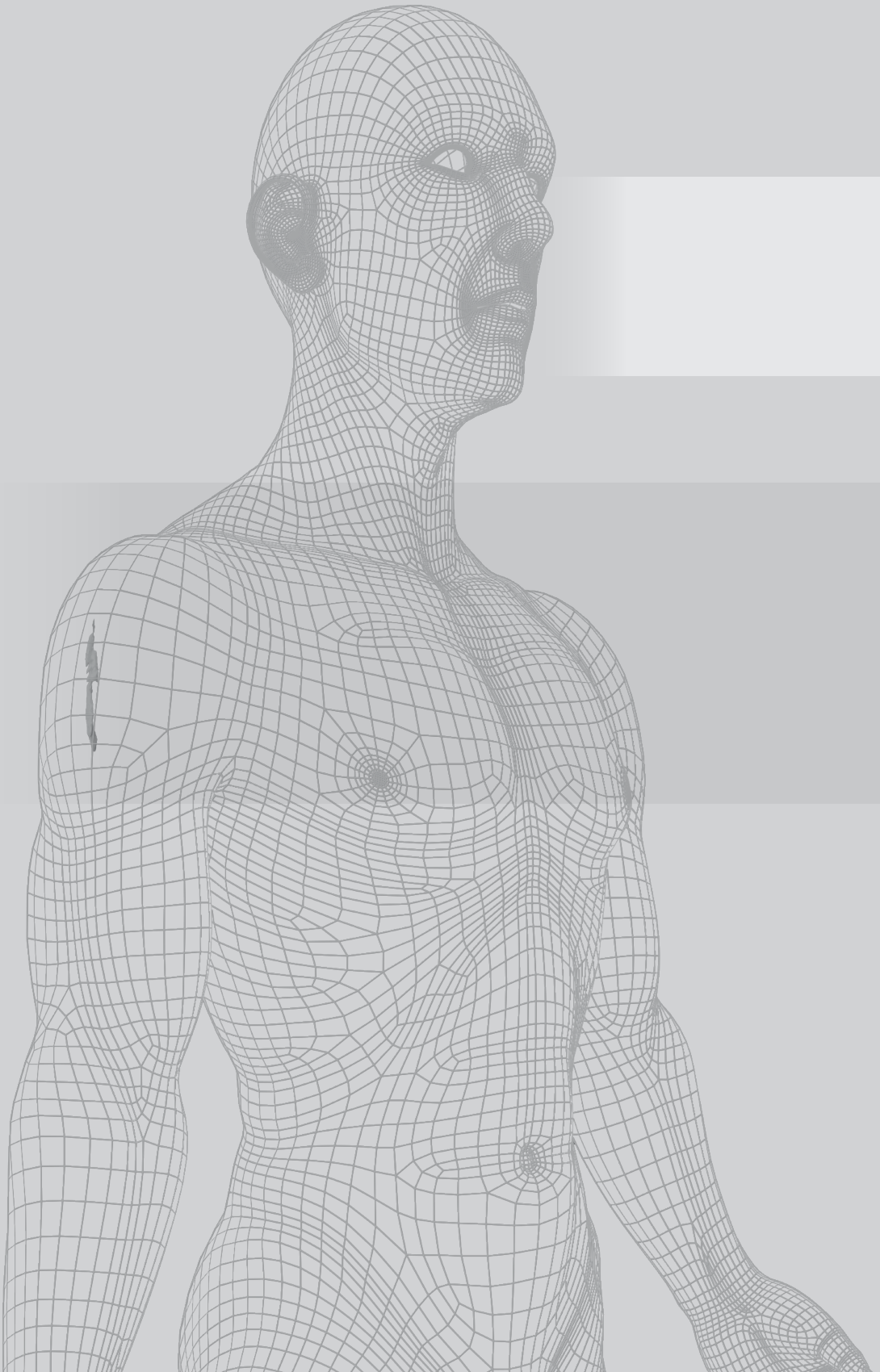
As mentioned previously, BOH and BA are processed as a preservative in several pharmaceutical drug products. BOH is a naturally occurring compound in food, for example in some fruits (< 5 mg/kg), black tea (1-15 mg/kg) and green tea (1-30 mg/kg) (76). As reported by the Scientific Commission of the European Union, the maximally allowed quantity of BOH in end products (foods and beverages) is 300 mg/kg (76). Although the quantities that can be consumed can be relatively high, these were apparently not taken by the volunteers as levels of BOH were below LoQ before depot injection as well as 52 hours after injection.

Serum levels of BA and HA may emerge from other sources. However, because BOH and BA levels correspond with each other and their AUC's are comparable, it is likely that the measured BA is mainly originated from BOH released from the depot.

#### CONCLUSIONS

This article reports the development of an assay for simultaneous determination of benzyl alcohol, benzoic acid and hippuric acid in human serum by HPLC. The assay is tested and validated conform the latest ICH Q2(R1) guideline and EMA Guideline for bioanalytical method validations. It appears to be accurate, selective, sensitive and reproducible for benzyl alcohol, benzoic acid and hippuric acid in human serum. The sample pre-treatment is simple to perform, because no pre-concentration, derivatization or extraction procedures are required. In addition, it has a lower LoQ compared to published methods using LC-MS/MS.

The newly developed method was applied to determine the pharmacokinetics of benzyl alcohol released from a subcutaneously injected oil depot, which contained 10% benzyl alcohol, nandrolone decanoate and cholecalciferol. The pharmacokinetic profile revealed that all benzyl alcohol was released from the depot within 52 hours after injection. This means that the release of the (active) substances from the oil depot may be affected in this period and therefore also the absorption *in vivo*. Interestingly, two peak levels of benzyl alcohol were determined in all volunteers. Further studies are needed to determine the cause of this phenomenon. A raise in benzoic acid level is observed simultaneously with the decrease in benzyl alcohol level, which can be explained by the mechanism of metabolism.



## Chapter 3

# Fundamental understanding of drug absorption from a parenteral oil depot

R.W. Kalicharan

P. Schot

H. Vromans

*European Journal of Pharmaceutical Sciences* 83 (2016) 19–27

### ABSTRACT

Oil depots are parenteral drug formulations meant for sustained release of lipophilic compounds. Until now, a comprehensive understanding of the mechanism of drug absorption from oil depots is lacking. The aim of this paper was to fill this gap. A clinical study with healthy volunteers was conducted. An oil depot with nandrolone decanoate and benzyl alcohol was subcutaneously administered in the upper arm of female volunteers. Pharmacokinetic profiles of both substances were related to each other and to literature data. Benzyl alcohol absorbs much more rapidly than nandrolone. In detail, it appears that benzyl alcohol enters the central compartment directly, while nandrolone decanoate is recovered in serum after a lag time. This lag time is also seen in literature data, although not reported explicitly. The absorption of nandrolone is enhanced by the presence of benzyl alcohol. This is most likely an effect of altered oil viscosity and partition coefficient between the oil and aqueous phase. The absorption rate constant of compounds is found to be related to the logP of the solubilized prodrug. The absorption rate is however not only determined by the physico-chemical properties of the formulation but also by the tissue properties. Here, it is argued that lymphatic flow must be considered as a relevant parameter.

## INTRODUCTION

Oily solutions of lipophilic compounds are widely used as a sustained release formulation. Although this pharmaceutical approach has been applied for several decades already, relatively little research has been published on the fundamental parameters that determine the absorption characteristics.

Generally, the formulation of an oil depot contains arachis or sesame oil as well as an amount of benzyl alcohol (BOH) which increases the solubility of the (pro)drug in the oil. In addition to these excipients, the formulation contains the active compound, most often as the esterified substance. Theoretically, there are a number of factors that determine drug absorption from a parenteral oil depot:

1. The drug dissolved in the oil is released as a result of the concentration gradient. Relevant parameters are a) the concentration in the oil, b) the thickness of the diffusion layer as well as the diffusion coefficient in the oil, c) the surface area of the depot, d) the partition coefficient ( $P$ ) between oil and tissue fluid and finally e) the thickness of the diffusion layer in the aqueous phase as well as the diffusivity in this compartment. Basically, this represents the rate at which the drug is transported through the tissue (29,30,40,42,44,47). A simplification of the real *in vivo* situation is depicted in Figure 3.1. The oil liquid is not injected directly in the blood stream, while yet the absorption is normally measured in this central compartment ( $C_{serum}$ ). Therefore, a membrane should be included in this model representing the tissue which is situated in between the oil and the central circulation.

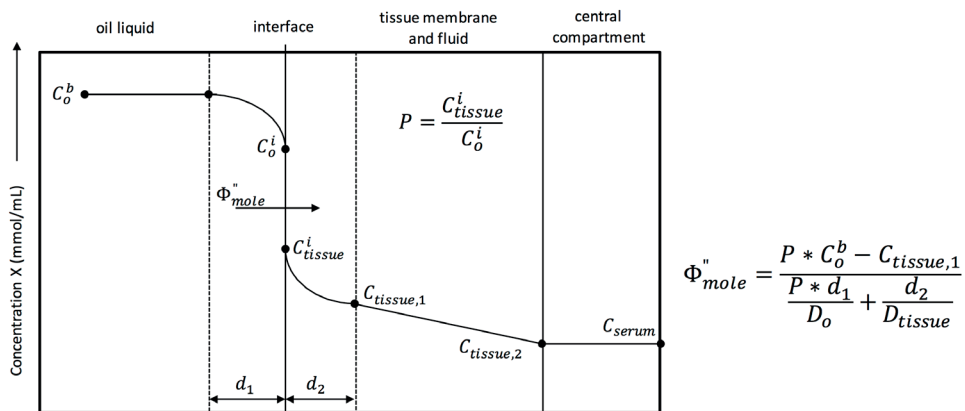


Figure 3.1 Schematic overview of the *in vivo* situation (left). Equation on the right presents the parameters which contribute to the mole flux ( $\Phi^m$ ). Abbreviations: bulk concentration (pro)drug in oil ( $C_o^b$ ), at oil interface ( $C_o^i$ ), at tissue interface ( $C_{tissue}^i$ ), in tissue beginning ( $C_{tissue,1}$ ), before entering central compartment ( $C_{tissue,2}$ ) and in serum ( $C_{serum}$ );  $d$  = diffusion layer in oil ( $d_1$ ) and tissue fluid ( $d_2$ );  $P$  = partition coefficient;  $D$  = diffusion coefficient in oil ( $D_o$ ) and in tissue fluid ( $D_{tissue}$ ).

2. BOH exhibits not only a significant solubility in the oil phase, but does also dissolve in the aqueous phase. Consequently, it will also be released out of the depot. Because of the different physico-chemical properties, it can be expected that BOH shows a completely different release profile than the prodrug. BOH in turn has a significant influence on the solubility of the active compound in both the oil and the aqueous phase (26). Therefore, it is obvious that the partition coefficient is not a constant value during the release from the depot. This is presented as the partition coefficient between the concentrations at the interface in Figure 3.1.
3. In most cases a lipophilic ester is used as a prodrug. After release out of the oil, this ester has to be hydrolysed to the parent drug. The prodrug exhibits a significantly higher logP than the parent compound. As a consequence, the transport through tissue can be considerably different; Highly lipophilic drugs show both retardation by tissue absorption effects and lymphatic transport whereas less lipophilic compounds diffuse directly to the central circulation. Hence, the speed and the place at which (enzymatic) hydrolysis occurs may have impact on the rate of absorption.

Other factors that may also contribute to the absorption rate are: injection depth (77), site of injection (78,79), lymphatic absorption (42), massage before injection (79) and muscle activity (79). Although these suggested and obvious factors could lead to a complete understanding of drug absorption from oil depots, no studies have been published on this topic so far. This article makes a distinction between *release* and *absorption kinetics*: substance *release* from the depot can be translated from the mass flux from oil towards the aqueous phase, while *absorption* represents the entire process in which the substance enters in de central compartment. Hence, absorption includes the release out of the oil and the subsequent transfer through the tissue to the blood stream.

The current study started with a clinical trial in which an oil depot containing nandrolone decanoate was used. Frequent sampling of volunteers enabled us to monitor the absorption phase in detail. The aim of this paper is to create further understanding of the fundamental mechanisms that determine the drug absorption from a parenteral oil depot. Second, this paper elucidates the effect of BOH on nandrolone absorption. The observations are compared with results reported in literature and put into perspective with the pharmacokinetic profile of BOH that has been published separately in *Chapter 2*.

## MATERIALS AND METHODS

### Experimental design

Drug product was manufactured under current Good Manufacturing Practice conditions in the hospital pharmacy at the University Medical Center Utrecht, the Netherlands. Each 1.0 mL of the solution contained 117  $\mu\text{mol}$  nandrolone decanoate (ND), 28,000 IU cholecalciferol,

926  $\mu\text{mol}$  (10% (m/v)) BOH and ad 1.0 mL sesame oil. In this study, 0.5 mL of the solution was subcutaneously (s.c.) injected in the upper arm. Fourteen female volunteers participated in this study. Full informed written consent was obtained from the volunteers, conform to the Declaration of Helsinki. Inclusion criteria were: good physically and mentally healthy Caucasian females with an age between 65-80 years old and a body mass index (BMI) between 20-30  $\text{kg}/\text{m}^2$ . Volunteers were excluded when using any drug, food or beverages that influence the metabolism of ND from 2 weeks or 5 half-lives of the medication (whichever is longer) prior to drug administration. Smoking was allowed, provided no more than 4 cigarettes or equivalents were used per day.

A validated LC-MS/MS bioassay was used to determine serum nandrolone concentrations (LoQ = 0.12  $\text{pmol}/\text{mL}$ ). Blood samples were taken directly after injection (0 hour) and 2, 4, 8, 12, 15, 22, 24, 36, 48, 72, 96, 168, 216, 264, 360, 456, 552, 648 and 840 hour after injection.

### Pharmacokinetic analysis

Pharmacokinetic parameters were examined using Microsoft Excel 2010. The following parameters were determined: maximum serum concentration ( $C_{max}$ ) and time to reach this concentration ( $T_{max}$ ); the area under the serum concentration-time curve (AUC) was calculated using the linear trapezoidal rule. All data are expressed as mean  $\pm$  standard error of the mean (SEM).

### Absorption analysis

Drug absorption from the depot was estimated by converting serum levels to total amount of absorbed drug. All serum levels were converted to molar concentrations. The amount of absorption was calculated using the Wagner-Nelson method as described previously (80). Analysis was performed by the following equation:

$$\frac{A}{V_d} = C_{serum} + k_e * \int_0^t C_{serum} * dt \quad [\text{Equation 3.1}]$$

wherein the maximum (cumulative) amount absorbed into the central compartment equals cumulative amount released by the depot, which was calculated according to

$$\frac{A_{max}}{V_d} = k_e * AUC_{0-\infty} \quad [\text{Equation 3.2}]$$

$$AUC_{0-\infty} = \left[ \int_0^t C_{serum} * dt \right] + \frac{C_{serum}^{final}}{\lambda_z} \quad [\text{Equation 3.3}]$$

where  $A$  and  $A_{max}$  are the amount absorbed at moment  $t$  and maximal amount absorbed, respectively;  $C_{serum}$  and  $C_{serum}^{(final)}$  are the serum concentration at time  $t$  and the last measured

plasma concentration, respectively;  $\lambda_z$  is the apparent elimination rate constant due to flip-flop pharmacokinetics (see below);  $V_d$  is the distribution volume and  $k_e$  is the elimination rate constant after intravenous injection. Values for  $k_e$ 's in this study were for nandrolone  $2.75 \text{ h}^{-1}$  (30), haloperidol  $0.03 \text{ h}^{-1}$  (81) and testosterone  $0.80 \text{ h}^{-1}$  (82).

Absorption rate constant ( $k_a$ ) was determined by calculating the elimination rate constant ( $\lambda_z$ ) using the least square method. *Wijnand et al.* pointed out that drug release from sustained oil depots shows flip-flop pharmacokinetics (32). As a result, during flip-flop pharmacokinetics the rate of absorption equals the decline of the terminal slope in the serum concentrations plot (83).

Recovery was calculated by dividing  $A_{max}$  ( $\mu\text{mol}$ ) by total injected dose ( $\mu\text{mol}$ ). It should be noted that all determined concentrations represent the levels of the parent compound. The depot contained a prodrug, i.e. the decanoate ester of the parent compound nandrolone.

### Viscosity measurement

The viscosities of the oil solutions were determined in an AR-G2 rheometer (TA Instruments, New Castle, USA) at  $23^\circ\text{C}$ . The shear rate was  $100 \text{ s}^{-1}$  and rotating frequency of  $2.0 \text{ rad/s}$ . Sesame oil mixed with different concentrations of BOH were measured in three-fold.

### Inclusion criteria of literature

A literature search was conducted within the PubMed/Medline database from January 1965 to May 2015. Mesh search query: (“Injections, Intramuscular”[Mesh]) OR “Injections, Subcutaneous”[Mesh]) AND “Delayed-Action Preparations”[Mesh] AND “Pharmacokinetics”[Mesh]). The following filters were applied: “Clinical trial”, “Review”, “Humans”. Articles were eligible for inclusion if they met: 1) The used injections had to be oil depots; and 2) Pharmacokinetic intravenous data of the APIs were known, otherwise data analysis could not be conducted.

## RESULTS AND DISCUSSION

The baseline characteristics of the fourteen females were (mean  $\pm$  standard deviation): Age =  $70.7 \pm 4.3$  year, length =  $1.65 \pm 0.06$  meter, weight =  $68.0 \pm 9.0$  kilogram and BMI =  $24.8 \pm 2.3 \text{ kg/m}^2$ . All subjects were included in the following analysis. No adverse reactions were reported during or after the study.

## Pharmacokinetic profile of nandrolone

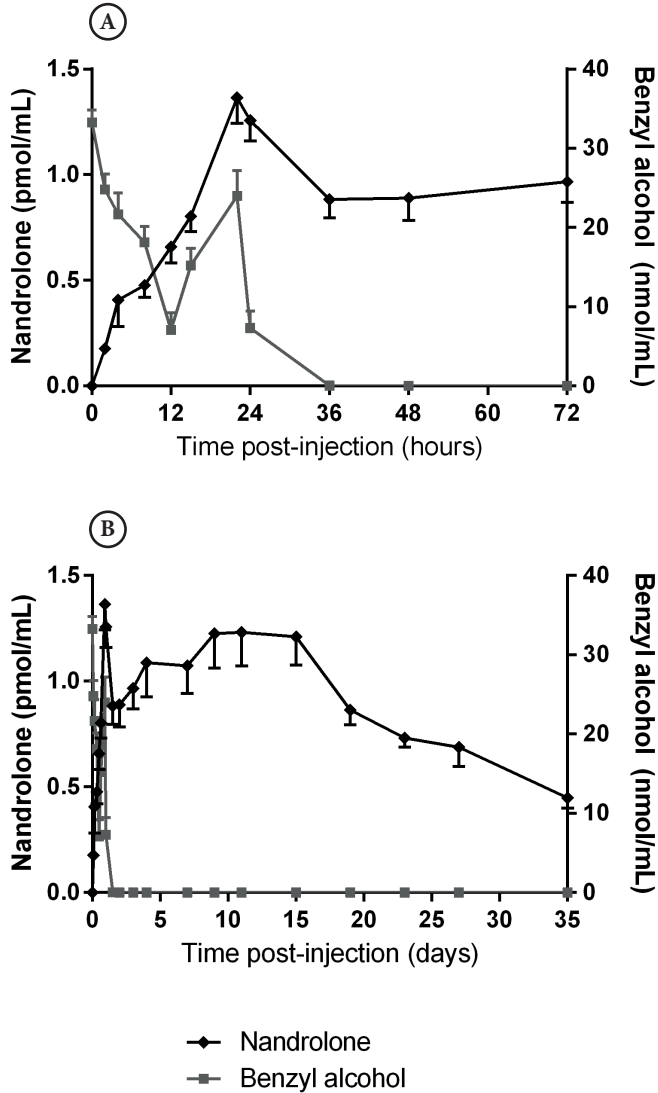


Figure 3.2: Nandrolone (◆) serum levels after subcutaneous injection of 58.3  $\mu\text{mol}$  of nandrolone decanoate ( $n=14$ ). Benzyl alcohol (■) serum levels were determined in another study (*Chapter 2*). Results expressed as mean and standard error of the mean, unless standard error is smaller than the symbol.

Table 3.1: Summary of pharmacokinetic parameters for nandrolone in serum (n=14).

Variable	(mean $\pm$ SEM)
<b><math>C_{max}</math> (pmol/mL)</b>	
First peak	1.42 $\pm$ 0.11
Second peak	1.50 $\pm$ 0.16
<b><math>T_{max}</math> (hours)</b>	
First peak	24.4 $\pm$ 1.8
Second peak	274.3 $\pm$ 38.0
<b>AUC (pmol/mL*h)</b>	
0-840 h	726.5 $\pm$ 52.4
0- $\infty$	1035.2 $\pm$ 74.7
<b>Amount absorbed (<math>\mu</math>mol)</b>	
0-840 h	22.9 $\pm$ 1.7
0- $\infty$	32.6 $\pm$ 2.4
$k_a$ ( $h^{-1}$ )	0.0021 $\pm$ 0.0003
<b>Recovery (%)</b>	
0-840 h	39.3 $\pm$ 2.8
0- $\infty$	56.0 $\pm$ 4.0

Abbreviations:  $C_{max}$  = maximum serum concentration;  $T_{max}$  = time post-injection to reach  $C_{max}$ ; AUC = area under the serum concentration-time curve; and  $k_a$  = absorption rate constant.

The serum profile of nandrolone is presented in Figure 3.2. The pharmacokinetic parameters are summarized in Table 3.1. Remarkably, Figure 3.2 shows two distinct  $C_{max}$  values; there is a peak at 22 h while a second maximum is reached between 9-15 days post-injection. Surprisingly, literature data (Table 3.2) show these double peaks in all nandrolone oil depot studies, although it is not mentioned explicitly. In clinical papers about oil depots containing antipsychotics, the occurrence of two peaks has been noted however (84). Here, the first peak was thought to be associated to the presence of a certain quantity of parent compound, i.e. the substance without the ester moiety. In our clinical study, no additional peaks were obtained during quality control analysis of the investigational medicinal product (IMP). This indicates no significant amount of parent compound in the IMP, which may cause the first nandrolone peak. This phenomenon will be discussed further below.

Figure 3.2 also shows the serum profile of benzyl alcohol. This has been reported earlier in Chapter 2, in a paper which also reports the development of a bioassay for BOH. As can be seen, BOH shows a completely different pharmacokinetic profile compared to the nandrolone profile; BOH is present in the central circulation at the earliest moment samples were taken, i.e. only a few minutes after the moment of injection. This suggests principally different mechanisms of absorption compared to nandrolone; BOH appears to absorb fairly rapidly, whereas nandrolone exhibits a slow absorption. Another observation is that the first nandrolone peak at 22 hours post-injection coincides with a peak in BOH level, after

which both substances show a decline in serum concentration (Figure 3.2A). Furthermore, the absorption of nandrolone is slower after 36 hours post-injection compared to the period directly after injection. BOH was only recovered during the first 36 hours post-injection, which may suggest that the initially increased absorption of nandrolone is related to the quick release of BOH; the obvious explanation can be that this will lead to a decrease in concentration of the solubilizing compounds in the oil phase while it will have the reverse effect in the aqueous phase at the same time. Basically, this means that the partition coefficient between oily and aqueous phase changes during the release of BOH until there is a full depletion. In addition, also the viscosity of the oil depot changes during BOH release (Figure 3.3). As expressed by the Stokes-Einstein law, the diffusion coefficient decreases upon increasing viscosity.



Figure 3.3: Viscosity of different concentrations benzyl alcohol mixed with sesame oil. No other substances were added. Results expressed as mean and standard error of the mean ( $n=3$ ), unless standard error is smaller than the symbol.

After the depletion of BOH, nandrolone clearly absorbs more slowly, resulting in a second prolonged serum peak, representing a steady state situation. Figure 3.4A depicts the cumulative absorption profile of nandrolone. These results were obtained by converting the serum level (Figure 3.2) to the amount of absorbed nandrolone (Figure 3.4) using the Wagner-Nelson method. The cumulative release of BOH is also given in Figure 3.4. This is in this case expressed as area under the curve instead of the percentage absorbed, because the Wagner-Nelson method could not be applied; the kinetic parameters *elimination constant* and the *distribution volume* are unknown for BOH. After 52 hours post-injection, no BOH was detected in serum anymore, which implies that the depot at this point is depleted of BOH. Therefore, we assume a nearly 100% recovery of BOH from the depot.

Table 3.2: Injections were administered in several muscles. Different vehicles (oil types and percentage benzyl alcohol) and chemical parameters (partition coefficient and molar weight) are shown of prodrug and corresponding parent compound.

Reference	Depot		Injection volume (mL)	Injection site	Type of oil	logP <sup>a,b</sup>			Molecular weight <sup>c</sup>			Recovery (%)	
	API	Dose (mmol)				BOH (%)	prodrug	parent	prodrug	parent	prodrug		parent
<i>Wijnand et al.</i> (32)	ND	0.23	1	Vastus lateralis	Arachis	10	7.9	2.6	428.6	274.4	2.7	0.0082	34
	ND	0.47	2	Vastus lateralis	Arachis	10	7.9	2.6	428.6	274.4	2.6	0.0055	22
<i>Minto et al.</i> (30)	NPP	0.25	4	Gluteal	Arachis	10	6.0	2.6	406.6	274.4	4.9	0.0112	45
	ND	0.23	4	Gluteal	Arachis	10	7.9	2.6	428.6	274.4	14.6	0.0056	45
ND	0.23	1	Gluteal	Arachis	10	7.9	2.6	428.6	274.4	11.4	0.0051	61	
	ND	0.23	1	Deltoid	Arachis	10	7.9	2.6	428.6	274.4	26.4	0.0036	49
<i>Bagchus et al.</i> (33)	ND	0.12	1	Gluteal	Arachis	10	7.9	2.6	428.6	274.4	10.8	0.0053	42
	ND	0.23	1	Gluteal	Arachis	10	7.9	2.6	428.6	274.4	12.0	0.0058	43
<i>Van Weringh et al.</i> (50)	ND	0.35	1	Gluteal	Arachis	10	7.9	2.6	428.6	274.4	15.9	0.0051	41
	HD	0.38	2	Gluteal	Sesame	1.5	6.9	3.2	530.1	375.9	29.8	0.0107	25
<i>Morgenthaler et al.</i> (13)	HD	0.57	3	Gluteal	Sesame	1.5	6.9	3.2	530.1	375.9	27.3	0.0122	29
	TD	1.69	1	Gluteal	Castor	0	8.6	3.3	442.6	288.4	24.2	0.0022	42

<sup>a</sup> data obtained from Clarke's Analysis of Drugs and Poisons (85)

<sup>b</sup> data obtained from ChemSpider (86)

<sup>c</sup> data obtained from The Merck Index, 14th ed (87)

Abbreviations: API = active pharmaceutical ingredient; ND = nandrolone decanoate; NPP = nandrolone phenyl propionate; HD = haloperidol decanoate; TD = testosterone decanoate; k<sub>a</sub> = absorption rate constant and BOH = benzyl alcohol

### Lag time

As can be seen in Figure 3.4B, the absorption phase for BOH is quick and complete. In contrast, the absorption of nandrolone is principally different; the exposure is not instantaneous. There appears to be a *lag time* before nandrolone enters the central circulation. From a physical perspective, it is obvious that the compound release starts immediately after injection. This has been confirmed in *in vitro* studies (35,36). It must be noted that these *in vitro* models did not include a membrane. BOH seems to behave according to these *in vitro* models, but knowing that there is no direct contact between blood and oil, it should be concluded that the lag time for BOH is extremely short. Hence, the transport through the tissue layer occurs very rapidly. The transport of ND from the oil to the central circulation appears to be slower however. Obviously, there is a retarding factor in the tissue and therefore it is clear that this lag time period reflects the mechanism of transport in the tissue. There were no relationships found between the volunteers' baseline characteristics (e.g. BMI, weight, length or age) and the lag time. In this study, nandrolone injected subcutaneously as decanoate, exhibits a lag time of about eight hours (Figure 3.4B).

Literature demonstrates that this phenomenon is not unique to a specific oil depot. A lag time is seen in all parenteral oil depot formulations (Table 3.2). This is not a constant interval however.

Several endogenous factors may contribute to this delayed absorption: (temporary) cell membrane adsorption, cell absorption, esterase activity, interstitial and/or lymph flow and/or alternative pathways. After injection of the depot into the tissue the prodrug starts to release and enters the interstitial space, in which the depot is injected. These prodrugs, being ester compounds, can spontaneously be hydrolysed with water or actively be hydrolysed by esterases. *Van der Vies et al.* published a half-life hydrolysis of 4 minutes for  $2.5 \times 10^{-3} \mu\text{mol/mL}$  ( $1 \mu\text{g/mL}$ ) nandrolone phenyl propionate in rat plasma (88). Although no hydrolysis data on nandrolone decanoate in human fluids have been published yet, *Wijnand et al.* assumed that the time needed for hydrolysis of  $2.3 \times 10^{-5} \mu\text{mol/mL}$  ( $= 0.01 \mu\text{g/mL}$ ) nandrolone decanoate in serum is presumably below one hour (32). They based their assumptions on data published by *Van der Vies et al.* (88). In the present study, released nandrolone decanoate will then be hydrolysed within one hour in plasma, because all nandrolone serum concentrations were below  $1.0 \times 10^{-5} \mu\text{mol/mL}$  (Figure 3.2B). Yet a delayed absorption is seen, indicating that ester hydrolysis is not occurring in the interstitial fluid, but probably only in the central circulation. When hydrolysis is not immediate, the prodrug may flow towards lymph vessels, whether or not linked to proteins such as globulins. Interstitial space consists of reticular and collagenous fibres (89), to which molecules could be adsorbed. The absorption rate into the lymph depends on the rate of diffusion through the interstitium (90) and pressure gradients (91). It has already been suggested by *Zuidema* and colleagues that the interstitial space can be compared to reversed-phase chromatography (47): the interstitial fluid acts as the mobile phase, whereas the cells and fibres represent the stationary phase. The lag time is probably a

combination of mentioned factors above.

The nearly immediate absorption of BOH suggests a fast pathway to the central compartment (Figure 3.1). Oil depots injected into muscle or subcutaneous tissues are surrounded by (micro) blood vessels. It is well known that blood vessels are natural barriers, because they are constructed out of a concatenation of endothelial cells. *Porter and Charman* showed that small molecules ( $< 2,000$  g/mole molecular weight) with a logP (octanol/water) under five enter the systemic circulation directly after oral ingestion (92). These substances can pass capillary walls which result in instantaneous absorption into the systemic circulation (93). Analogous to oral absorption, parent compounds can immediately enter the bloodstream when they meet the two chemical properties molecular weight and logP.

It is interesting to realize that drug absorption from an oil depot is not well described by a simple two phase mass transfer model. There is obviously a considerable resistance towards mass transfer in the tissue surrounding the depot, which is given in Figure 3.1 as a tissue membrane. The presence of this membrane fits with the finding of a substantial lag time for nandrolone. The difficulty with this theoretical presentation is that this membrane represents body tissue where not only diffusion takes place, but where also lymphatic transport and hydrolysis may play a role.

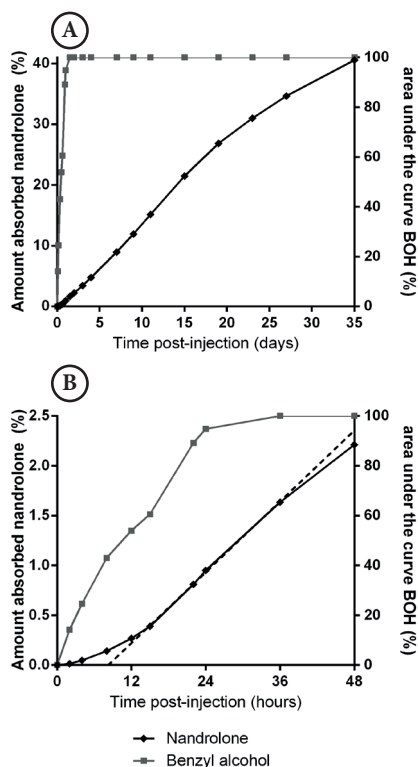


Figure 3.4: Cumulative amount of absorbed nandrolone (◆) is represented as percentage of the recovery in serum at the left y-axis. The right y-axis shows the cumulative AUC of BOH (■) as percentage of total AUC. (B) The intercept of the dashed line with the x-axis shows the lag time of nandrolone.

## Absorption

After the lag time period, a steady absorption is established (Figure 3.4), resulting in a plateau as seen in Figure 3.2B. In general, the obvious parameters that have influence on drug release can be understood from Figure 3.1; the higher the concentration in the depot, the higher the driving force for release (33). The same holds for the surface area. *Minto et al.* (30) have shown that a simultaneous increase in volume and proportional decrease in concentration does not change the absorption significantly (Table 3.2). It has been postulated (38,40) that the digestion of oil would play a role in the rate at which compounds are absorbed, but that is not confirmed by our data.

After approximately two weeks, the plasma profile declines, which in fact reflects the depletion of the depot; the concentration gradient gradually decreases because of the amount of drug that already has been released. This is generally referred to as ‘flip-flop’ pharmacokinetics; what might be perceived as the elimination rate constant basically equals the absorption rate constant ( $k_a$ ) from the formulation (32,83). In the case of the oil depots studied, a higher  $k_a$  reflects a faster depletion of the depot, which actually means that the resistance towards mass transfer in the surrounding tissue is relatively low. As discussed above, this mass transfer is determined by e.g. the diffusion through the interstitial fluid and the flow of the lymphatic system into the circulation.

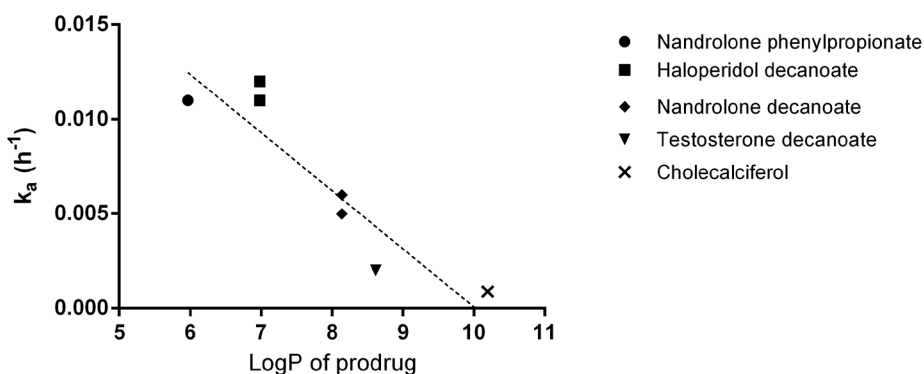


Figure 3.5: Absorption rate constant ( $k_a$ ) of the parent compound as a function of the prodrug partition coefficient. Figure includes only depots administered in the gluteal muscle. The dashed line represents the ‘best-fitted’ relation of prodrug logP with  $k_a$ . Here, logP is the theoretical distribution between octanol and water. See Table 3.2 for raw data and references (cholecalciferol (94)).

Figure 3.5 shows that the absorption of ingredients from depots injected in the gluteal muscle is determined by the partition coefficient of the prodrugs. The role of logP is twofold; it determines the concentration  $C_{tissue}^i$ , which means that a high logP will yield a low  $C_{tissue}^i$  and subsequently a low driving force for mass transfer in the aqueous phase (Figure 3.1).

At the same time, a high logP results in increased absorptive and adsorptive interactions with tissue components by which the permeability decreases. Similar relationships have been published for intramuscularly injected beta blockers (aqueous solutions) in pigs (44) where the absorption rate appeared also to be affected by the lipophilicity. Remarkably, there is no such relationship as depicted in Figure 3.5 for the parent compound, which seems to confirm our conclusion that it is the prodrug that is transported through the tissue and that conversion to the parent compound takes place in the central compartment.

Absorption rate constants of different compounds were compared after administration in the gluteal muscle (Figure 3.5). In contrast, Figure 3.6 shows the normalised profiles of equal formulations injected in different muscles: As can be seen, the site of injection appears to have a considerable influence on the absorption. For comparison, also the subcutaneous injection of the present study is given. It must be noted however that used oil as well as volume of injection were different. Our own experiments (based on (95), procedure 2) showed that the type of oil does not affect the partition coefficient of nandrolone decanoate:  $\log P(\text{sesame oil}:\text{serum}) = 2.36$  and  $\log P(\text{arachis oil}:\text{serum}) = 2.44$  (both mixed with 10% BOH), which emphasizes the low absorption from the subcutaneous injection.

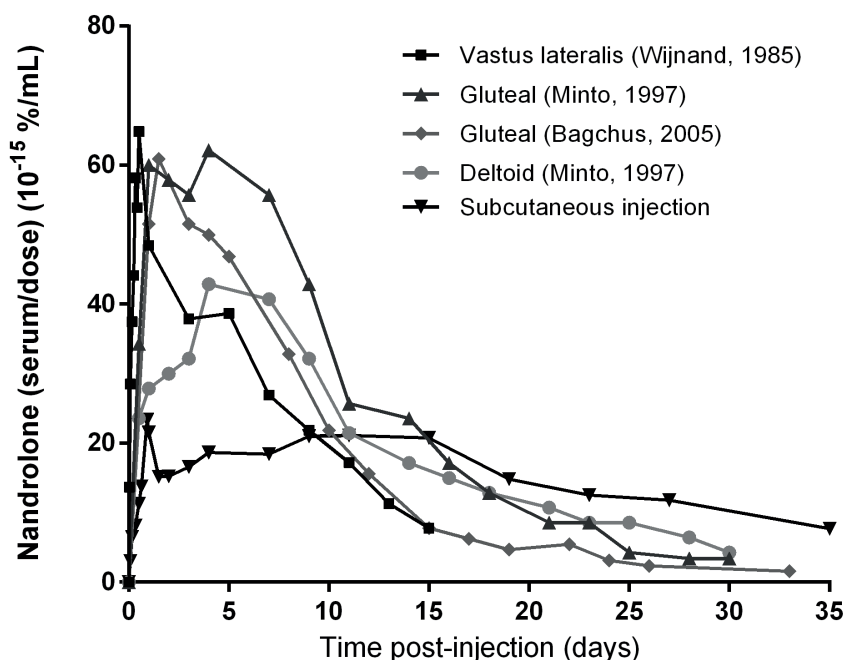


Figure 3.6: All i.m. administered injections (deltoid (●), gluteal (◆ and ▲), vastus lateralis (■)) were 1 mL at a concentration of 233  $\mu\text{mol/mL}$  nandrolone decanoate. The 0.5 mL s.c. injection (▼) had a concentration of 117  $\mu\text{mol/mL}$  nandrolone decanoate. Y-axis shows the concentration in percentage of serum level divided by amount administered. See Table 3.2 for raw data and references.

The i.m. depot formulations were equal, i.e. they contained the same compound at the same concentration in the same volume. This limits the amount of explanations for these differences. First, it can be speculated that the surface areas of the depots were different in the three muscles because of differences in spreading. The larger the surface, the larger the total mass flux ( $\Phi$ ). Unfortunately, the surface areas of injected oil depots are unknown. This has been a reason for us to start a study to visualise the fate of oil when injected in muscles, results of which will be reported later. The role of surface area may also be relevant for the s.c. injection; the absorption was significantly lower, which can be attributed to the smaller surface area of the depot as it is likely that the shear forces in subcutaneous tissue are substantially lower than those in muscles. In addition, the way the compound is being transported through the different tissues may be different. In this respect, the lymphatic flow rate may therefore be interesting to study as well.

Figure 3.6 shows that absorption from the deltoid muscle is much lower compared to that from gluteal and vastus lateralis muscles. This is counterintuitive, since blood flow in deltoid muscle is higher than the flow in gluteal and vastus lateralis (96). However, as has been argued, it is not the blood perfusion but the lymphatic drainage that determines drug absorption in this case. Table 3.2 shows that the ND absorption rate constant from the deltoid muscle is lower compared to the gluteal and vastus lateralis muscle. There appears to be a relationship between the absorption rate constant and the lag time within one muscle group (Figure 3.7). The reasonable explanation for this must be that both parameters may be a result of the same variable. For example, when the differences in release are due to different surface areas, the lag time would be the same, since the way the compound is transferred to the blood stream would not be changed. Therefore, it is more likely that the differences in transport through tissue, such as lymphatic transport may determine the absorption phase. This would also explain the considerably deviating results of the s.c. injection; the low release rate may be attributed to a low surface area, whereas the relatively short lag time may be a result of relatively high lymphatic flow or shorter lymph vessel. Unfortunately, little is known about the human lymphatic flow rate in the studied muscles, although one article reported a lymph flow rate of 0.25-0.41 mL/h in the superficial lymph vessel of the leg (97). In rats and rabbits however, skin lymph flow (measured as albumin clearance rate) is shown to be higher compared to the muscle lymph flow (98,99). Of course, this does not necessarily mean that this also applies to the human situation.

Another approach to verify the suggested mechanism would be to change the lymphatic flow. Two studies report a raised lymph flow (measured as albumin clearance rate) in the lymphatic vessels of the vastus lateralis muscle during exercise (100) or during massage (rabbits) (101). However, Soni et al. (79) described no increased absorption of fluphenazine after exercise or massage from a fluphenazine decanoate sesame oil depot, injected in the thigh and buttock

skeletal muscle. Clearly, there is no unambiguous explanation for the observed differences at this moment. Future studies on this subject should provide clarity.

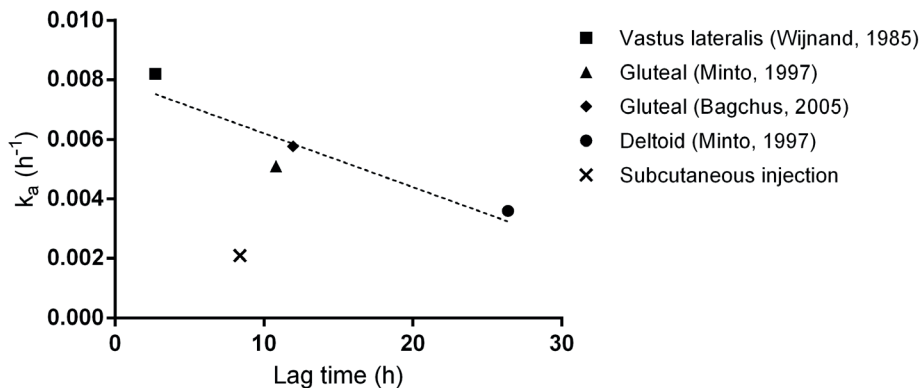


Figure 3.7: Plot of absorption rate constant ( $k_a$ ) and lag time of nandrolone administered at different injection sites: deltoid (●), gluteal (◆ and ▲), vastus lateralis (■) muscle and subcutaneous tissue (x). All i.m. injections were 1 mL at a concentration of 233  $\mu\text{mol}/\text{mL}$  nandrolone decanoate. The s.c. injection (0.5 mL) had a concentration of 117  $\mu\text{mol}/\text{mL}$  nandrolone decanoate. See Table 3.2 for raw data and references.

## CONCLUSIONS

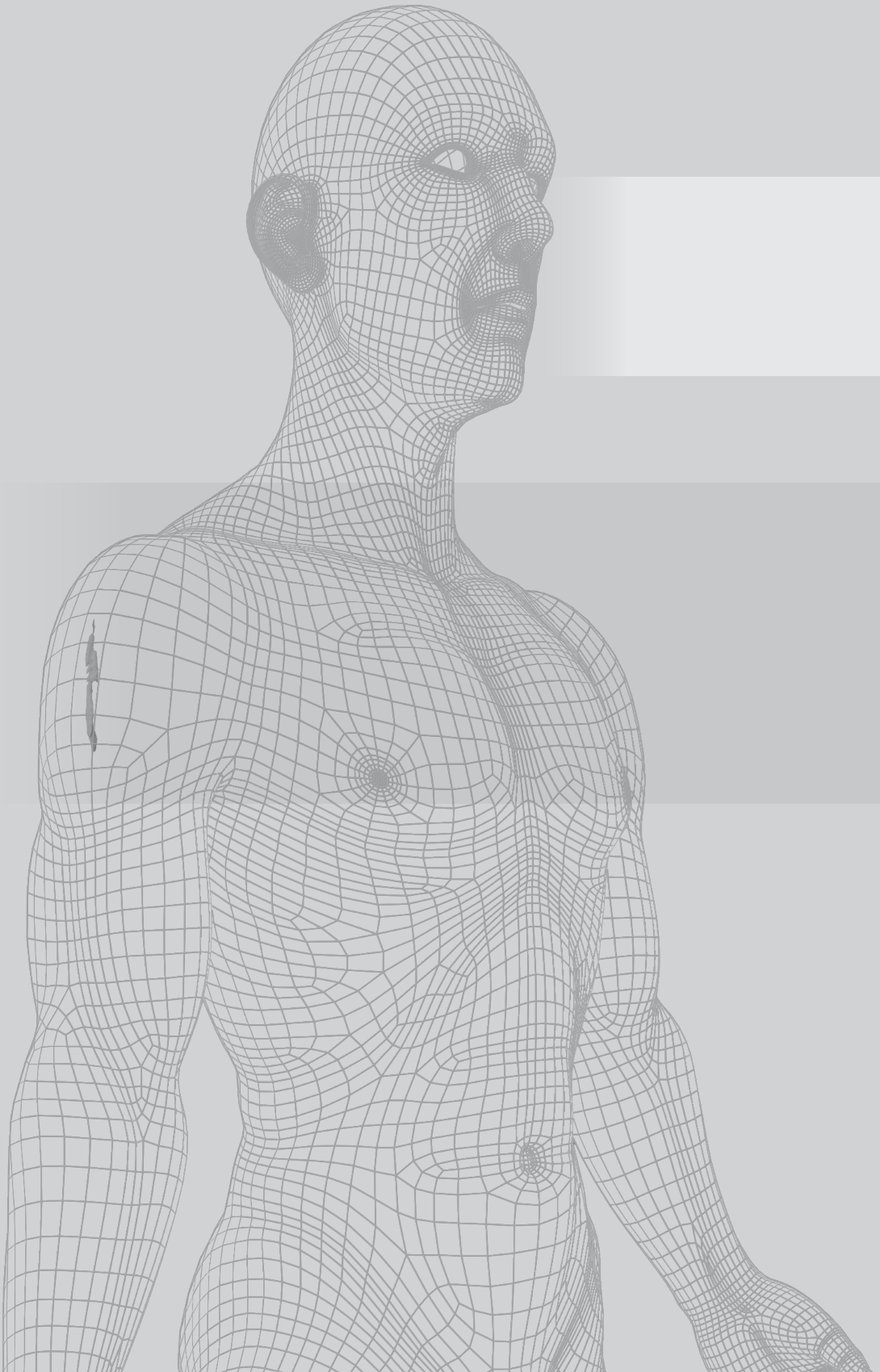
This study discusses critical parameters that determine the release and absorption mechanisms of (active) substances from oil depots. It is shown that small molecules (e.g. BOH) are directly and fully absorbed, while larger, more lipophilic substances (e.g. prodrugs) exhibit an incomplete and slow absorption pattern. A lag time is seen, which is a critical parameter for absorption into the systemic circulation. This means that the absorption of compounds from a depot is significantly affected by the mass transfer in the tissue. The more lipophilic the compound, the more this plays a role. It is suggested that concentration of the compound in the oil, the *in situ* surface area of the depot as well as the partition coefficient of the compound are the most important formulation parameters. The mass transfer is mainly determined by the lipophilicity of the compound, while also the lymphatic flow is suggested to be relevant for drug absorption. In oil depots, BOH is often used as an excipient. It appeared that the absorption of nandrolone is enhanced by the presence of benzyl alcohol in the first few days. Subsequently, upon BOH depletion, a change in absorption of nandrolone is seen. Injections of equivalent formulation in different muscles demonstrate that the mass transfer through these tissues is not the same. It is argued that this may be due to differences in lymphatic transport.

### Acknowledgements

The authors would like to thank dr. J.H. Proost and dr. M.P.H. van den Broek for their useful scientific discussions about this paper.

### Conflicts of interest

The authors declare no conflict of interest.



## Chapter 4

# Spatial distribution of oil depots monitored in human muscle using MRI

R.W. Kalicharan

P. Baron

C. Oussoren

L.W. Bartels

H. Vromans

*International Journal of Pharmaceutics* 505 (2016) 52–60

### ABSTRACT

Oil depots are parenteral drug formulations meant for sustained release of lipophilic compounds. According to mass transport models, the drug-release rate from these injections is determined by the surface area of the oil depot. Until now, the size of the surface area of injected depots has not been assessed, however. MRI provides an excellent possibility to distinguish between water and adipose tissue. The aim of this study was to investigate whether MRI can be used to determine the shape and hence the surface area of oil depots in muscle tissue. The developed MRI-scan protocol is demonstrated to be suitable for visualising oil depots. It was applied to determine the surface area of 0.5 mL oil, i.m. injected in healthy volunteers. The mean ( $\pm$ RSD) surface area and volume of the depots recovered after injection was  $755.4 \text{ mm}^2$  ( $\pm 26.5$ ) and  $520.1 \text{ mm}^3$  ( $\pm 24.6$ ). It is shown that the depot disappearance from the injection site is very variable between volunteers. It is suggested that the oil is first solubilized and subsequently distributed. In all cases, the oil was not detectable after 14 days. These factors are relevant for the understanding of the mechanism by which compounds are released out of oil depots.

## INTRODUCTION

Sustained delivery of drugs is an important method of drug administration for a number of diseases that require long-term drug treatment, such as psychiatric disorders (50,102–104) and hormone-dependent conditions (5,13,105). The most commonly used drug-delivery systems, which can release drugs for a longer period of time, are parenteral injections. In general, long-acting parenteral injections are mostly administered by the intramuscular (i.m.) and subcutaneous (s.c.) route (106).

A considerable number of long-acting i.m. injections are available on the market. Conventional sustained release injections often consist of lipophilic compounds dissolved in vegetable oils. For example, arachis oil depots containing nandrolone decanoate (30,32,33) and castor oil depots containing testosterone undecanoate (13) or estradiol valerate (107) have been marketed several decades ago and are still available on the market. Furthermore, i.m. oil depots are widely used as parenteral depot formulations of antipsychotic drugs, such as haloperidol decanoate (50). Since these long-acting formulations are administered every few weeks, they require fewer injections and result in improved drug compliance.

Although many i.m. oil depots for sustained drug delivery have been marketed, the rate and extent of drug release is often difficult to predict. The drug-release and absorption rate from the oil solution is controlled by the drug partitioning between the oil vehicle and the tissue fluid (*Chapter 3*). However, several other factors such as the injection site (30,79,108), injection volume (30), the rate of bioconversion of the prodrug into the parent drug, the absorption and distribution of the oil vehicle and the extent of spreading of the depot at the injection site might affect the overall pharmacokinetic profile of the drug (38,48). Most studies focus on the pharmacokinetics of the drug rather than on the fate of the oil depot formulation (13,32,33,50,79,109). Thus far, only few researchers have reported on the rate and extent of disappearance of the injected formulation. In 2001 *Larsen et al.* reported a disappearance half-life of 21.4 days of an iodine-125 labelled oil depot after i.m. injection in the lower back of pigs (110). Radioactivity was monitored by placing the scintillator probe directly on the skin surface. To date, no studies on the fate of oil depots in humans have been published yet.

Drug-release rate from depot injections are estimated according to mass transport models. A parameter for this release rate is the surface area of the oil depot (111). These mass transport models are often based on the assumption that the injected depots are spherically shaped. However, until now, the shape, and therefore the associated surface area, of injected depots had not been known. The surface area is the interface between a hydrophilic and lipophilic phase. In the case of an i.m. oil depot, the interface is formed by the muscle interstitial fluid and the oil formulation, respectively. Since the size of the surface area of the oil depot determines the extent of mass transport over the interface, this plays an important role in the rate and extent of drug release from i.m. injected oil depots (111).

Until now, there are no published methods to visualise small volumes of oil *in situ* without an invasive procedure. Hence, the value of the surface area of a perfect sphere is used for

modelling the release rate of substances. As a result, absorption profiles of active substances originating from oil depots cannot be accurately predicted and the pharmacokinetic profiles and therapeutic efficacy cannot be estimated.

In this study, magnetic resonance imaging (MRI) was used to determine the surface area of oil depots in a non-invasive manner. MRI provides excellent soft tissue contrasts and this feature can also be used to distinguish water and adipose (fat) tissue. The fat/water contrast in images can be provoked in two different ways: 1) by signal weighting on the basis of the magnetic relaxation times (T1 and T2 for the longitudinal and transverse magnetization component, respectively) of protons in the oil depot and of those in the surrounding tissue or 2) by the difference in chemical shift (112). Each nuclei has a different spin frequency and this frequency is also influenced by nearby nuclei (e.g. in a molecular environment by chemical bonding). Chemical shifts are relative frequency differences within one voxel. Initially, both imaging techniques were used in preliminary studies. Later on, the focus was shifted to the difference in chemical shift, because this technique is generally known for obtaining fat fractions (small portions of lipophilic liquid or tissue) adequately in a quantitative result. This is relevant in this current study.

The aim of this study was to investigate whether MRI can be used to determine the surface area of oil depots in muscle tissue *in situ*. Subsequently, the developed MRI-scan protocol was applied to determine the surface area of i.m. injected oil depots in human volunteers.

## MATERIAL AND METHODS

### Materials

Fresh pigskin (from epidermis till muscle tissue) was obtained from the Central Laboratory Animal Research Facility (Utrecht University, the Netherlands). Fresh chicken breast (muscle tissue) was obtained from the local butchery. Sesame oil (Ph. Eur.) and benzyl alcohol (Ph. Eur.) were purchased from Fagron BV (Capelle aan den IJssel, the Netherlands). A BD Microlance 3<sup>®</sup>, 21-gauge needle was used in all experiments.

### Oil depot injections

Oil depots contained sesame oil mixed with 10% (m/v) benzyl alcohol, unless otherwise defined. Subsequently, the mixture was sterilised by filtration (0.2  $\mu\text{m}$ , Mini Kleenpak Fluorodyne II, Pall Corporation, USA) and packed under current Good Manufacturing Practice conditions in the Clinical Pharmacy University Medical Center Utrecht, the Netherlands.

## Preliminary studies

### Magnetic resonance imaging and set-up

Preliminary MRI scans were performed on a clinical 3.0-T MRI-scanner (Achieva, Philips Healthcare, Best, the Netherlands). T1 and T2 relaxation times of the oil depot injections and tissues were determined with the following parameters: “mixed weighted 2D sequence”-sequence (echo time (TE) = 20, 40, 60 and 80 ms; repetition time (TR) = 700 and 2000 ms; field of view (FOV) = 70 x 150 x 150 mm; slice thickness = 1 mm). MR Spectra were obtained with the following parameters: “single voxel press”- sequence (TE = 31 ms; TR = 2000 ms; FOV = 10 x 10 x 10 mm; number of scans = 128).

Examined liquids were 100% sesame oil and sesame oil mixed with 10% (m/v) benzyl alcohol that were packed in plastic syringes. Syringes were fixed to pig tissue with tape and placed in a 2 litre water bath (36.4°C). The whole set-up was placed in centre of the bore of the 3.0-T MRI-scanner and a micro coil (inner diameter 47 mm), the detection device, was used as a radio frequency (RF)-receive coil.

## Oil in muscle tissue studies

### Magnetic resonance imaging

Both *ex vivo* animal and *in vivo* human imaging studies were performed on a clinical 1.5-T MRI-scanner (Achieva, Philips Healthcare, Best, the Netherlands). The parameters for the MRI-scan protocol were: “multi-echo 3D spoiled gradient-echo”-sequence (also known as the Dixon-scan), voxel size = 1 x 1 x 1 mm, TE<sub>0</sub>= 2.1 ms, ΔTE=1.6 ms, repetition time = 25 ms, flip angle = 50°. Field of View: 180 x 164 x 80; total scan duration = 4 minutes and 4 seconds. A SENSE Flex S coil, the detection device, was used as a RF-receive coil.

### Sensitivity

Sensitivity was determined by a visual observation of the oil liquid in muscle tissue after MRI scan. For this, chicken breast tissue was injected with 0.05 mL sesame oil mixed with 10% (m/v) benzyl alcohol. Subsequently, this tissue was placed in centre of the bore of the MRI scanner. Three scans were conducted to assess the visibility of oil liquid in muscle tissue.

### Accuracy and precision

Intra- and inter-scan accuracy and precision of spatial oil volume determination were performed with a fixed volume of oil. A commercial soft gel capsule (alfacalcidol 0.25 microgram, Pharmachemie B.V., Haarlem, the Netherlands) containing arachis oil was inserted into chicken breast. The real capsule volume was determined in water: the increased water volume represents the capsule volume after the capsule was immersed in water. This experiment was repeated three times, with different capsules.

Initially, the tissue was scanned with MRI for the intra-scan accuracy and precision (n=3). Subsequently, inter-scan accuracy and precision were conducted by repositioning the surface

coil slightly: after the first scan (*Position 1*), the surface coil was repositioned (*Position 2*) and the tissue was scanned again (n=3). Accuracy was determined by comparing the mean real capsule volume with the volume obtained from post processing and the obtained volumes between Position 1 and 2. A volume difference of  $\pm 3\%$  was considered as acceptable. The precision (relative standard deviation; RSD) was calculated by dividing the standard deviation (SD) by the square root of N. A RSD of  $<10\%$  was considered as acceptable.

### Subjects

Four male volunteers participated in the study (characteristics of the volunteers are summarized in Table 4.1). Ethical approval for the study was obtained from the ethical committee of the University Medical Center Utrecht, the Netherlands (protocol number: 14-401/D). Written informed consent according to the latest Declaration of Helsinki was obtained from all volunteers. Inclusion criteria were: healthy males with an age between 18-65 years old. Exclusion criteria: claustrophobic, metal clips or wires in the upper arm, implanted pacemakers, allergies to sesame oil or benzyl alcohol, other depots present in the same muscle or smoking.

Table 4.1: Volunteer baseline characteristics (n=4)

	Mean $\pm$ SD
Age (years)	37.8 $\pm$ 12.8
Length (meters)	1.8 $\pm$ 0.1
Weight (kilograms)	79.8 $\pm$ 12.6
BMI (kg/m <sup>2</sup> )	23.5 $\pm$ 2.9

### Clinical study

Before injection, a planning (blank) scan was made by positioning the surface coil on the upper arm of the volunteer. Immediately after the planning scan, an oil depot with a volume of 0.5 mL was injected in the left biceps brachii (upper arm). The volunteers remained on the MRI table and were not allowed to move the upper arm during the planning scan, the injection and the scan immediately after the injection. Initially, MRI scans of the injection site were made in week 2, 3 and 4 after injection, unless otherwise stated.

### Volume and surface analysis

Firstly, the volume and surface area of the oil depot were determined by obtaining fat fractions maps directly after the MRI scan. These fat fraction maps were calculated using the clinical software program of Philips Healthcare and exported as PAR/REC-files. Data processing was performed using MeVisLab 2.7 (MeVis Medical Solutions AG, Bremen, Germany) (113).

Secondly, the fat fraction images were used to visually delineate the oil depot from the

muscle tissue, using an isoline spline drawing technique as implemented in an in-house developed program based on MeVisLab (113,114). This manual delineation was used because it was unknown whether volunteer movement or the presence of BOH in the oil depot had any influence in obtaining the oil volume automatically. Otherwise, automatic volume and surface calculations from the fat fraction maps were preferred.

Lastly, after delineation, a binary image (1 = 100% fat and 0 =100% water) was obtained and interpolated and combined with the triangulation method (with cut-off voxel intensity value of 0.5). This was used to create a smooth surface area from which the volume and surface area could be determined. The triangulation method was performed using the IsoSurface module, included in MeVisLab 2.7 (113). No analysis was performed in the absence of a visual oil depot.

## RESULTS AND DISCUSSION

This study reports the development of a MRI method to visualise the surface area of an i.m. oil depot injection. Firstly, preliminary studies were conducted in order to develop an appropriate MRI-scan protocol. Secondly, the developed scan protocol was assessed on suitability for use in humans. Lastly, the MRI-scan protocol was used to determine the surface area of i.m. injected oil depots in healthy volunteers.

### Development and suitability of the MRI-scan protocol

#### Preliminary studies

Distinction between the oil depot and muscle tissue was firstly attempted based on signal weighting: differences in T1 relaxation times may cause an adequate fat/water contrast image. These differences were obtained in successive layers of the scanned body area, which result in a tomographic map. A tomographic map is a matrix of successive, two-dimensional images (pixels) to form volumetric pixels (voxels). The preliminary studies were conducted *ex vivo*. To represent the human arm tissue, pigskin was used consisting of muscle and subcutaneous tissue. Syringes with oil depot liquid were externally attached to pig tissue. This research showed a significant difference in relaxation times between oil (with or without benzyl alcohol) and muscle tissue (Table 4.2). The relaxation times of adipose tissue are reported in Table 4.2.

Despite the fact that significant differences in relaxation times between oil (with or without benzyl alcohol) and muscle tissue was seen, this fat/water contrast image based on signal weighting was not further developed. The decision was taken, because the relaxation times of adipose tissue and oil were relatively similar (within 10% of each other). Before the start of the clinical study, it was not clear how deep the oil depot would be injected into the biceps brachii. A confusion between adipose tissue and oil depot was possible.

Table 4.2: Relaxation times of pig tissue and sesame oil (pure or mixed with benzyl alcohol)

	Relaxation time (ms)	
	T1	T2
Muscle tissue	1475.0 (305.7)	3.8 (1.6)
Adipose tissue	336.3 (16.0)	50.7 (0.8)
Sesame oil	354.7 (3.9)	53.1 (0.5)
Sesame oil + 10% BOH	322.3 (5.5)	48.6 (0.4)

Data are presented as mean  $\pm$  standard deviation (n=3). Temperature = 36.4 °C. BOH = benzylalcohol; ms = milliseconds

Contrast images were therefore created using the differences in chemical shift. This technique is generally known as a more reliable method for quantitative spatial volume determination. It gives fat fractions as output data variable, which was used for oil depot volume calculations. The development started by obtaining MR spectra of pure sesame oil and sesame oil + 10% benzyl alcohol (BOH) (Figure 4.1). Unfortunately, the MR spectra corresponded to the MR spectrum of adipose tissue (115,116), which also contains triglycerides (116). Therefore, automatic contrast imaging to obtain the oil depot could not be done. Figure 4.1 shows a benzyl alcohol peak in the sesame oil + 10% benzyl alcohol sample around 6 ppm. By focussing on this peak, contrast images could be created. Unfortunately, oil depots are fully depleted of benzyl alcohol after three days (*Chapter 2*), so this peak will not appear anymore after three days. The here developed visualisation method must be applicable to visualise the oil depot directly after injection, during the release of benzyl alcohol and after benzyl alcohol depletion.

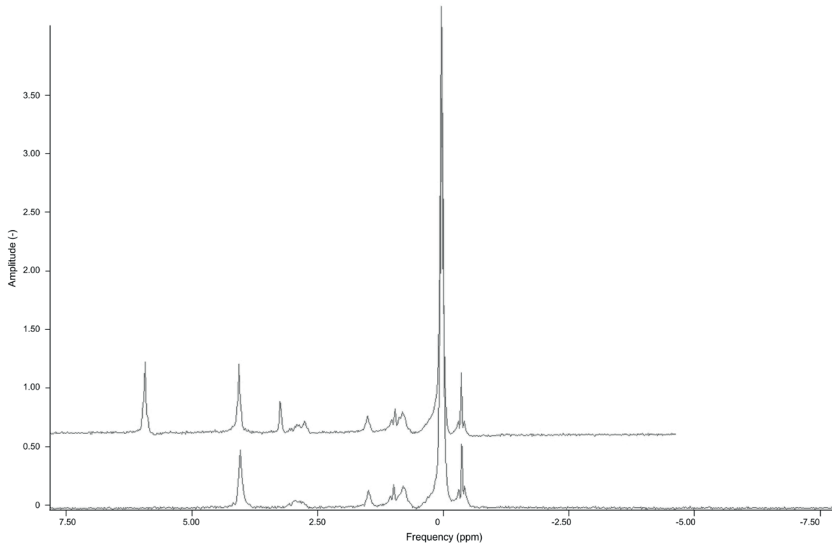


Figure 4.1: MR Spectra images of pure sesame oil (lower line) and sesame oil mixed with 10% benzyl alcohol (upper line). Specific benzyl alcohol in sesame oil frequency was around 6 ppm.

As mentioned before, fat/water contrast images were created using the differences in chemical shift. A commonly used method is the Dixon method (117), which is an existing MRI-scan method to discriminate between fat and water fractions (118,119). This method was then modified to visualise the oil depot from muscle tissue more adequately, even on a lower magnetic field strength MRI-scanner. As a result, it was decided to continue the *ex vivo* experiments and *in vivo* study with a clinical 1.5-T MRI-scanner

The surface area and volume of the oil depot were determined from the raw data of the complete tomographic map. The fat fraction is measured in voxel intensity value, wherein a voxel intensity value of zero means that a voxel contains 100% water and a voxel intensity of 1 is labelled as 100% oil. In this study, the voxel intensity value of 0.5 was arbitrarily chosen as a cut-off value for a fat fraction per voxel. The oil volume was obtained by the summation of all fat fractions. All square surfaces ( $1 \text{ mm}^2$ ) at the interface between oil and water formed the total surface area of the depot. Via post-processing, three-dimensional images were built up from voxels.

#### Sensibility, accuracy and precision

Sensibility, accuracy and precision studies of this method were investigated on samples of chicken breast muscle instead of pig tissue, because of the lower amount of fat in chicken tissue.

In Figure 4.2, the result of a MRI scan to determine the sensitivity is shown. Blank sample of 0.05 mL sesame oil mixed with benzyl alcohol was injected in chicken breast muscle. The mixture is harder to distinguish from muscle tissue because of a smaller difference in

relaxation times compared to pure sesame oil (Table 4.2). Immediately after injection, muscle tissue was scanned with the here developed scan protocol. The scan was visually examined by voxel intensity value, based on white pixels. The number of white pixels is a measure for the fat fraction in muscle tissue.

Scan of muscle tissue with sesame oil mixed with benzyl alcohol (0.05 mL) is shown in Figure 4.2B. The oil depot resulted in 3 pixels and 8 voxels. Thus, the developed method was sensitive enough to determine 0.05 mL 10% (m/v) benzyl alcohol in sesame oil.

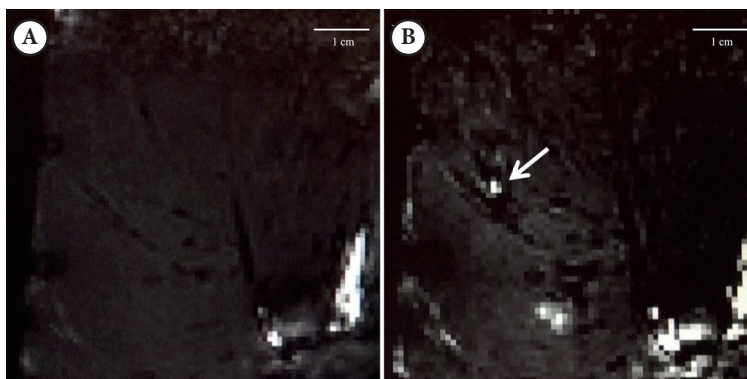


Figure 4.2: chicken breast muscle was used for this experiment to determine the sensitivity of the scan procedure. Blank sample (a) was injected with 0.05 mL sesame oil mixed with benzyl alcohol (10% (m/v)) (b). The white arrow indicates the oil liquid.

Accuracy and precision of the scan protocol were performed with a fixed oil volume, which represented the oil depot. The fixed volume was an oil capsule, containing arachis oil and was inserted into fresh chicken breast. As with the sensitivity determination, voxels were obtained for accuracy and precision determination.

The oil capsule had a mean ( $\pm$  RSD) volume of  $240 \text{ mm}^3 (\pm 20)$  ( $n=3$ ). The results of volume determination with MRI are summarized in Table 4.3. Normally, MRI-signals from objects of interest are received via surface coils. This is a coil made of copper and receives spin frequencies from protons. This experiment was repeated with a slightly changed position of the surface coil to determine the volume repeatedly. Obtained volumes of position 1 and 2 after post-processing were  $244.6 (\pm 5.4)$  and  $240.6 \text{ mm}^3 (\pm 1.3)$ , respectively. This was comparable with the real capsule volume. Regardless to the position of the surface coil, the obtained volume was not significantly changed and met the predefined requirement of  $\pm 3\%$  in volume difference. The attachment of the surface coil to enrolled volunteers is therefore not very critical. Repeated analysis resulted in a precision of maximal 5.4%, which met the predefined requirement of  $<10\%$ .

Table 4.3: Volume and surface area of oil capsule determined by post processing

Position	Volume (mm <sup>3</sup> )		Surface area (mm <sup>2</sup> )	
	1	2	1	2
N	3	3	3	3
Mean	244.6	240.6	199.7	209.8
RSD (%)	5.4	1.3	2.2	3.2

In addition, a reconstruction of the capsule was made by post-processing (Figure 4.3). It appeared that the surface of the capsule was not perfectly spherical. An explanation for these irregular edges could be that the shell of the soft capsule consists of gelatine. Gelatine is composed from animal material, which may contain fat.

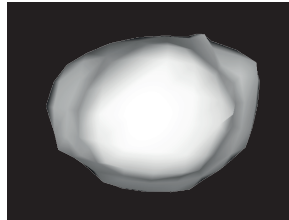


Figure 4.3: reconstructed alfalcidol capsule. The edges were irregular instead of a smooth, round capsule surface.

The suitability experiments showed that this newly developed MRI-scan protocol was sensitive enough to determine small amounts of oil depots. Furthermore, the obtained oil volume was recovered accurately and precisely during post-processing. Subsequently, the developed MRI-scan protocol above was used in a clinical study with healthy volunteers.

### Clinical study

To study the surface shape of an oil depot in human, four healthy male volunteers were injected with an oil depot in the biceps brachii of the left arm. The baseline characteristics of the volunteers are summarized in Table 4.1. The study was designed to scan each volunteer four times in total. This number was requested to keep the burden for the volunteer as low as possible, while we were still able to obtain the rate of disappearance from the injection site (zero- or first-order clearance kinetics).

The mean ( $\pm$  RSD) surface area and volume of the depots recovered after injection was 755.4 mm<sup>2</sup> ( $\pm$  26.5) and 520.1 mm<sup>3</sup> ( $\pm$  24.6). All oil depots were injected between 15-22 mm deep. No adverse reactions upon injection were reported.

As can be seen in Figure 4.4, the injected depots were oblong in all volunteers. This stretched shape was confirmed by post-processing the data (Figure 4.5). Apparently, the oil liquid follows the fibres in muscle. A schematic cross-section of the muscle before and after injection is represented in Figure 4.6. The resolution of the MRI scanner was not sufficient

enough to visualise perimysia and fascicles. Therefore, it cannot be determined how the oil liquid is spread through the perimysium and several fascicles. However, based on the size of the needle, it is assumed that the perimysium between fascicles will be pierced by the injection needle. Consequently, as a result of the injection, the oil liquid will spread across multiple fascicles and will form a bulk (continuous) phase (Figure 4.6). This is substantiated by the visualisation of the oil depots immediately after injection (Figure 4.5), wherein the oil depot forms a thin, long shape.

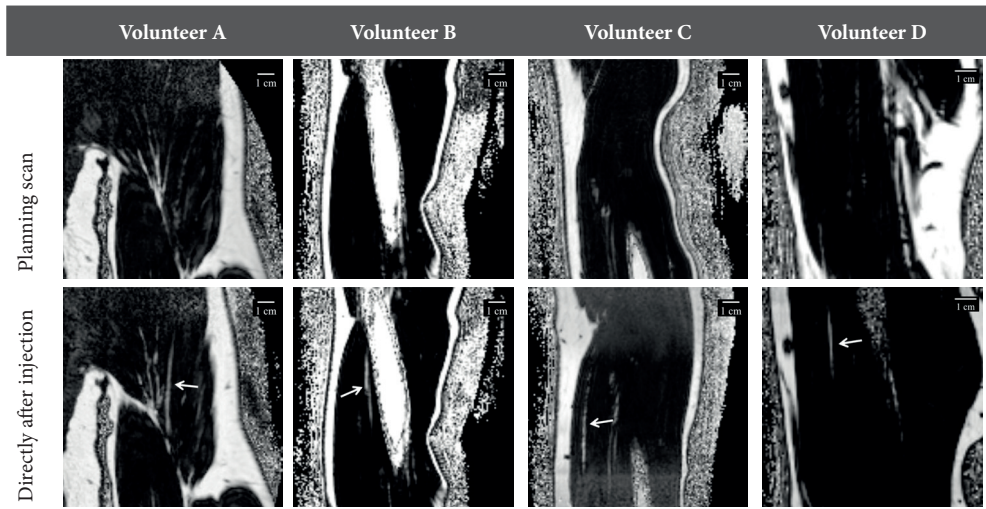


Figure 4.4: An overview of the upper arms of the volunteers. Top row shows the planning (blank) scan where a proper injection site was chosen. The second row shows the oil depot directly after injection (white arrow). The white tissues represent tissues that contain a higher fat/water ratio: subcutaneous and bot tissue. Dark areas contain relative more water, such as muscle tissue.

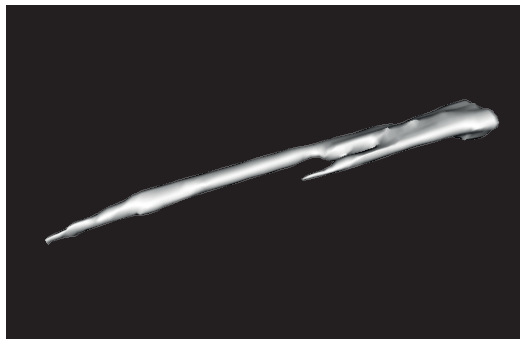


Figure 4.5: The oil depot directly after injection from volunteer C was obtained via post-processing whereby every voxel was analysed to the amount of voxel intensity. This 3D-picture contains every voxel that had a voxel intensity of  $\geq 0.5$ , which was marked as fat-fraction.

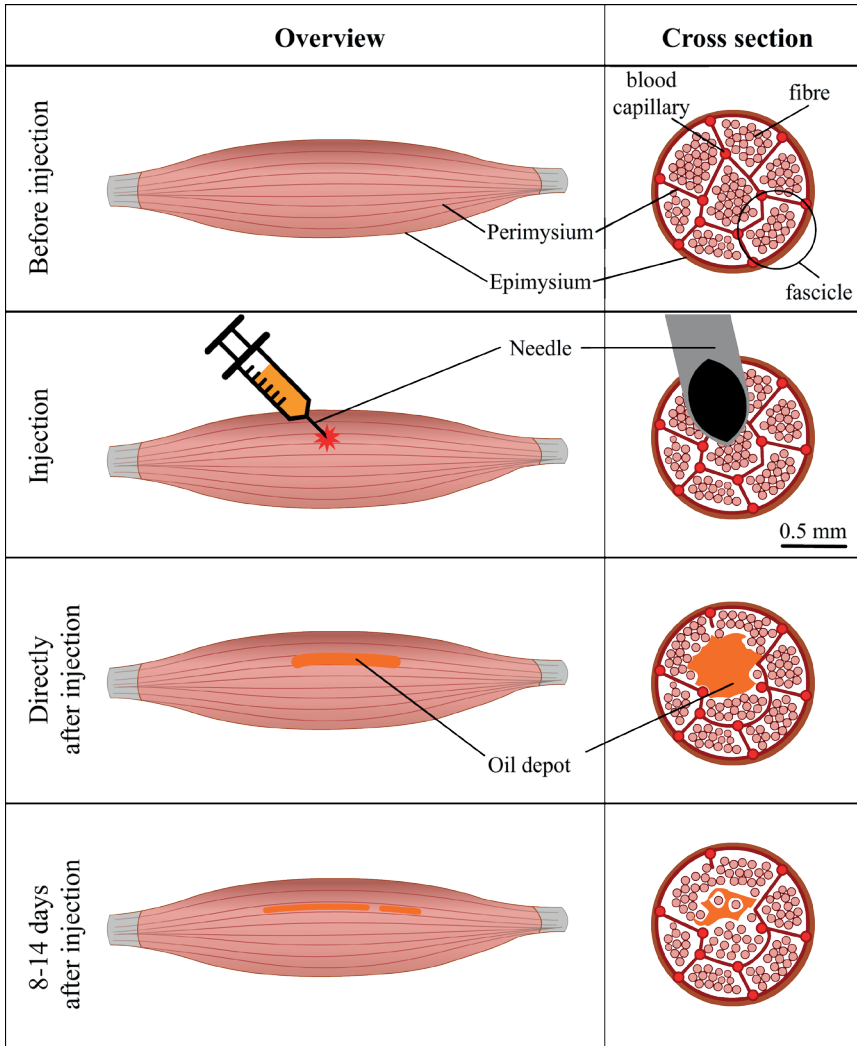


Figure 4.6: A schematic image of the muscle before and after injection. The diameter of the needle is 0.5 mm. It is assumed that the perimysium between fascicles is pierced by the injection needle. Consequently, as a result of the injection, the oil depot will spread across multiple fascicles and push aside the muscle fibres to form a bulk (continuous) phase.

Disappearance rate from the injection site

In addition to visualisation of the shape of the oil depot, the rate of disappearance of the oil depot from the injection site was also determined. As stated before, the reported disappearance half-life of an i.m. depot in pigs was 21.4 days (110). Based on these data, it was estimated that the depot would stay for 4-5 weeks at the injection site. Therefore, a total of 4 MRI-scans were scheduled for every volunteer in the consecutive weeks after injection.

Volunteer A and B received the first oil injections and scanned according to the scan

schedule as mentioned in the study protocol. In the second week after injection, the oil depot volume in volunteer A decreased from 506.0 to 178.6 mm<sup>3</sup>; this was a reduction of 327.4 mm<sup>3</sup> (-65%) within 10 days (Figure 4.7A). Furthermore, the depot could not be visualised anymore at day 14. Speculatively, a merge with adipose tissue occurred or the oil depot was fully stretched out, probably due to oil digestion. See an evaluation of applied method below.

The second MRI-scan for volunteer B was, as scheduled, in the second week after injection. The depot was not visible anymore at that moment (Figure 4.7). Hence, it was unclear when the depot disappeared exactly, but it was within 2 weeks.

The scan schedule for volunteer C and D was therefore intervened. The period between the MRI-scans for volunteers C and D was shortened. The oil depot in volunteer C was determined at day 0, 4, 8 and 14 (Figure 4.7). Clearly, the oil depot was split into 2 or more parts (Figure 4.8).

The oil depot in volunteer C still showed a fast disappearance rate from the injection site (Figure 4.7). Therefore, it was decided to modify the scan intervals for volunteer D by scanning the upper arm every day with a maximum of 4 scans. The depot volume was 540.8 mm<sup>3</sup> immediately after injection. The volume was reduced by 430 mm<sup>3</sup> after the first day. A full disappearance was seen at day 2. This volunteer had normal motility during these days. There was neither sport activity, nor heavy objects were lifted.

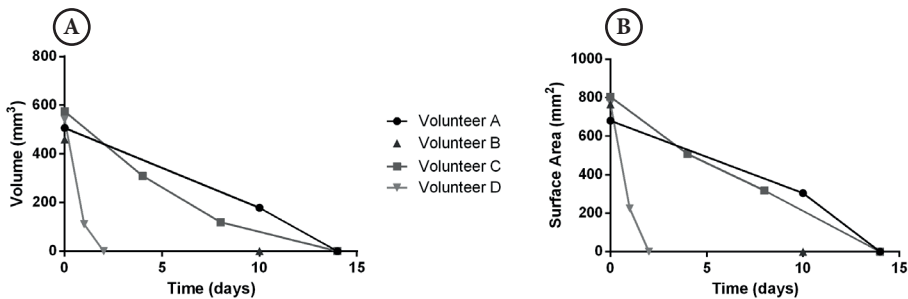


Figure 4.7: The depot volume (A) and surface area (B) reduced in time after injection. No line was drawn for volunteer B, because it was unclear at which time-point the depot disappeared.

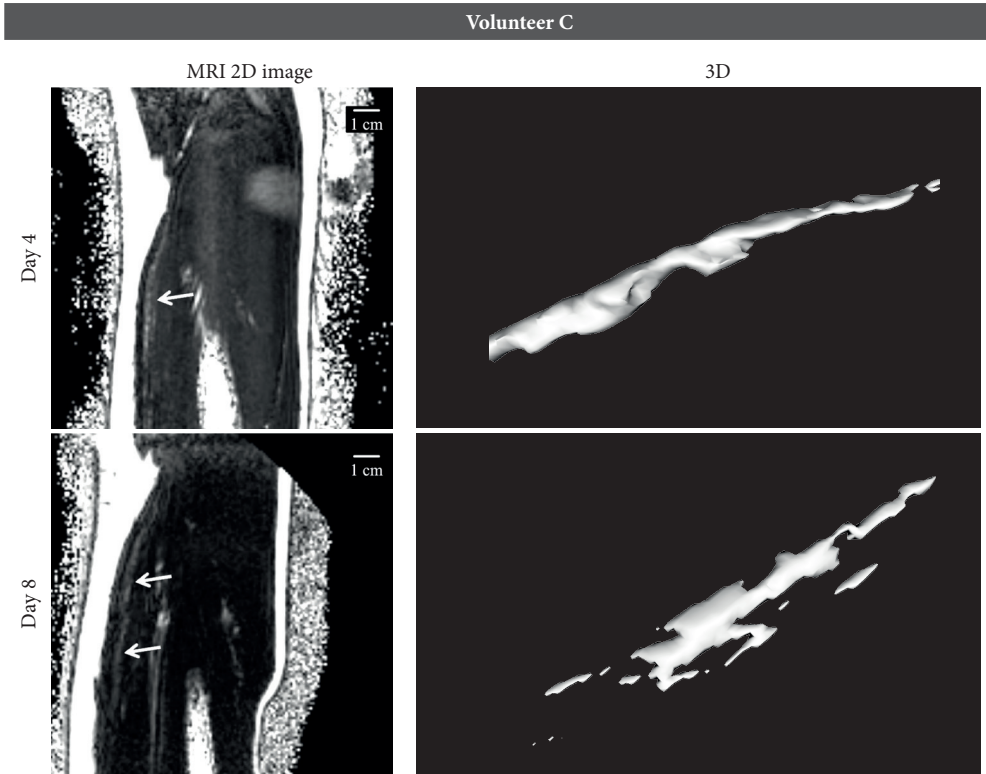


Figure 4.8: Visualisation of the oil depot in volunteer C. The images show the depot at day 4 and 8. White arrows indicate the oil depot in tissue.

#### Evaluation of applied developed method in current clinical study

The here developed MRI scan method is accurate, precise and sensitive and it is therefore applied in the current clinical study. An arbitrary cut-off voxel intensity value of 0.5 was used to label fat fractions. Figure 4.9 shows two other evaluated cut-off voxel intensity values. Logically, the surface area and volume increases by a cut-off voxel intensity value of 0.3 for the fat fraction, whereas these oil depot properties decrease when using 0.7. Interestingly, the 3D image shows a smaller oil depot by a cut-off voxel value of 0.7. It seemed that the whole oil depot contained less fat fractions by, speculatively, an increased amount of water per voxel. This may result in a fine dispersion of small oil droplets emulsified in interstitial fluid. These droplets are not anymore attached to the main part of the oil depot. It can be speculated that these small droplets are individually cleared from the injection site. Although there is no clearance or digestion mechanism published yet, it can be suggested that these droplets can be transported towards the lymphatics or stay attached to the muscle fibres (Figure 4.6). As a result of this speculation, these small droplets have a relatively high surface area that may cause a quicker oil depot depletion of compounds.

The variety in depot disappearance rates from the injection site is noticeable in Figure 4.7.

The residence time of the i.m. oil depots in our volunteers seems to be much shorter than in pigs, as reported by *Larsen et al.* (110). In human, the depot could be visualised for 2-14 days after injection, whereas the half-life of 21.4 days in pigs was reported. Because of the accuracy studies with the fixed oil volumes, the voxel intensity value of 0.5 was considered as reliable. An obvious explanation for this difference in disappearance rate may be the contraction frequency of the injection site. It is assumed that the human upper arm muscle may have a higher frequency compared to neck muscle in pigs. As a result, this may increase drug release and subsequently absorption from oil depots. Although the drug absorption from oil depot injections during exercise is unknown, the drug absorption from aqueous injections (e.g. insulin injections) during exercise is increased (120–123).

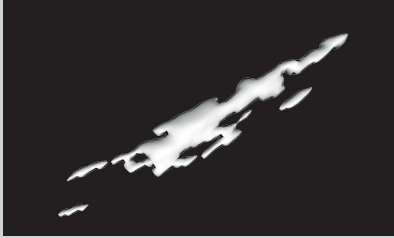
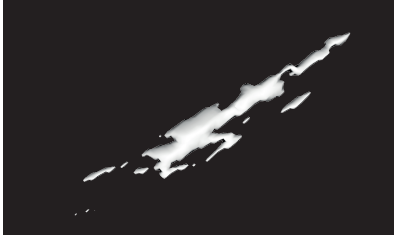
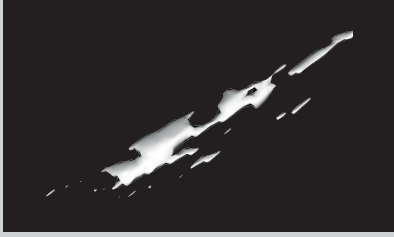
Volunteer C - Day 8			
Cut-off voxel intensity value	Volume (mm <sup>3</sup> )	Surface area (mm <sup>2</sup> )	3D
0.3	245.6	549.9	
0.5	138.6	395.2	
0.7	65.5	253.7	

Figure 4.9: Different depot properties using 0.3, 0.5 and 0.7 as cut-off voxel intensity value for fat fraction labelling. Data was obtained from volunteer C at day 8.

## CONCLUSION

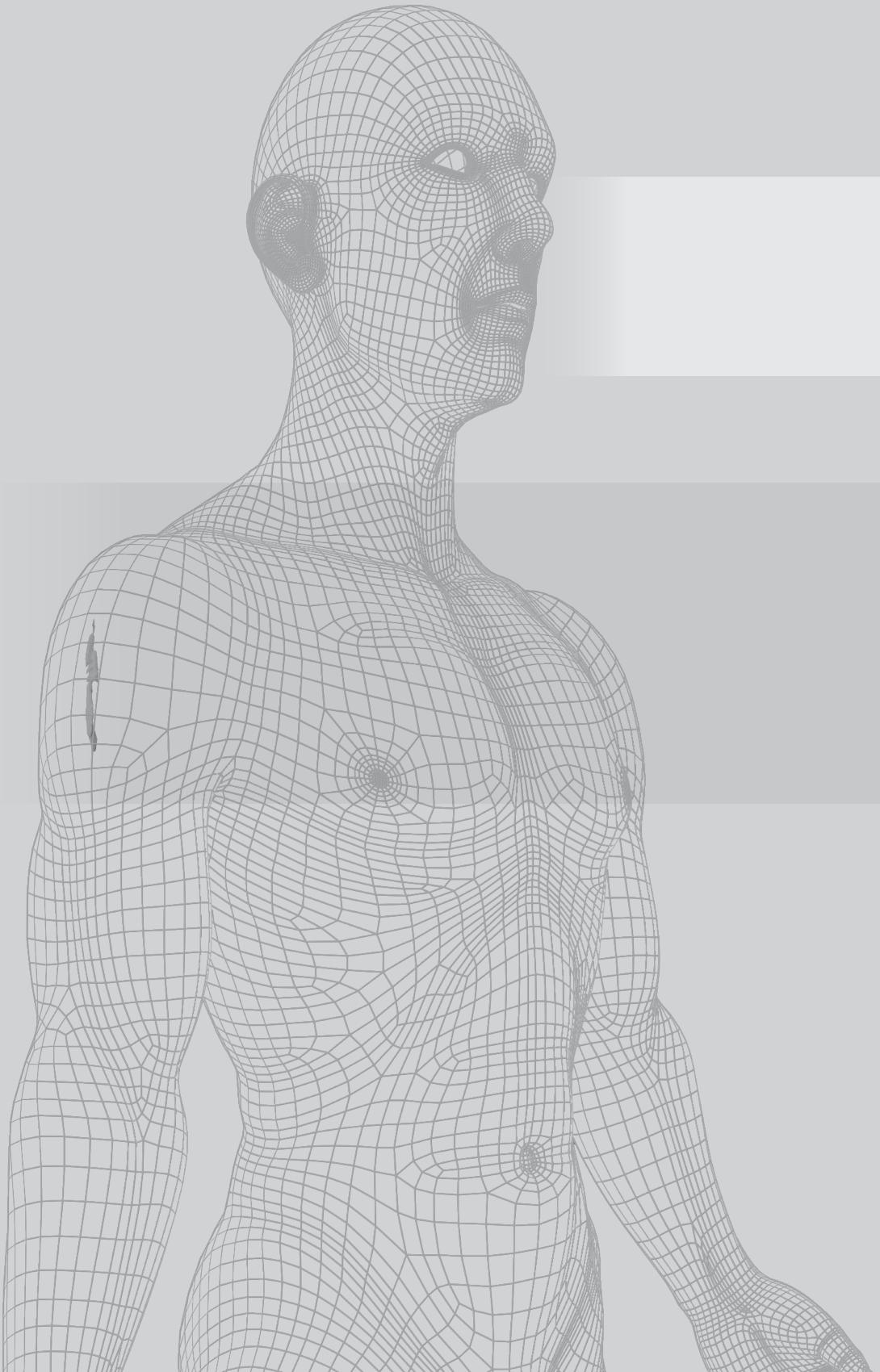
The MRI method applied in this study is able to visualise the shape of an oil depot when injected in the muscle. The method enables to estimate the surface area as well as the way the oil is disappeared from the injection site. From this, further understanding can be obtained about the mechanism of drug absorption from oil depots. During the development of an i.m. injection, it should be taken into account that a stretched shape of the oil depot is formed in muscle. It can be argued that the oil depot is squeezed between the muscle fibres, which explains the obtained shape. As a result of this shape, the determined surface area is much larger than that of a perfect sphere that is used in mathematical models. Although the surface areas were approximately the same in all volunteers directly after injection, this was not the case in the successive days. Furthermore, the oil depot disappearance from the injection site is very variable between patients after i.m. injection. In all cases, the oil depot was disappeared from the injection site within 14 days. These factors are relevant for the absorption kinetics of active substances from oil depots and therefore contribute to the optimal therapeutic treatment in patients.

## Conflicts of interest

The authors declare no conflict of interest.

## Acknowledgments

The authors would like to thank nurses Loes ten Brink and Albertine van der Veen-Selderbeek for their contribution to this research.



## Chapter 5

### The *in-vivo* fate of an oil depot in different tissues

R.W. Kalicharan

C. Oussoren

P. Schot

E. de Rijk

H. Vromans

*Submitted*

## ABSTRACT

Sustained release of lipophilic compounds can be achieved with oil depots. These parenteral formulations are generally injected in the vastus lateralis and deltoid muscle. It is known that the absorption rate differs between these two muscles. The reason for this is not fully understood. The aim of the current study was to investigate whether a distinction in disappearance rate of the oil is responsible for the variation in absorption rate.

A clinical study with healthy volunteers was conducted to determine 1.0 mL oil depots in the vastus lateralis and deltoid muscle for two weeks. The spatial distribution of the oil depots was determined using MRI. Additionally, a study in rats was conducted to microscopically examine the oil immediately and after 31 days of injection. All rats were injected with a 0.1 mL oil depot with and without benzyl alcohol (BOH), a commonly used excipient in oil depots.

In humans, it was shown that all oil depots were equal in volume and surface area directly after injection. Moreover, the disappearance rate for all oil depots was similar; within one week there was no depot visible anymore by MRI. This in contrast to the depots in rats, which were still microscopically visible after 31 days. It is concluded from these observations that the oil is dispersed to small droplets in the course of time. The resulting increase in surface area does not lead to an increase in absorption rate however.

The results of this paper show that the variation in drug absorption as found for the two muscles is not caused by a distinction in surface areas or disappearance rates of the oil depots. Therefore, it is concluded that the local tissue drainage (e.g. lymph flow) plays a considerable role in drug absorption from oil depots, whereby the lymph flow differs between the muscles. A higher muscular lymph flow is expected from the lower parts than compared to the upper parts of the body.

## INTRODUCTION

Long-term drug treatment is optimised using sustained delivery of drugs. These are used for a number of diseases, such as hormone-related (13,105) and psychiatric disorders (50,102–104). This method of drug delivery can be achieved with the use of parenteral oil formulations. Long-acting parenteral injections are administered intramuscularly (i.m.) or subcutaneously (s.c.) (106).

A considerable number of oil depots is registered for clinical use. These sustained release formulations are composed out of lipophilic compounds, dissolved in vegetable oils (arachis, sesame or castor oil). A commonly used additive is benzyl alcohol (BOH), which enhances the solubility of the lipophilic compound in the oil, decreases the oil viscosity to ease the administration and provides some local anaesthesia. Examples of oil depots registered on the market contain nandrolone decanoate (ND) (30,32,33), testosterone undecanoate (13), estradiol valerate (107) or haloperidol decanoate (50). In all cases, the drug substance is compounded as a lipophilic prodrug. These oil depots are administered only once every 2-3 weeks.

In the recent years, new insights into the fundamental mechanisms of drug absorption from an oil depot have been obtained (*Chapter 3*). Here, it is necessary to distinct the drug release out of the oil depot and the absorption into the central circulation (*central compartment*). After injection of the oil depot, the inactive prodrug (e.g. nandrolone decanoate) is released into the aqueous phase (*interstitial fluid*). This drug release is described by mass transport models, in which the release is determined by the drug partition coefficient ( $\log P$ ), the concentration gradient between the oil and aqueous phase and the surface area of the oil depot. It has been assumed by *Shaffer et al.* that an injected oil depot forms a spherical shape in muscle tissue (41). In theory, a 0.5 mL injected oil depot would result in a spherical object with a surface area of 304.6 mm<sup>2</sup>. In our previous study we showed with MRI that the *in situ* surface area of a 0.5 mL administered oil depot is approximately 750 mm<sup>2</sup> (*Chapter 4*). This measured surface area is much larger due to the spatial distribution of the oil liquid throughout the muscle fibres. Obviously, the shape was definitely not spherical, but stretched.

Once released from the oil depot, the prodrug must be hydrolysed into its active (parent) compound to become therapeutically active. It is generally known that hydrolysis of prodrugs with an ester bond can occur via chemical or enzymatic routes. Recently, it was concluded that enzymes are responsible for the fast conversion of the prodrug. At the same time, it was pointed out that this enzymatic hydrolysis does not occur at the injection site due to the absence of carboxylesterases in the interstitial fluid. It was illustrated that it neither occurs in cells near the site of injection because of the slow permeation of the lipophilic prodrug through tissue (*Chapter 6*). Therefore, it was argued that the inactive prodrug is drained via the lymphatic system to the central circulation (*Chapter 3 and 6*). After absorption into the central circulation the prodrug is hydrolysed into the parent compound. In *in vitro* studies

with the model compound ND, this process only took place in human whole blood and not in human plasma or human serum (*Chapter 6*). It was also shown that the ND hydrolysis did not start immediately, but after a delay of approximately half an hour. These experiments indicated that the carboxylesterases are located intracellularly. The delayed appearance of nandrolone after hydrolysis can be referred to as the *hydrolysis lag time*. After intracellular hydrolysis, the parent compound diffuses back to the systemic circulation and can be determined in blood. The overall lag time, or simply *lag time*, is the total time delay between the moment of injection and the appearance of the active substance steady-state release in the central circulation.

The rate at which the drug substance enters the blood stream is determined by the factors that have been described; The so-called *absorption rate constant* ( $k_a$ ) was found to be mainly determined by the partition coefficient of the prodrug and the site of injection (*Chapter 3*). The three mentioned absorption variables (lag time,  $k_a$  and site of injection) are summarized in Figure 5.1 for ND. It has been shown that there is a relationship between the *lag time* and  $k_a$  in appearance of nandrolone after injection in the deltoid, gluteal or vastus lateralis muscle (*Chapter 3*). The explanation for the differences in kinetic parameters is still lacking. Figure 5.1 also shows that a ND oil depot administered in the subcutaneous tissue results in a low nandrolone absorption rate constant and a relatively short lag time.

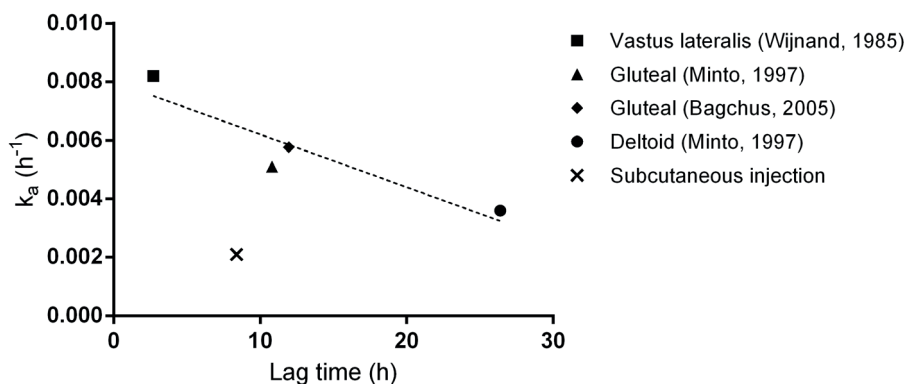


Figure 5.1: obtained from (*Chapter 3*). Plot of absorption rate constant ( $k_a$ ) and lag time of nandrolone administered at different injection sites: deltoid (●), gluteal (◆ and ▲), vastus lateralis (■) muscle and subcutaneous tissue (x). All i.m. injections were 1 mL at a concentration of 233  $\mu\text{mol/mL}$  nandrolone decanoate. The s.c. injection (0.5 mL) had a concentration of 117  $\mu\text{mol/mL}$  nandrolone decanoate.

Although the mechanism of drug absorption from an oil depot has become somewhat more clear, there are still some phenomena that should be studied. First of all, the oil depot formulations and volumes in Figure 5.1 were equal for the i.m. injection, and therefore, it is likely that the different  $k_a$ 's are caused by factors within the body. For example, the shape and hence the surface area of the depot may differ. Also, although it is still unknown how

rapidly the oil depot (with the prodrug) disappears from different muscles after injection, it is possible that the disappearance rate differs between these muscles. In this respect it should be noted that there were some remarkable results in the previous study in which the spatial distribution of an administered oil depot was determined: a significant variation in oil depot disappearance rate was noticed (*Chapter 4*). The period in which the oil depot seemed to disappear from the biceps branchii varied between 2 and 14 days. Although this injection site is never used in pharmacokinetic studies with oil depots, it is not unlikely that this also happens in other muscles where oil depots are administered. Until now, all pharmacokinetic studies on oil depots show at least 2 weeks of sustained levels of the active substance (30,32,33,50,84), indicating that the functionality of sustained drug release is maintained during this period.

In this current study, the surface areas and disappearance rates of oil depots injected in the vastus lateralis and deltoid muscle were determined *in situ* using MRI. Although this technique was suitable to visualize oil in tissue, there is a possibility that it exhibits a too low sensitivity to detect oil that is spread out in the tissue (*Chapter 4*). Therefore, this paper covers also a histology study in animals to determine whether such a dispersion of oil develops in tissue after injection.

The aim of this current study was to investigate the fate of an oil depot in different tissues to elucidate whether the disappearance rate of oil is the cause of observed differences in absorption rate.

## MATERIALS AND METHODS

### Chemical substances

Benzyl alcohol (Ph. Eur.) and sesame oil (Ph. Eur.) were purchased from Fagron NL BV (Capelle aan den IJssel, the Netherlands).

### Oil depots

Oil depots contained sesame oil mixed with 10% (m/v) benzyl alcohol. The formulation was sterilised by filtration (0.2 mm, Mini Kleenpak Fluorodyne II, Pall Corporation, USA) and packed under current Good Manufacturing Practice conditions in the Clinical Pharmacy University Medical Center Utrecht, the Netherlands.

### Clinical study

#### Volunteers

Four healthy male volunteers participated in the study. The characteristics of the volunteers are summarized in Table 5.1. Ethical approval for the study was obtained from the ethical committee of the University Medical Center Utrecht, the Netherlands (protocol number: 14-401/D). Written informed consent according to the latest Declaration of Helsinki was obtained from all volunteers. Inclusion criteria were: healthy males with an age between 18

and 65 years old. Exclusion criteria: claustrophobic, metal clips or wires in the upper arm or thigh, implanted pacemakers, allergies to sesame oil or benzyl alcohol, other depots present in the same muscle or smoking.

Table 5.1: Volunteer baseline characteristics (n = 4).

	Mean ± Standard deviation
Age (years)	28.5 ± 4.5
Length (meters)	1.8 ± 0.1
Weight (kilograms)	76.8 ± 9.0
BMI (kg/m <sup>2</sup> )	23.7 ± 1.3

### Magnetic resonance imaging

A clinical 1.5-T MRI-scanner (Achieva, Philips Healthcare, Best, the Netherlands) was used to perform the imaging studies. The MRI scan parameters and methods used in the current study are described elsewhere (*Chapter 4*).

### Study design

Each volunteer received one 1.0 mL injection in both the left deltoid and left vastus lateralis muscle. Before each injection, two separate planning (blank) scans were made with MRI by positioning the surface coil on the muscle of interest. These scans were used to determine the injection location in the specific muscle of the oil depot. Subsequently, 1.0 mL oil depot was injected with a 21G needle in each muscle directly after each other. MRI scans of the injection sites in both muscles were made immediately after injection and 1, 2, 3, 6, 8, 10 and 13 days after injection. The scanning of the injection site was stopped if the oil depot could not be detected on two consecutive scan days.

### Data processing

The oil depot volume and surface area were determined using the procedure as described previously (*Chapter 4*). All data is depicted as mean ± SD. An unpaired t-test was conducted to compare the different surface areas and volumes with each other. A *P*-value less than 0.05 was considered as significantly different. All data and statistical analysis were performed in GraphPad Prism version 6.02.

### Animal study

#### Rats

18 male Wistar rats (CrI:WI(Han); Charles River Deutschland, Sulzfeld, Germany) were used in the current study. All rats were approximately 5 weeks old and weighed at least 120 g. Subcutaneous (group 1 and 2) and intramuscular (group 3) injections were administered using a 25G needle. Environmental controls for the animal room were set to maintain 18

to 24°C, a relative humidity of 40 to 70%, approximately 15 room air changes/hour, and a 12-hour light/12-hour dark cycle (nightlight during the night period). Group housing of 3 animals per sex per cage. The animals were housed in labelled Macrolon cages (type IV; height 18 cm) with sterilized sawdust as bedding material (Litalabo, S.P.P.S., Argenteuil, France) and paper as cage-enrichment (Enviro-dri, Wm. Lilico & Son (Wonham Mill Ltd), Surrey, United Kingdom).

#### Study design

All rats were injected once on day 1 and once on day 31 with 0.1 mL oil depot. The vehiculum of the oil depot differed per study group, as given in Table 5.2. Each study group consisted of six rats. All rats of group 1 and 2 were subcutaneously injected at the left caudal side of the back (day 1) and at the left cranial side of the back (day 31). All rats of group 3 were intramuscularly injected at the left hind leg (lateral) (day 1) and at the left hind leg (medial) (day 31). Necropsy was on day 32 and all injection sites (including from day 1) and gross lesions in the skin were evaluated to assess local irritation of the test substances. Randomization was conducted by computer-generated random algorithm according to body weight, with all animals within  $\pm$  20% of the mean.

Table 5.2: Study design of rat study

Group	Percentage of BOH	Route of administration
1	0	s.c.
2	10	s.c.
3	10	i.m.

Abbreviations: BOH = benzyl alcohol; s.c. = subcutaneous; i.m. = intramuscular

#### Necropsy and Histopathology

Animals were deeply anaesthetized using isoflurane (Abbott B.V., Hoofddorp, the Netherlands) and exsanguinated. Subsequently, all animals were subjected to examination of the injection site and surrounding area.

All injection sites were collected from all animals at necropsy and fixed in 10% buffered formalin (neutral phosphate buffered 4% formaldehyde solution, Klinipath, Duiven, the Netherlands). Sections were cut at a thickness of 2-4  $\mu$ m and stained with hematoxylin and eosin and evaluated using a light microscope.

## RESULTS AND DISCUSSION

This study reports the *in situ* surface area and disappearance rate of an oil depot injected in the deltoid and vastus lateralis muscle in human male volunteers using MRI. In addition, the oil depot is characterized in rat muscle and subcutaneous tissue via histopathology.

### Clinical study

Healthy male volunteers (n=4) were included in the current study. The baseline characteristics are summarized in Table 5.1. All oil depots were injected between 10 and 20 mm deep. Unfortunately, in one volunteer, the oil depot appeared to have leaked from the deltoid directly after injection. In retrospect, this oil depot was injected insufficiently deep (10 mm). No adverse events were reported during the complete study duration.

The *in situ* volume and surface area of the oil depots (mean ( $\pm$  SD)) were significantly equal in the deltoid and vastus lateralis directly after injection (Table 5.3). All oil depots showed comparable spatial distribution in muscle tissue as reported in our previous study (Chapter 4) (Table 5.4). It is assumed that the oil spreads across multiple fascicles to form a continuous phase in both muscles.

During the successive 6 days, all oil depots disappeared completely from their injection site (Figure 5.2). Furthermore, the disappearance rates did differ to what has been reported in our previous study (Study 1 in Figure 5.2): here, two oil depots were still visible for more than 10 days.

The differences between the two studies are the injected volume and place of injection: in the current study a 1.0 mL oil depot was injected in deltoid and vastus lateralis, whereas in the previous study biceps brachii was provided with a 0.5 mL oil depot. In both studies, the procedure of drug administration, type of needle and nursing personnel were comparable. Although a larger amount of oil seems to disappear quicker, there was one 0.5 mL oil depot that disappeared within 2 days in the previous study (▼). Interestingly, one participant (■) was included in both studies: in the previous study, the oil depot was not detectable anymore within 14 days, while in the current study both oil depots disappeared within 6 days. These combined results show that the speed at which an oil depot is removed from the injection site appears to be highly variable, both inter- and intra-individually. To our knowledge, the mechanism of oil clearance from the injection site is unknown. Data of both studies suggest that a 0.5 mL oil depot is cleared somewhat slower from the injection site than 1.0 mL oil depots.

Table 5.3: Overview of injected oil depots in each muscle. Volume and surface area are measured directly after injection.

	Deltoid (n=3)	Vastus lateralis (n=4)	<i>P</i>	Mean (n=7)
Volume (mm <sup>3</sup> )	891.7 ± 87.7	999.5 ± 66.1	0.1203	953.3 ± 89.8
Surface (mm <sup>2</sup> )	1163.7 ± 164.5	1693.7 ± 407.1	0.0910	1466.5 ± 414.9

Data is shown as mean ± standard deviation.

Table 5.4: Visualisation of the oil depot in the deltoid and vastus lateralis muscle of volunteer C. The images of the planning scan (first row with images) show no oil depot. White arrows indicate the oil depot in tissue (second row with images). The 3D-picture of the oil depot is given in the third row with images.

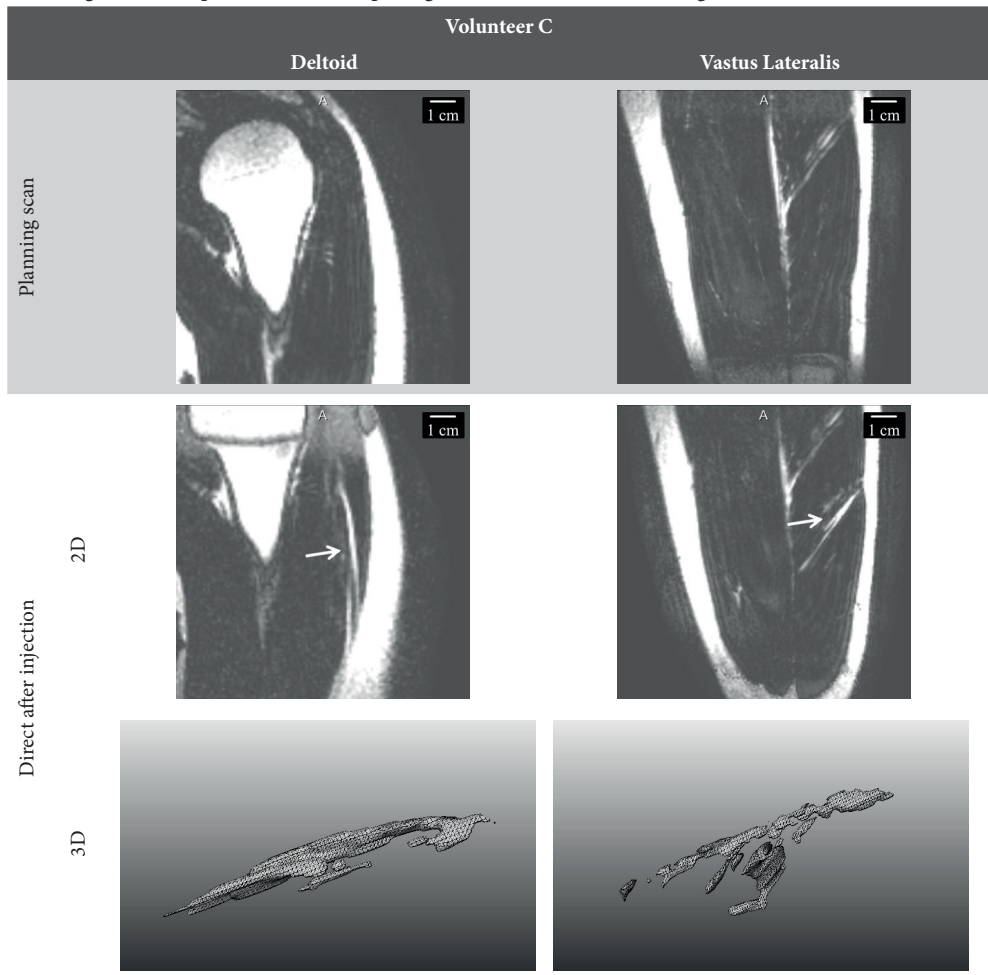
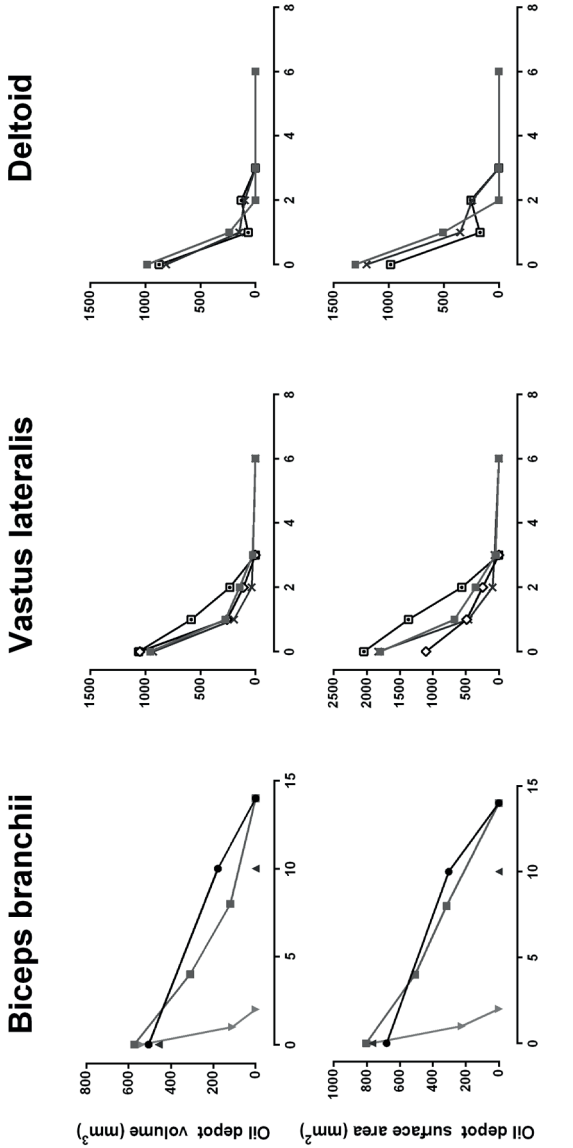


Figure 5.2: Time course of oil depot volumes and surface areas after injection in the biceps branchii (0.5 mL; data from previous study (*Chapter 4*)), the vastus lateralis and the deltoid muscle (both 1.0 mL).



Time after injection (days)

	Participated		
	Study 1	Study 2	
		Vastus lateralis	Deltoid
● Volunteer A	x		
▲ Volunteer B	x		
■ Volunteer C	x	x	x
▬ Volunteer D	x		
◇ Volunteer E			x
* Volunteer F		x	x
▣ Volunteer G		x	x

As earlier indicated, we have previously shown that the release characteristics of a ND oil depot differed between the muscles (Figure 5.1). The current study shows that this cannot be explained by the results obtained with MRI as these suggest that there is no significant difference between the oil depot surface area nor the disappearance rate from the injection site in the different sites of administration (Figure 5.2). Furthermore, there seems to be a discrepancy between the oil disappearance rate and the exposure of the active substances in clinical studies. Two independent clinical studies with 1.0 mL ND oil depots showed that the nandrolone levels persisted for at least two-three weeks (30,32). These oil depots were either injected into the deltoid muscle or the vastus lateralis. It should be noted in this respect that the oil depot disappearance rates are determined on the basis of MRI voxels which represent a certain resolution. The measurements had a detection limit of 0.05 mL (= 8 voxels of 1x1x1 mm) of the oil (*Chapter 4*). As already suggested in our previous paper, it is possible that the injected oil depot is dispersed in time into fine oil droplets with volumes <0.05 mL which are invisible for the MRI assessment. As a result, the oil depot seems to be disappeared, but is actually still present as small droplets. For this reason, histological studies were conducted to further investigate the fate of oil *in situ*.

#### Oil depots in rats

The spatial distribution and local reaction studies were conducted in rats. No mortality was seen during the study period. There were no relevant test-substance related clinical signs after the first injection (day 1). After the second injection (day 31), mild clinical signs in all subcutaneously injected rats consisted of scabs and/or swelling at the flanks. These were not seen in the intramuscularly injected rats.

#### Necropsy and Histopathology

The most relevant microscopic findings in both the subcutaneously and intramuscularly injected groups consisted of the presence of vacuoles (Figure 5.3). These vacuoles were morphologically characterized as clear, round to oval spaces, surrounded by a thin layer of some inflammatory cells. It is likely that these vacuoles represent the injection fluid, which was washed out during the histology sample preparation process. As can be seen in Figure 5.3, the oil is not a distinct continuous phase but represents several separate droplets. This is already noticeable after 1 day. The microscopical resolution in the histopathology study is much better than that of the MRI, as can be seen in this figure where scale bars show a length of 1000  $\mu\text{m}$ . When a fine dispersion of droplets develops in human, it is most probably not measured anymore by MRI. As has been illustrated in the previous study by alteration of the cut-off value intensity the MRI measurement was suggesting that more oil could be present than detected (*Chapter 4*). This indicates in fact that a MRI-scanner with a higher resolution is needed to determine smaller fractions oil accurately during spatial distribution analysis. The disappearance of the oil from the injection as seen in Figure 5.2 is therefore be an apparent

disappearance, as the fine droplets may still be present at the injection site.

In contrast to the current and previous study in human where the oil disappeared for MRI detection within respectively one and two week(s), the oil depot in rats is still microscopically visible after 31 days. Combining the results from both approaches, it can be concluded that the oil depot does not represent a discrete, continuous phase but is dispersed into separate droplets. This occurs already in the first few days. Clearly, the oil is still present after a month, albeit that it may consist of a dispersion of small droplets.

In the subcutaneous administration group, macroscopically a discoloration of the subcutis was observed. At the microscopic level these findings were correlating with tissue damage. These local reactions of the dermis are considered to be an effect of the injection procedure and not of the drug product. At day 1, some early collagen development in group 2 was seen. This was not noticed in group 1, which indicates that the presence of BOH stimulates the formation of collagen by for instance the (enhanced) activation of the immune system (124,125). The release of BOH from an oil depot is expected to be species independent, as the mass transport over the interstitial layer is mainly regulated by its partition coefficient. In a previous study, we reported a complete release of BOH after injection of an oil depot within 48 hours (*Chapter 2*). It can therefore be expected that a collagen formation will occur in human after the injection of an oil depot that contains BOH.

In the intramuscularly injected group, there was a moderate degree of myofiber degeneration, which is a logical consequence after an injection in this tissue. Similar to the s.c. administrations, these local reactions are considered to be a normal reaction pattern of the injection procedure in rats. Collagen formation was slightly noticed around the oil after 1 day and 31 days of injection.

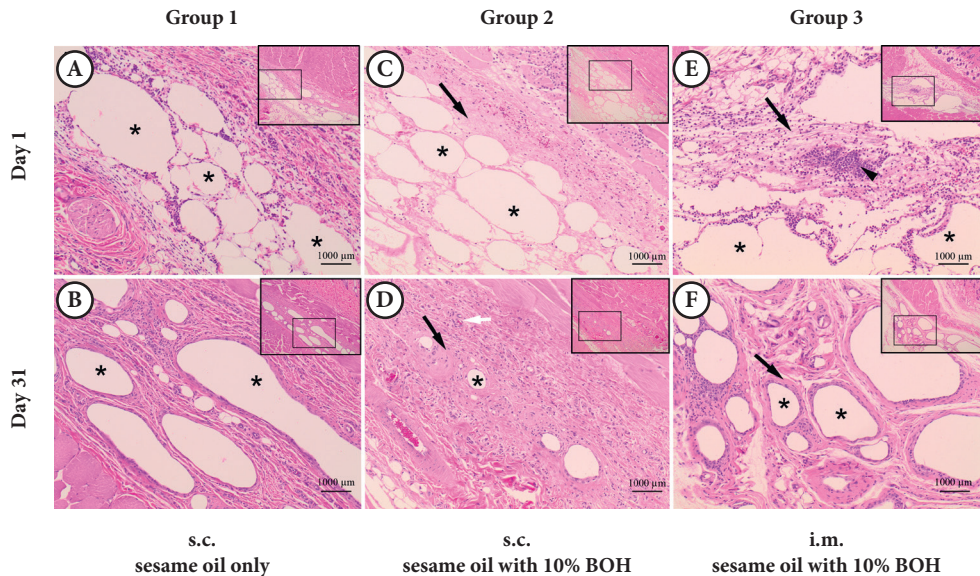


Figure 5.3: Histopathology of the rat subcutaneous (A-D) and intramuscular (E and F) injection sites at day 1 and 31. Representation of the oil is indicated with asterisks (\*). Black arrows show the collagen formation (C-F). Neovascularization is seen in group 2 after 31 days (see white arrow in figure D).

### The contribution of local effects on drug absorption from oil depots

The rat study shows that the oil depot is not necessarily one continuous oil phase, but becomes a dispersion of oil droplets at the site of injection. Microscopical examination shows that the oil does not completely disappear within a couple of days from the site of injection, as is suggested by MRI scanning, but seems to be still present after a month.

The fact that the oil is obviously still present in the tissue explains the continuing exposure of the active substance. However, an interesting aspect of the formation of small droplets is that this results in an increase in surface area. Mass transfer models state that the surface area of the oil depot is relevant for the release rate of the compound. An increased surface area should then lead to a higher release. This is not what is seen in pharmacokinetic studies (30,32,33,50). The obvious explanation for this is that the surface area of the separate droplets is apparently of minor importance. In this respect, it can be argued that the drug release rate is determined by the outer-layer of the assembly of small droplets, encapsulated at the injection site (as seen in Figure 5.3F); Consequently, the droplets in the centre of the fragmented oil depot have minor contribution to the drug release rate.

As has been discussed, there is a difference between the rate of absorption when nandrolone decanoate depots are injected in the deltoid muscle and vastus lateralis. The current study shows that there is no reason to assume that the local conversion of the oil is responsible for this. Therefore, it must be concluded that the cause of the difference must be found in the elsewhere in the body. Several body parameters have been suggested to be relevant during

drug absorption (42,47,106): type of tissue, blood and lymph flow in tissues, physical activity of the tissue and the local activation of the immune system.

The types of muscle tissue in the deltoid and vastus lateralis are the same. They both belong to the phasic muscles, which promote physical activity instead of body stability (126). The mean blood flow in the deltoid muscle is about 11.6 mL/100 g tissue/min, whereas the mean blood flow in the vastus lateralis is about 10.8 mL/100 g tissue/min (96). This difference in blood flow is not only insignificant, it is also inconsistent with the nandrolone absorption rate constants (Figure 5.1). Although lymph flow in the deltoid muscle is unknown, a higher lymph flow is seen in the lower part of the body compared to the upper part after intradermal injections of Technetium-99m ( $^{99m}\text{Tc}$ ) antimony sulphide colloid (127,128). Gravity pulls blood down, making it more difficult to reach the heart via the veins from the lower body parts than when it comes via the veins from the upper body parts (e.g. blood from the shoulders). Muscle contractions (100) and arterial blood pressure (93) in the lower parts of the body should ensure a higher compensation lymph flow. Similar to dermal lymph flow, lymph flow in the vastus lateralis (lower body part) is suggested to be higher than the lymph flow in the deltoid muscle (upper body part). The higher lymph flow is in accordance with the higher nandrolone absorption rate constant administered in the vastus lateralis.

Local activation of the immune system can be of great influence during drug absorption from administered oil depots. *Darville et al.* showed that paliperidone palmitate suspension i.m. injections caused local reactions (129). The authors also reported the effect of co-administered clodronate to inhibit the recruitment of macrophages towards the injection site. An increased infiltration of macrophages towards the injection site was seen which caused a significantly lower  $C_{max}$  of the active substance, but an insignificantly changed  $T_{max}$  compared to group with co-administered clodronate. Therefore, besides the suggested differences in lymph flow at the injection site, the amount macrophages infiltrated, and the material phagocytosed could also differ. For aqueous suspensions, solid particles can be phagocytosed by macrophages, whereas also fine droplets originating from the oil depot can be assumed to be taken up. These macrophages can digest foreign body material (e.g. oil and solvated compounds), which also can digest the prodrug compound via metabolism. The resulting products (either active or inactive) can then also be metabolised into inactive molecule fragments. This digestion in the macrophage decreases the availability of the active substance in the systemic circulation. This negative effect is seen in all administered oil depots: Low recoveries of these active substances are noticed (*Chapter 3*).

The local tissue damage in the rat study could also explain the relatively quick disappearance of both 1.0 mL administered oil depots in contrast to the 0.5 mL oil depot from previous study: a higher injected volume of non-endogenous material enhances the local activity of the immune system. This enhancement could result in an increased clearance of this material locally. In accordance with the arguments above where macrophages could decrease the

maximum concentration of active substances, this oil clearance could therefore also have a negative effect on drug absorption. A lower drug absorption has been demonstrated in a clinical study in which different volumes of nandrolone decanoate oil depots were applied: *Minto et al.* reported that (although not significant) a 1.0 mL oil depot yielded an AUC (mean  $\pm$  SD) of  $193 \pm 29$  nmol\*day/liter nandrolone compared to an AUC of  $144 \pm 30$  nmol\*day/liter after injection of a 4.0 mL oil depot (30). In this study, the drug dose (100 mg nandrolone decanoate) and other parameters were kept constant (30). This phenomenon could be a result of an increased local clearance due to a higher amount of non-endogenous material.

Figure 5.1 shows that not only the drug absorption rate constant and lag time between i.m. injected oil depots differ, but also the subcutaneous from the intramuscular injection. It was already argued that drug absorption of lipophilic prodrugs starts with uptake via the lymphatic system, which consists of lymph vessels and lymph nodes. It is generally known that the body contains several of these nodes, which are temporary collectors of lymph fluid supplied through the vessels. It can be argued that subcutaneous and intramuscular tissue have separate afferent lymph vessels towards the nodes. Once transported towards the lymph node, the prodrug enters the *vena cava superior* and the central circulation. Here, it is hydrolysed. The difference in drug *absorption rate constant* and *lag time* from s.c. or i.m. injected oil depots can therefore be explained by different absorption path lengths via tissue specific lymphatic vessel lengths and lymph flows.

The lower nandrolone  $k_a$  after a s.c. injection as shown in Figure 5.1 is probably due to a lower drainage flow from the subcutaneous tissue towards lymph nodes (130). *Stanton et al.* showed that  $^{99m}\text{Tc}$ -human IgG (a radiolabelled macromolecule) was almost twice as fast cleared from muscle tissue compared to s.c. tissue. In this respect, it is good to realize that macromolecules are also drained via lymph vessels (131).

The shorter nandrolone *lag time* after a s.c. injection (Figure 5.1) must then be due to a shorter pathway towards the central circulation: Drug absorption from s.c. administered oil depots appears earlier in time (shorter *lag time*), but at a lower velocity (lower  $k_a$ ). This in contrast to drug absorption from i.m. injected oil depots from the same organ, where drugs appear after a longer period (longer *lag time*), but at a higher velocity (higher  $k_a$ ). Figure 5.4 depicts an illustration of this concept. This makes sense from an evolutionary perspective, because leukocytes take the shortest way to eliminate exogenous material after infection in the skin. Unfortunately, the differences of lymph vessel length and fluid flow towards the central circulation from the s.c. or muscle tissues from the same human organs are to our knowledge still unknown.

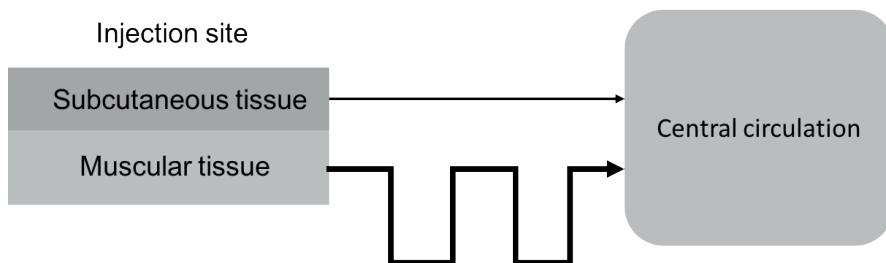
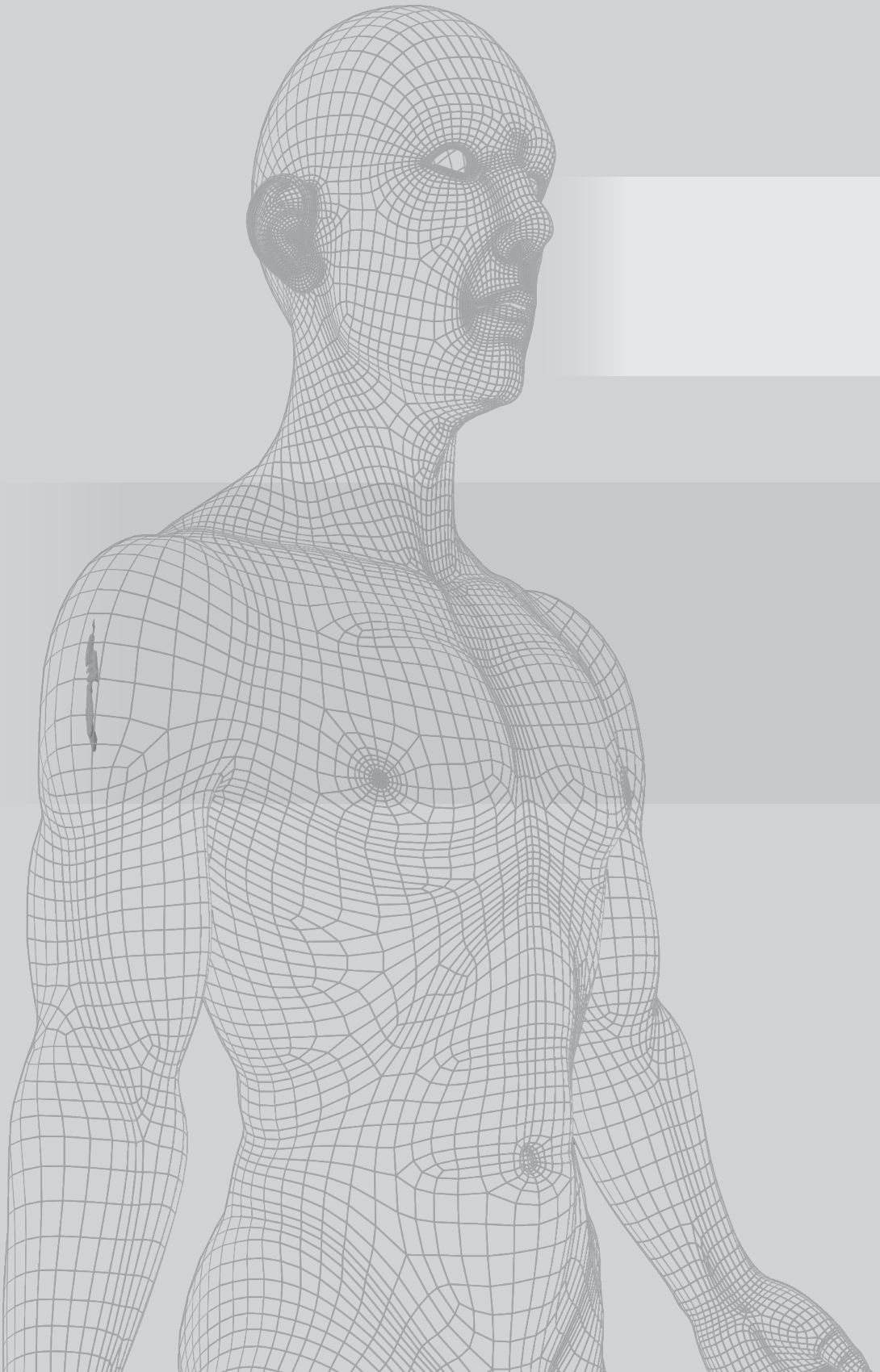


Figure 5.4: Schematic overview of suggested drug transport pathways from the subcutaneous and muscular tissue to the central circulation. Drug transport from the subcutaneous tissue will occur at a lower flow rate and via a relative short pathway, whereas the drug transport from muscular tissues will occur at a higher flow, but via a longer pathway.

## CONCLUSION

In this paper, the rate of disappearance of oil depots from the vastus lateralis and deltoid muscle is shown. It is concluded that differences in drug absorption cannot be explained by drug product properties such as the surface areas. Therefore, body factors such as the activated immune system can influence this drug absorption. The lymph flow and path length at the injection site is argued to be the dominating factor in drug absorption of the released compounds from oil depots.





Chapter 6  
**Where does hydrolysis of nandrolone decanoate  
occur in the human body after release from an oil  
depot?**

R.W. Kalicharan  
M.R. Bout  
C. Oussoren  
H. Vromans

*International Journal of Pharmaceutics* 515 (2016) 721–728

### ABSTRACT

Long-term therapy of nandrolone (N) is recommended to increase mineral density and muscle strength. Using a parenteral sustained release drug formulation with nandrolone decanoate (ND), therapeutic N levels can be achieved and maintained. Until now, it is unknown if hydrolysis of ND into N occurs in tissue at the injection site or after systemic absorption. Therefore, hydrolysis studies were conducted to investigate the location and rate of ND hydrolysis after its release from the oil depot.

ND hydrolysis was studied in porcine tissues, to mimic the human muscular and subcutaneous tissues. Additionally, the ND hydrolysis was studied in human whole blood, plasma and serum at a concentration range of 23.3-233.3  $\mu\text{M}$ .

ND hydrolysis only occurred in human whole blood. The hydrolysis did not start immediately, but after a lag time. The mean lag time for all studied concentrations was  $34.9 \pm 2.5$  minutes. Because of a slow penetration into tissue, hydrolysis of ND is found to be very low in surrounding tissue. Therefore, the local generation of the active compound is clinically irrelevant.

It is argued that after injection of the oil depot, ND molecules will be transported via the lymphatic system towards lymph nodes. From here, it will enter the central circulation and within half an hour it will hydrolyse to the active N compound.

## INTRODUCTION

Androgens can be used to increase bone mineral density and muscle strength (132–135). For this purpose, long-term therapy of nandrolone is recommended. Therapeutic nandrolone levels in blood can be maintained using a parenteral sustained release drug formulation (30,32,33). An example of such a parenteral drug formulation is an oil depot. In general, slow release from oil depots is a result of the high partition coefficient of lipophilic compounds; The release rate decreases when the compound is more lipophilic. Increased lipophilicity can be accomplished through esterification with a fatty acid. For nandrolone, the decanoate has been selected as the appropriate moiety. In contrast to nandrolone (the active parent compound), nandrolone decanoate (ND) is an inactive prodrug. Oil depots with ND have been applied in several clinical studies, in which they were administered by intramuscular (i.m.) (30,32,33) or subcutaneous (s.c.) routes (*Chapter 3*).

Although pharmacokinetic profiles of nandrolone depots have been published, the fundamental mechanisms of drug release and absorption into the central circulation have hardly been studied. In theory, ND is released from the oil depot into the interstitial (tissue) fluid. The rate at which this occurs is largely determined by the compound concentration in the oil formulation and its partition coefficient. Subsequently, ND is hydrolysed into nandrolone. Until now, it is generally assumed that ND is hydrolysed in serum and not in the tissue (fluid) at the site of injection (32).

Recently, we have demonstrated that there exists a delay (*lag time*) in the appearance of nandrolone in the central circulation (*Chapter 3*). Since nandrolone has a  $\log P$  of 3.0 (86) and therefore will be absorbed relatively rapidly, this observed lag time indicates that immediate hydrolyses of ND does not occur. The lag time can be affected by several factors, such as diffusion in tissue fluid, cell membrane adsorption and cell absorption (*Chapter 3*). On the one hand, at the site of injection, interstitial fluid transport is slower than blood flow. On the other hand, this transport is faster than diffusion. Another factor, cell membrane adsorption is relevant, because lipophilic prodrugs have high affinity with lipophilic cell structures such as cell membranes and membrane proteins. Due to the adherence to the cell membrane, cell absorption seems a logical consequence. Once absorbed, the lipophilic prodrug can be hydrolysed by esterases (if present) localized in cytosol and microsomes (136–138). After hydrolysis, efflux of the active parent compound out of the cell must occur in order to reach the central circulation. All these factors may contribute to a prolonged residence time of the lipophilic prodrug in tissues and fluids around the injection site.

Hydrolysis can occur via chemical processes or by carboxylesterases (136,137,139). These enzymes hydrolyse a different ester prodrug, haloperidol decanoate (140,141). Because the ester bond in this prodrug is similar to the ester bond in ND, it is likely that ND hydrolysis also occurs by carboxylesterases. To our knowledge, this has however never been published yet and will be studied in this paper.

Interestingly, carboxylesterases are inhibited by benzil (142). This compound shows great similarity on molecular structure with a commonly added oil depot additive: benzyl alcohol (BOH). Although BOH is processed in a significant quantity in oil depots of 1-10% (m/v) (30,32,33), any inhibitory effect of BOH on carboxylesterases is yet unknown but can be clinically relevant if it inhibits carboxylesterases.

The time period between ND release from the oil depot and metabolism in the liver may account for the complete lag time, but it is also well possible that hydrolysis occurs earlier in the absorption phase. Until now, this has never been unambiguously demonstrated.

The aim of this research was to determine whether ND hydrolysis occurs at the injection site after its release from an oil depot. This paper covers the ND hydrolysis in human blood, plasma, and serum. Hydrolysis in interstitial fluid was also indirectly studied, as interstitial fluid originates from blood plasma (34,143). Furthermore, the rate of ND hydrolysis is studied in muscle and subcutaneous tissue from pigs to mimic the injection site in respectively human muscle and subcutaneous tissue. Usability of carboxylesterases from porcine liver was evaluated in an experimental setup using newborn calf serum (NBCS). This was also used to check whether carboxylesterases from porcine could induce ND hydrolysis in human intravascular fluids, as a positive control in the experimental setup. The evaluation took into account the effects of BOH on carboxylesterases.

## METHOD

### Chemicals and Reagents

Nandrolone decanoate (ND) (Ph. Eur. quality) was purchased from MSD (Oss, the Netherlands). Nandrolone (N) (analytical standard), spironolactone (analytical standard), benzyl alcohol (BOH) (analytical standard), zinc sulphate (analytical standard), RIPA-buffer and carboxylesterases from porcine liver (lyophilized powder,  $\geq 15$  units/mg solid) were purchased from Sigma Aldrich, USA. HPLC-grade methanol and acetonitrile were obtained from Merck (Darmstadt, Germany). Phosphate-buffered saline (PBS) was manufactured under current Good Manufacturing Practice conditions in the hospital pharmacy at the University Medical Center Utrecht, the Netherlands.

### Biological materials

Newborn calf serum (NBCS) was purchased from Life Technologies (Carlsbad, CA).

Human blood (HB) was obtained by drawing blood into a BD Vacutainer® with anticoagulant (18.0 mg  $K_2EDTA$ ). Human plasma (HP) was obtained by centrifuging HB for 10 min at 4000 rpm. Human serum (HS) was obtained by drawing blood into a BD Vacutainer® (REF 367896) with clot activator (micronized silica particles).

Muscle (gluteus maximus) and subcutaneous tissues were obtained from porcine (hind left

leg) at the Central Laboratory Animal research facility (Utrecht University, the Netherlands). Before euthanizing with pentobarbital (barbiturate), esketamine (anaesthetic) and midazolam (benzodiazepine) were administered to the animal. Directly after termination, the tissues were cryopreserved with liquid nitrogen until usage.

### HPLC system and conditions

The reversed phase-HPLC system was from Agilent Technologies 1100 series with a UV-vis detector (G1314A VWD). A Phenomenex guard column (C18, 4 x 2 mm ID, 5.0 µm particle size) was used to filter out contaminants from each injection. Compound separation was carried out on a LiChrospher 100 RP-C18 column (125 x 4 mm ID, 5.0 µm particle size). The column temperature was kept at 30°C during analysis. The autosampler kept the samples at 4°C. A volume of 15 µL for samples originating from serum/plasma or 30 µL for samples originating from blood were injected per run of 10 minutes. The flow rate was set at 1.0 mL/min. The eluted peaks were subsequently detected at a wavelength of 240 nm. The mobile phase was set as a gradient with a mixture of methanol absolute/distilled water, as listed in Table 6.1. Software used for equipment control and data acquisition was Chromeleon, version 7.1.3.2425 from ThermoFisher Scientific (Waltham, MA).

Table 6.1: Schematic representation of the used gradient. The gradient allowed elution within 10 minutes of the three substances: spironolactone, nandrolone and nandrolone decanoate.

Time (minutes)	Distilled water (%)	Methanol (%)
0.00	34.0	66.0
3.30	34.0	66.0
3.40	2.0	98.0
7.00	2.0	98.0
7.10	34.0	66.0
10.00	34.0	66.0

### Standards

A calibration curve of the mixed stock solution was made of 2, 25, 100, 250, 500 and 1000 µg/mL for both ND and N in ethanol absolute. Internal standard (IS) spironolactone was prepared as a 25 µg/mL acetonitril solution. A stock concentration of 300 units/mL carboxylesterases (originating from porcine liver) was prepared in 10mM borate buffer (pH 6.0) conform protocol Sigma Aldrich. A freeze and thaw experiment of the carboxylesterases was evaluated on enzyme activity conform protocol Sigma Aldrich. Freeze-thaw cycles from -70°C to ambient temperature in 10mM borate buffer were performed 4 times, whereby samples were stored 6 h at ambient temperature.

### Incubation studies

*Newborn calf serum.* Ten microliters of ND solution was added to 490  $\mu\text{L}$  NBCS. To each studied NBCS sample, 100  $\mu\text{L}$  10mM borate buffer was added. The borate buffer was replaced with 100  $\mu\text{L}$  carboxylesterase solution for the positive control samples. Final ND concentrations were 212.3, 396.6, 977.6 and 1957.5  $\mu\text{M}$ .

*Human intravascular fluids.* Five microliters of ND solution was added to 245  $\mu\text{L}$  human serum, plasma or blood. To the studied samples, 50  $\mu\text{L}$  10mM borate buffer was added and to the positive control samples 50  $\mu\text{L}$  carboxylesterase solution was added. Final ND concentrations were 23.3, 58.3, 116.7 and 233.3  $\mu\text{M}$ .

Inhibition studies with BOH were performed by replacing a volume fraction of NBCS or human intravascular fluids by a percentage (v/v) of BOH.

*Porcine tissues.* Whole muscle (690 mg) and subcutaneous (590 mg) tissues were incubated in 50 mL tubes (polypropylene, sterile and with screw cap, Greiner bio one, Germany). Each tissue was washed with approximately 5 mL PBS. Subsequently, to lose potential lysate of leaking cells, the solution was gently centrifuged at 300g for 5 min, and the supernatant was poured away. This wash procedure was repeated three times in total. Hereafter, 4917  $\mu\text{L}$  PBS and 83  $\mu\text{L}$  ND solution were sequentially added. Final ND concentration was 700.1  $\mu\text{M}$ . To positive control samples, 50  $\mu\text{L}$  PBS was replaced with 50  $\mu\text{L}$  carboxylesterase solution.

All solutions were incubated at 37°C. Incubation period for NBCS was 90 minutes. For human intravascular fluids samples and porcine fluids, the incubation period was 300 minutes. All experiments were conducted in triplicate.

### Sample Preparation

*Newborn calf serum.* One hundred microliters of incubation fluid in NBCS was mixed with 200  $\mu\text{L}$  IS in 1.5 mL mixing tubes (Eppendorf, Hamburg, Germany). Hereafter, the tubes were vortexed for 10 seconds to precipitate serum proteins. Subsequently, samples were centrifuged for 5 min at 14,000 rpm. Supernatant was analysed using HPLC.

*Human intravascular fluids.* Fifty microliters of incubation fluid in human serum/plasma was mixed with 100  $\mu\text{L}$  IS in 1.5 mL mixing tubes (Eppendorf, Hamburg, Germany). Hereafter, the tubes were vortexed for 10 seconds to precipitate serum proteins. For human blood samples, 50  $\mu\text{L}$  blood was sequentially mixed with 50  $\mu\text{L}$  zinc sulphate and 200  $\mu\text{L}$  IS. Human blood samples were vortexed for 40 seconds. Subsequently, samples were processed as described above.

*Porcine tissues.* Fifty microliters of incubation fluid was mixed with 50  $\mu\text{L}$  Radio-Immuno precipitation Assay (RIPA)-buffer and 100  $\mu\text{L}$  IS in 1.5 mL mixing tubes. The mixtures were vortexed for 40 seconds. Subsequently, samples were processed as described above.

### Data analysis

All data will be depicted as mean  $\pm$  SD. Michaelis-Menten parameters and plots were obtained using a non-linear fit. To analyse the inhibition studies with BOH to ND hydrolysis in NBCS, a one-way ANOVA test was conducted to compare the control sample (0.0% BOH) to the samples with 0.5, 1.0 and 2.0% BOH. For the inhibition study with BOH to ND hydrolysis in human blood, an unpaired t-test was conducted to compare the control sample (0.0% BOH) to the sample with 1.0% BOH.

In both statistical studies, a *P*-value less than 0.05 was considered as significantly different to the control samples. All data and statistical analysis were performed in GraphPad Prism version 6.02.

Lag time was calculated by extrapolating the trend line of the last 3 sample points to the x-axis. The lag time was defined as this intercept.

## RESULTS

### Hydrolysis of nandrolone decanoate in newborn calf serum

To study whether ND is hydrolysed by carboxylesterases, the rate of hydrolysis from ND into N was determined without and in the presence of porcine carboxylesterases (50 units/mL) in NBCS. A range of 212.3-1957.5  $\mu\text{M}$  ND was chosen because of the good detection of ND and N, not for any clinical relevance.

Hydrolysis to N was only observed in the presence of carboxylesterases. A typical hydrolysis profile is given in Figure 6.1. Michaelis-Menten kinetics was observed with a maximum reaction rate of 7.2  $\mu\text{M}/\text{min}$  and a Michaelis constant of 483.1  $\mu\text{M}$  (Figure 6.2). No hydrolysis appeared in samples without carboxylesterases.

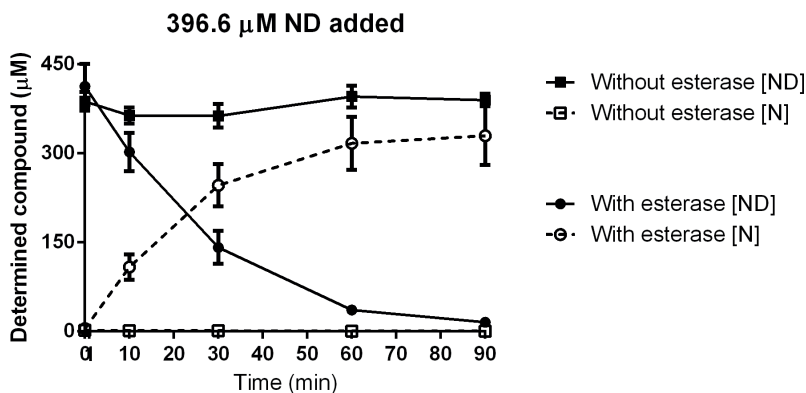


Figure 6.1: Hydrolysis of 396.6  $\mu\text{M}$  ND in newborn calf serum ( $n=3$ ). Hydrolysed ND samples (■) without carboxylesterases resulted in N (□), whereas hydrolysed ND samples (●) with added carboxylesterases from porcine liver resulted in N (○). Incubation studies were conducted at 37 °C for 90 minutes. Results expressed as mean  $\pm$  SD, unless SD is smaller than the symbol.

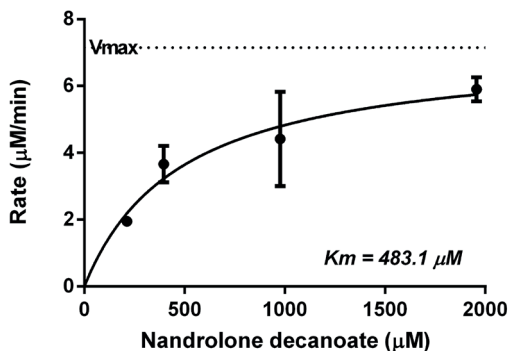


Figure 6.2: Typical Michaelis-Menten plot of ND kinetics catalysed by carboxylesterases from porcine liver ( $n=3$ ). Results expressed as mean  $\pm$  SD, unless SD is smaller than the symbol.

### Hydrolysis in human intravascular fluids

Incubation studies in human intravascular fluids were carried out according to the same method as was used for the hydrolysis assay of ND in NBCS. The rate of hydrolysis of ND was examined over a period of 5 hours in human blood (HB), human plasma (HP) and human serum (HS). To these fluids, an amount of ND in a range between 23.3–233.3  $\mu\text{M}$  was added.

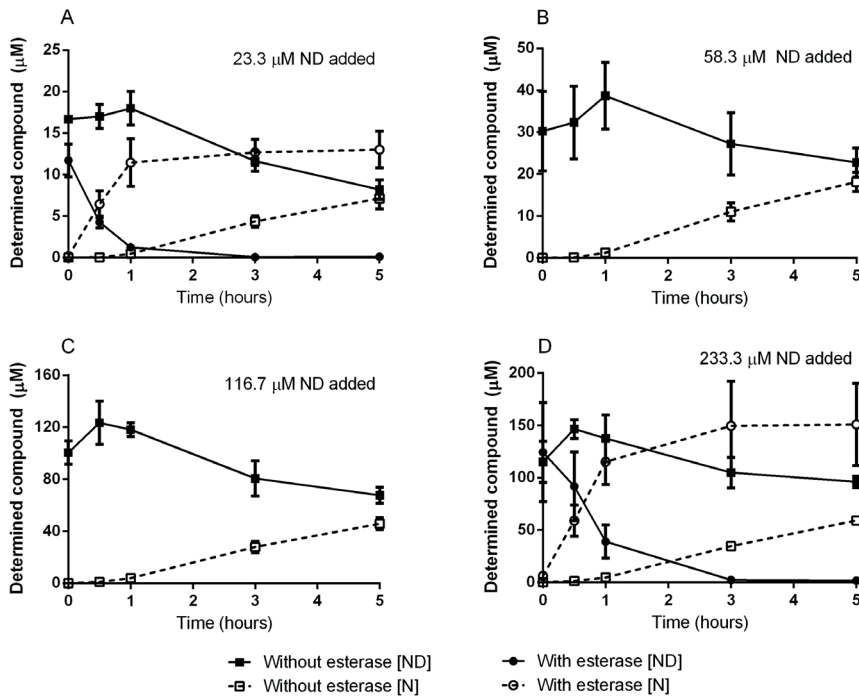


Figure 6.3: Hydrolysis of ND in human whole blood for four different concentrations ( $n=3$ ). Hydrolysed ND samples (■) without carboxylesterases resulted in N (□), whereas hydrolysed ND samples (●) with added carboxylesterases from porcine liver resulted in N (○). Incubation studies were conducted at 37 °C for 5 hours. Results expressed as mean  $\pm$  SD, unless SD is smaller than the symbol.

Figure 6.3 shows the hydrolysis of ND to N at four different concentrations in HB. During 5 hours of incubation, ND partially hydrolysed to N in HB. The hydrolysis of ND did not start immediately, in contrast to the positive control samples. Only a very low amount of N was observed after 30 minutes of incubation time. This lag time lasted  $34.9 \pm 2.5$  min ( $n=12$ ) in all studied concentrations. There was no relationship between lag time and ND concentration. After one hour of incubation, a significant amount of N (approximately 2.3%) was measured. During the first 5 hours, approximately 30% of ND was converted to N in HB, regardless of the added ND concentration. In contrast to the results obtained with carboxylesterases in NBCS where Michaelis Menten kinetics were observed (Figure 6.2), a linear correlation

between ND concentration and hydrolysis rate was obtained (Figure 6.4).

No hydrolysis of ND to N occurred in HP or in HS. Carboxylesterases from porcine liver (50 units/mL) were added to the lowest (23.3  $\mu\text{M}$ ) and highest (233.3  $\mu\text{M}$ ) ND sample as a positive control to check whether hydrolysis occurred in specific medium (positive controls, see Figure 6.3A and D). In all HP and HS positive controls, ND was also converted to N (data not shown).

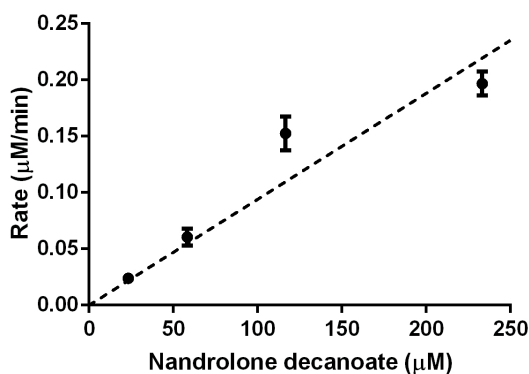


Figure 6.4: Hydrolysis rate plot of ND kinetics in human blood (n=3). Results expressed as mean  $\pm$  SD, unless SD is smaller than the symbol. Dotted line represents the linear regression line (forced through 0,0) with equation:  $Y = 0.0009414 \cdot X - 0.0$

### Hydrolysis in porcine muscle and subcutaneous tissue

To study hydrolysis of ND in muscle and subcutaneous tissue whole porcine tissues were incubated to mimic human tissues. These incubation studies were carried out according to the same method that was used for the hydrolysis assay of ND in NBCS and human intravascular fluids. The realistic situation was to expose the tissues to an oil depot with ND, but preliminary experiments showed that there was no ND released from an oil depot in aqueous media (data not shown). Therefore, ND solution (ethanol absolute) was added to the experimental setup, to determine any hydrolysis activity in these tissues. Concentrations ND below  $700.1 \mu\text{M}$  were not hydrolysed after 5 hours of incubation.

Figure 6.5 shows the percentage recovery of N in the muscle and subcutaneous tissues. In this figure, N recovery in HB is added to compare the relevance of ND hydrolysis in these tissues. During 5 hours of incubation, nandrolone was just above the detection limit in the incubation tissue media: Less than 1% N was recovered during incubating ND with porcine muscle tissues. No N was obtained in ND incubated porcine subcutaneous tissues. Error bars represent standard deviation (SD).

Carboxylesterases from porcine liver (50 units/mL) were added in all media as a positive control to check whether ND hydrolysis occurred in the specific medium. In all media, the positive controls yielded full N within 5 hours incubation. A control freeze-thaw experiment with carboxylesterases from porcine liver did not affect the hydrolysis activity to obtain N from ND (data not shown).

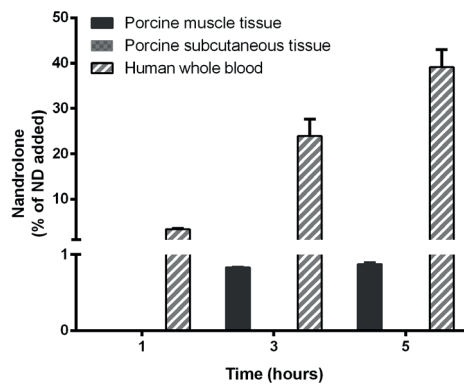


Figure 6.5: Bars represent the percentage recovery of N after 1, 3 and 5 hours of incubation ( $37^{\circ}\text{C}$ ) corrected for the amount ND added. Diagonally striped bars show the recovery of N obtained from human whole blood (originated from Figure 6.3C.), whereas black and grey bars represent respectively porcine muscle and subcutaneous tissues. Results expressed as mean  $\pm$  SD, unless SD is smaller than the symbol.

### Inhibitory effect of BOH on hydrolysis

To study the inhibitory effect of BOH on ND hydrolysis, NBCS containing ND was incubated with carboxylesterases. Upon addition of relatively high amounts of BOH to NBCS solutions, precipitation was visually noticeable. Full precipitation, presumable of protein aggregates, was seen upon addition of 10.0% BOH. Therefore, it was decided not to proceed with 10.0% BOH in the inhibition study. Precipitation was not visible after adding 2% BOH or less.

The inhibitory effect of 0.5, 1.0 and 2.0% (v/v) BOH on the ND hydrolysis activity of porcine liver carboxylesterases (50 units/mL) in NBCS is given in Figure 6.6. Complete inhibition of ND hydrolysis was examined with the addition of 2.0% BOH during 90 minutes of incubation ( $P = 0.011$ ) (Figure 6.6). One percent of BOH resulted in a significant inhibition of ND hydrolysis ( $P = 0.035$ ) whereas the addition of 0.5% BOH exhibited only a slight effect on ND hydrolysis. In the 1.0% BOH control sample without added carboxylesterases, no ND hydrolysis was observed (negative control). Additional control experiments (Figure 6.1), demonstrated that in NBCS in the presence of carboxylesterase ND is hydrolysed to N. Moreover, no spontaneous ND hydrolysis was observed in NBCS (Figure 6.1). Therefore, this medium was suitable to study the inhibitory effect of BOH on carboxylesterase with respect to the conversion of ND to N.

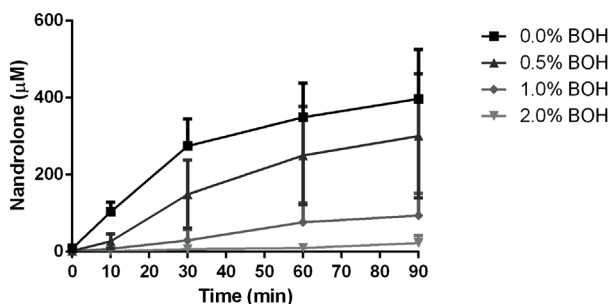


Figure 6.6: Inhibitory effect of BOH on 977.6  $\mu\text{M}$  ND hydrolysis in newborn calf serum ( $n=3$ ). The ND hydrolysis is inhibited by a raising BOH concentration. Results expressed as mean  $\pm$  SD, unless SD is smaller than the symbol.

Similar to the BOH inhibition study in NBCS, 1.0% BOH significantly inhibited the conversion to N in HB ( $P < 0.01$ ) (Figure 6.7). Without BOH, the obtained concentration of N was  $45.8 \pm 2.6 \mu\text{M}$  ( $n=3$ ), whereas the N concentration with 1.0% BOH was  $5.7 \pm 1.5 \mu\text{M}$  ( $n=3$ ). Both conditions contained the initial ND concentration of  $117 \mu\text{M}$ . No precipitation was noticed.

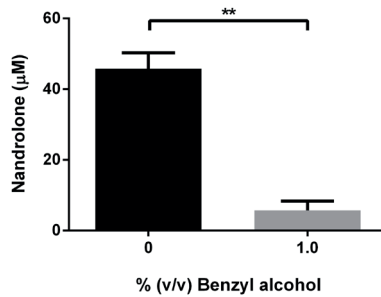


Figure 6.7: 1.0 % Benzyl alcohol resulted in a significant inhibition of  $116.7 \mu\text{M}$  ND hydrolysis in human blood after 5 hours of incubation ( $n=3$ ). \*\*,  $P < 0.01$ . Results expressed as mean  $\pm$  SD.

## DISCUSSION

This research aimed to study whether locally injected ND as an oil depot is hydrolysed at the site of injection. Drug absorption from a locally injected oil depot into the central circulation exhibits a delayed absorption pattern, which is defined as *lag time* (*Chapter 3*). About 8 hours after a s.c. ND oil depot injection, N is observed in the central circulation (*Chapter 3*). Remarkably, this lag time is much shorter when the oil depot is injected in the vastus lateralis muscle (2.7 hours), about the same when injected in the gluteal muscle (11-12 hours) and much longer when injected in the deltoid muscle (26.4 hours) (*Chapter 3*). This phenomenon of various lag times will be discussed in another article. This lag time is most likely caused by the postponed ND hydrolysis which would mean that hydrolysis does not take place in the tissue around the site of injection, but rather occurs in the central circulation or in the liver. This research elucidates whether the hydrolysis of N occurs at the injection site, or in the central circulation.

In literature, a half-life time hydrolysis of 4 min for  $2.5 \times 10^{-3}$   $\mu\text{mol/mL}$  (1  $\mu\text{g/mL}$ ) nandrolone phenyl propionate in rat plasma has been reported (14). Based on these data, the duration time to hydrolyse  $2.3 \times 10^{-5}$   $\mu\text{mol/mL}$  (=0.01  $\mu\text{g/mL}$ ) ND in HS was proposed by *Wijnand et al.* (32) to be below one hour. However, as reported by *Li et al.* and *Rudakova et al.* (138,144), no carboxylesterases are present in HP. This implies that no enzymatical hydrolysis of ND to N can occur in HP and HS, which is confirmed in this current study: In human serum and plasma, no hydrolysis of ND occurred during 5 hours of incubation. Also, no chemical hydrolysis of ND occurred in these media. Moreover, this entails that ND hydrolysis does not occur in interstitial fluid since interstitial fluid originates from blood plasma. It contains water and molecules less than approximately 40 kD molecular weight (34,143). This means that even when carboxylesterases would be present in human blood plasma, they would not appear in the interstitial fluid as the molecular weight of human carboxylesterases is approximately 60 kD (139).

This paper demonstrates that ND hydrolysis does occur in human blood. Apparently human blood contains carboxylesterases. The appearance of N was observed after an average lag time of  $34.9 \pm 2.5$  minutes. Noticeable was the absence of Michaelis-Menten behaviour. Instead of nonlinear enzyme kinetics, a linear rate of hydrolysis was seen (Figure 6.4). These observations suggest that the carboxylesterases, involved in ND hydrolysis, must be present in the blood cells since the distinction between whole blood and plasma is the presence of cells. Hydrolysis can occur either on the blood cell membrane, or occurs intracellularly. Because a *lag time* of N appearance was noticed, carboxylesterase activity on the cell membrane is apparently not very pronounced. Otherwise, the N recovery should be seen instantaneously. It can therefore be concluded that hydrolysis occurs after membrane diffusion and, subsequently intracellularly in erythrocytes cytosol (145) and probably in leukocytes. This is in line with literature, where it is reported that carboxylesterases are present in the endoplasmic reticulum

and cytosol in human cells.

In porcine muscle and subcutaneous tissues, little hydrolysis of ND occurred in porcine muscle tissue during 5 hours of incubation (Figure 6.5). The tissues were chosen to be originated from a pig instead of other species (such as rats) to prevent false-positive results. Similar to human tissues, interstitial fluid between porcine tissue cells does not contain carboxylesterases (138). Because the penetration depth of lipophilic molecules into tissue is very low (146), it is relevant to study the carboxylesterase activity in cells that are in the direct proximity of the oil depot. The results with tissue conclude that hydrolysis in porcine muscle and subcutaneous cells occurs slowly, indicating that only little ND has reached an enzyme. In line with hydrolysis in HB, this also suggests that *in vivo* hydrolysis only occurs intracellularly, because immediate (within 30 minutes) N appearance was absent.

Before intracellular hydrolysis can occur, ND must diffuse through the cell membrane. As can be seen in Figure 6.4, the enzymatic conversion is proportional to the concentration of the substrate. This suggests that there must be another process that plays a role. This process is the diffusion of ND through the cell membrane which is the rate-limiting step. Otherwise, Michaelis-Menten kinetics would have been observed and a lag time absent. As ND is more lipophilic ( $\log P = 8.1$  (86)) than N ( $\log P = 3.0$  (86)), we assume that the limiting step in mass transfer is the cell influx of ND rather than the cell efflux of N. Therefore, the N efflux will be neglected in the following estimation. With the value of lag time being roughly 2100 s and the literature value of the erythrocyte membrane thickness ( $h$ ) ( $7 \times 10^{-7}$  cm (147)), the diffusion coefficient ( $D$ ) of ND through this membrane can be estimated to be  $3.9 \times 10^{-17}$  cm<sup>2</sup>/s according to the following equation:

$$\text{Lag time} = \frac{h^2}{6D} \quad [\text{Equation 6.1}]$$

This calculated value of the diffusion coefficient is much lower than other steroid diffusion coefficients. For example, the  $D$  of testosterone in percutaneous absorption has been reported to be  $1.95 \times 10^{-11}$  cm<sup>2</sup>/s (148). Calculated lag time for this testosterone would be  $4.2 \times 10^{-3}$  s ( $h$  was kept constant), which gives a negligible corrected (for the N efflux) diffusion coefficient for ND in current study ( $D$  remains  $3.9 \times 10^{-17}$  cm<sup>2</sup>/s). There is a significant difference between the values of ND and testosterone and this may be a source of some discussion. However, it is at least a reflection of the large difference that exists between a prodrug having a  $\log P = 8$  and a parent drug having a  $\log P = 3$ . The conclusion of this observation is that ND hardly does permeate through tissue. This indicates that ND must be absorbed into the central circulation via other routes, as direct absorption is excluded due to the high partition coefficient. It is assumed that ND subsequently adheres to small proteins (< 40 kD) and migrates into lymph vessels to be absorbed into the central circulation.

Recently, it was shown that the *in situ* surface of a 0.5 mL injected oil depot is 755.4 mm<sup>2</sup> (Chapter 4). As can be seen in Table 6.2, the amount of cells per 1000 mm<sup>2</sup> tissue is around 10<sup>5</sup>-10<sup>8</sup> cells, which is negligible with the amount of cells in blood (10<sup>15</sup> cells/mL). Another advantage of blood, is that it is continuously refreshed (*sink conditions*).

Table 6.2: Estimation of amount of cells in studied media nandrolone decanoate may encounter during absorption into the central circulation.

Type	Amount of cells	Amount of cells available for ND at tissue surface <sup>†</sup>
Subcutaneous cells*	2.6 * 10 <sup>3</sup> cells/mg tissue	1.4 * 10 <sup>2</sup> cells/mm <sup>2</sup>
Muscle cells**	9.3 * 10 <sup>4</sup> cells/mg tissue	3.2 * 10 <sup>5</sup> cells/mm <sup>2</sup>
Erythrocytes	4.2-5.5 * 10 <sup>15</sup> cells/ml blood	-

\*= The volume of human adipose cells is 660 \* 10<sup>-6</sup> mm<sup>3</sup> (149). The 590 mg porcine subcutaneous tissue had a volume of approximately 1 cm<sup>3</sup> (= 1000 mm<sup>3</sup>).

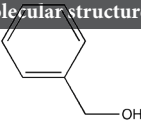
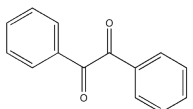
\*\*= No dimensions of human muscle cells are published. The following data is used: rat myocytes have a volume of 15.6 \* 10<sup>-6</sup> mm<sup>3</sup> (150). The 690 mg porcine muscle tissue had a volume of approximately 1 cm<sup>3</sup> (= 1000 mm<sup>3</sup>).

† = the diameter of human subcutaneous cells and muscle cells are respectively 94 and 2 μm (151,152).

Benzyl alcohol (BOH) is commonly used in oil depots at a concentration of 1-10% (m/v) (30,32,33,50). It is used as viscosity reducer, local anaesthetic and as co-solvent in oil depots (26). Recently, BOH was reported to have a very different absorption profile than N (Chapter 3). In contrast to N, BOH was detected in the bloodstream within minutes after injection. Furthermore, whereas N was measured for 5 weeks after injection, BOH was cleared from the central circulation within 36 hours (Chapter 2).

The BOH molecular structure shows great similarity to the one of benzil (Table 6.3), which is an inhibitor of carboxylesterases (142). The inhibition is due to steric interaction of the benzene ring of benzil with the pocket of human carboxylesterase 1 (hCE1) (153). This was the reason to study the influence of BOH on ND hydrolysis. As observed, the addition of 1.0% BOH significantly inhibits the ND hydrolysis in human blood.

Table 6.3: Summary of benzyl alcohol and benzil and their molecular properties.

Component name	Molecular formula	Molecular structure	Molecular weight (g/mole)	Log P (o/w)
Benzyl alcohol	C <sub>7</sub> H <sub>8</sub> O		108.1	1.03
Benzil	C <sub>14</sub> H <sub>10</sub> O <sub>2</sub>		210.2	3.38

Source: <http://www.chemspider.com/> (86), visited at July 15, 2016

Although not investigated, the effect of BOH on the carboxylesterases in porcine muscle and subcutaneous tissues can be predicted. This can be estimated by calculating the amount of BOH locally using the  $\log P$  of BOH. The  $\log P$  of BOH is 1.03 (86) which indicates a distribution in the water phase (*interstitial fluid*) of approximately 10% of the total amount injected BOH. The processed amount BOH in oil depots is 10% (m/v), which would result in a concentration less than 1% in the water phase. In the current study, 1.0% BOH significantly inhibited carboxylesterases in whole blood. Therefore, it is possible that this inhibition will also occur in the proximity of the oil depot. This is only temporary however, since nearly all BOH in the oil depot is released within 36 hours. Indicating a large amount of BOH that enter the interstitial fluid and diffuses through the tissues near the injection site, and, consequently, it will temporary inhibit the carboxylesterases in these tissues.

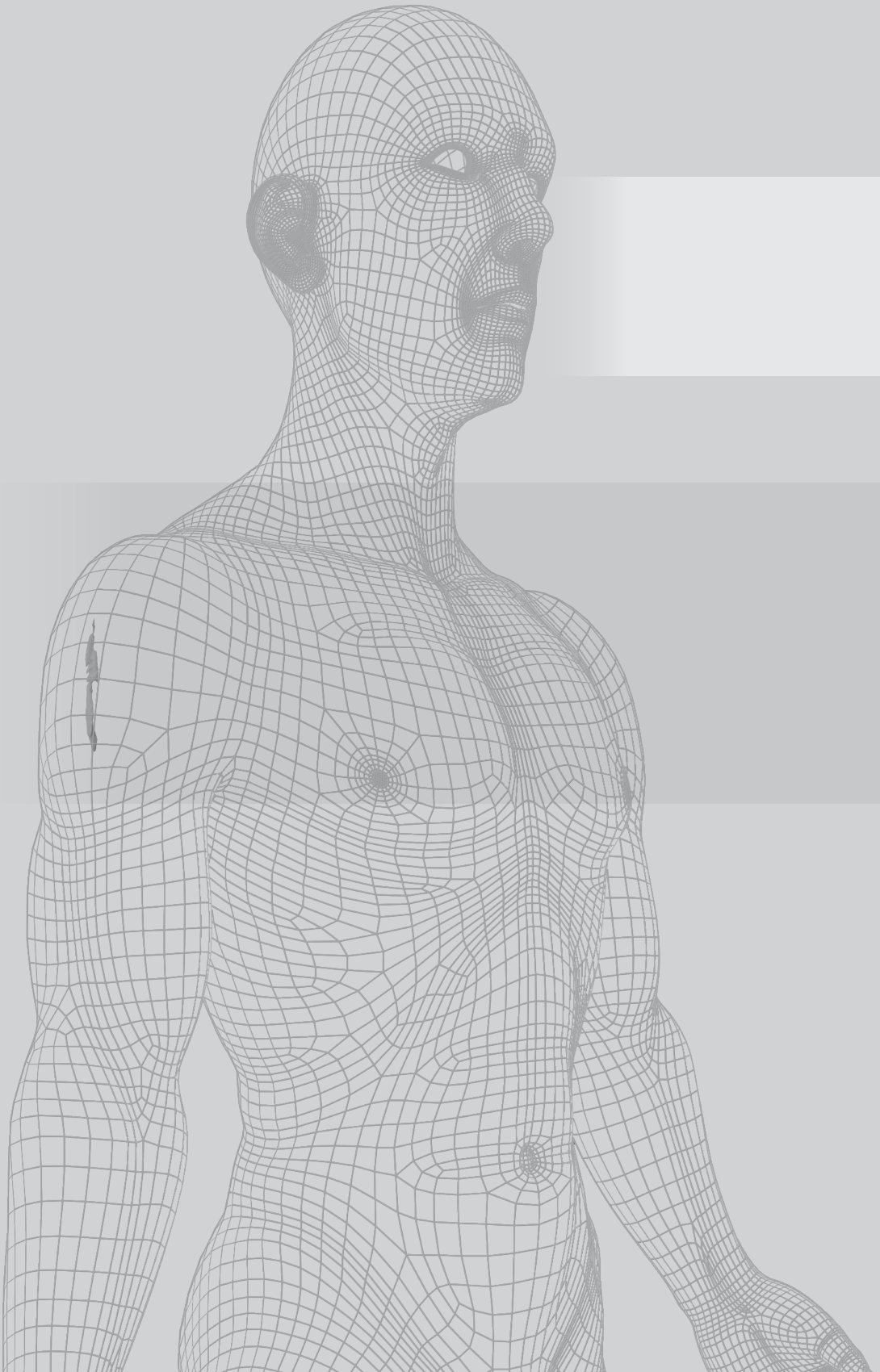
This study reveals that ND is stable in NBCS during incubation for 90 minutes at 37°C (Figure 6.1). This implies the absence of chemical and enzymatic degradation of ND in NBCS (Figure 6.1). It also has been shown that carboxylesterases from porcine liver are active in tissues from other species than pigs since porcine carboxylesterase also induced hydrolysis in newborn calf serum (NBCS) and in human blood. This experimental setup was therefore suitable for use with human intravascular fluids.

#### CONCLUSION: CONTRIBUTION OF NANDROLONE DECANOATE HYDROLYSIS TO NANDROLONE ABSORPTION

After injection of the oil depot, the released ND molecules appear in the interstitial tissue. Due to the high partition coefficient ( $\log P = 8.1$  (86)) of ND, it is likely that ND adheres to small proteins (<40 kD) in the interstitial fluid. As argued above, the prodrug is neither hydrolysed in the interstitial fluid nor is able to diffuse in a significant way into the tissue. The interstitial fluid is drained via the lymph vessels, and therefore ND absorption into the central circulation via the lymphatic system is in fact the only likely route. Therefore, it can be reasoned that ND is hydrolysed when entering the central circulation. Alternatively, it is possible that the cellular components in the lymphatic system take care of (a part of) the hydrolysis.

Once entered in the central compartment, it will take about half an hour before ND hydrolysis will occur. All these phenomena, transport through the lymph and diffusion through cell membranes, contribute to the lag time observed after the injection of an oil depot.

Although this article focusses on the location and rate of ND hydrolysis, the outcome is also applicable for other esterified prodrugs processed in oil depots and i.m. or s.c. injected, such as haloperidol decanoate (50), fluphenazine decanoate (79) or testosterone undecanoate (13).



## Chapter 7

### **General discussion**



The development of oil depots has been based on trial and error for a long time. As stated in the introduction (*Chapter 1*), most studies regarding oil depots focussed on either the drug release out of the depot or pharmacokinetics. These studies are certainly of importance during the development of an oil depot formulation: However, until now, it has hardly been studied what happens with the prodrug once it has been released from the oil depot until the appearance of the parent compound in the central circulation, i.e. the absorption process.

This dissertation aimed to create a better understanding on the fundamental parameters that influence drug absorption from oil depots. This final chapter provides a general discussion of all new insights into drug absorption from oil depots. At the end of this chapter, a future perspective and an overall conclusion will be given.

### MECHANISM OF DRUG ABSORPTION FROM OIL DEPOTS, UNTIL NOW.

Until now, the biopharmaceutical assumptions of drug absorption from oil depots can be summarized in Figure 7.1 below. These assumptions are based on *in vitro* experiments (35–37) and animal studies with model compounds (4). More information about this figure can be found in the introduction (*Chapter 1*).

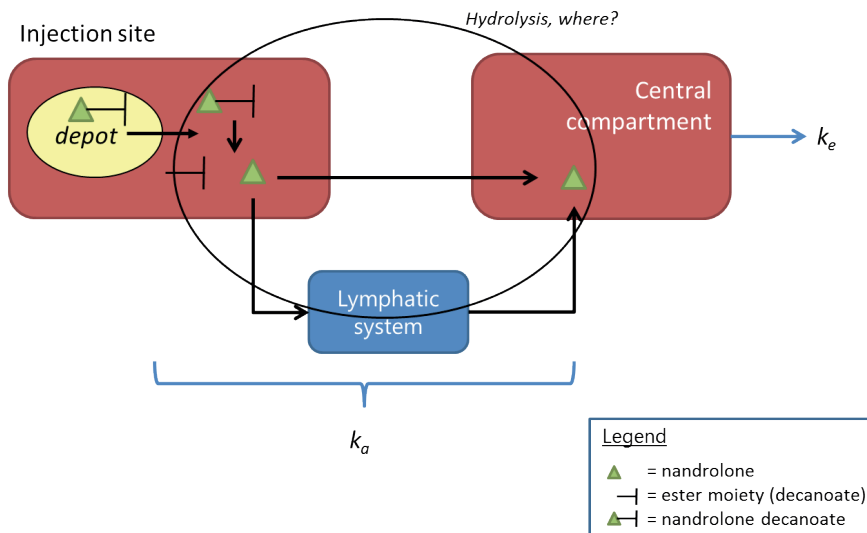


Figure 7.1: Schematic overview of the mechanism of drug absorption from oil depots until now. After release from the oil depot (yellow circle at the injection site), it is assumed that the prodrug is hydrolysed in serum. If this occurs locally, the active substance can be absorbed directly into the central compartment. Otherwise, the prodrug can be hydrolysed in the lymphatic system or at the end of the pathway in the central compartment. These pathways were already suggested by *Larsen et al.* (48).  $k_a$  = absorption rate constant;  $k_e$  = elimination rate constant.

### Lag time

The *in vitro* study by *Thing et al.* (36), showed that immediate appearance of naproxen (a model compound in the used oil depot) was observed in the acceptor phase when the oil depot was brought on this aqueous phase. Based on these results, our work started to study this phenomenon in humans. *Chapter 3* shows the *in vivo* absorption kinetics of benzyl alcohol (BOH) and nandrolone (N). In this chapter, a clinical study was conducted with a subcutaneously (s.c.) injected oil depot with BOH and nandrolone decanoate (ND). Both compounds have a relatively low molecular weight (<500 Da), but differ in lipophilicity: The first compound has a log P of 1.1 (86), whereas the second has a log P of 8.1 (86). Note that nandrolone decanoate is the prodrug of nandrolone, which has a log P of 3.0 (86). It is the ND compound that is released from the oil depot, whereas it is the nandrolone (the parent compound) that was measured in blood.

Interestingly, BOH was absorbed instantaneously, which is comparable with the *in vitro* release of naproxen. Nandrolone absorption was however much slower: there appeared to be a *lag time* of approximately 8 hours. Furthermore, BOH was fully absorbed within 52 hours after injection. This in contrast to the nandrolone, which was absorbed for approximately 40% within 35 days after injection. Both differences in absorption were remarkable and not immediately understood. A literature study was therefore conducted to investigate absorption kinetics of drugs from administered oil depots. Unfortunately, no clinical study was included that used s.c. administered oil depots, therefore only absorption kinetics of drug from intramuscularly (i.m.) injected oil depots were studied. All included studies administered oil depots with prodrugs (nandrolone decanoate, nandrolone phenylpropionate, haloperidol decanoate and testosterone undecanoate). All these prodrugs contain an ester bond with fatty acids, which increases the lipophilicity of the parent compound (*Chapter 3*).

Similar to the nandrolone absorption in our clinical study, the absorption of the other parent compounds occurred also slowly: in all studies, a *lag time* was noticed. These *lag times* varied between 2.6-29.8 hours after injection. This was unexpected, because *Wijnand et al.* (32) assumed that hydrolysis occurs in human serum and it therefore also may occur locally (based on research of *Van der Vies* (88), see details in *Chapter 3* and 6). Moreover, the prodrugs were expected to be partially hydrolysed directly after release from the oil depot to parent compounds (Figure 7.1). These parent compounds have log P's between 2.6-3.3 (86), which is assumed to lead to direct absorption into the systemic circulation. This assumption is based on a paper by *Porter and Charman* which showed that small molecules (<2000 Da) with a log P under five enter the systemic circulation directly after oral ingestion (92). These substances can easily pass capillary walls which result in instantaneous absorption into the systemic circulation (93). Analogous to oral absorption, we suggest that parenterally administered compounds can immediately enter the bloodstream when they meet the two chemical criteria towards molecular weight and log P. As noticed in our study (*Chapter 3*), the assumed direct absorption did not occur *in vivo*, which indicates that either the results of *Porter et al.* are not

applicable for parenteral administrations, or that prodrugs are not hydrolysed near the site of injection. Because this dissertation aims to unravel the fundamental mechanisms of drug absorption from oil depots, a logical next step was to initiate a hydrolysis study with prodrugs to examine this process locally.

### Hydrolysis of prodrug

After injection of the oil depot into tissue, the prodrug is transferred to the interstitial space, in which the oil depot is injected. Prodrugs, being ester compounds, can spontaneously be hydrolysed by water or actively be hydrolysed by carboxylesterases (136,137,139). Carboxylesterases have a molecular weight of approximately 60 kDa (139). This size already predicts that the likelihood of prodrug hydrolysis in the interstitial fluid will be low; Interstitial fluid originates from blood plasma, and it contains water and molecules of approximately 40 kDa molecular weight (34). Thus, when carboxylesterases would be present in human blood plasma, they would most probably not appear in the interstitial fluid. The carboxylesterase activity in human blood, plasma and serum was examined *in vitro* with the model compound (ND) which was incubated at 37°C. The degradation of ND and the appearance of the parent compound (nandrolone, N) were determined.

*Chapter 6* shows that carboxylesterases are absent in human blood plasma and serum, as the ND did not hydrolyse to N in these media. Moreover, the prodrug remained intact during 5 hours of incubation at 37°C, which indicates that even chemical ND hydrolysis did not significantly occur. In contrast, ND hydrolysis was observed in human whole blood. Remarkably, this was not immediate but after a *hydrolysis lag time* of approximately 35 minutes. Immediate ND hydrolysis only occurred in the positive control samples (human whole blood, plasma and serum) in which carboxylesterases were added. These combined results demonstrate that the carboxylesterases that are responsible for ND hydrolysis are located intracellularly.

Muscular or subcutaneous cells surround the oil depot after its injection. In general, it is possible that a prodrug (e.g. ND) is absorbed by such cells after its release from the oil depot. The hydrolysis study was therefore expanded to examine ND hydrolysis with muscular and subcutaneous tissues from pigs. It was found that the contribution to the hydrolysis can be neglected, as only a small fraction of N appeared after 3 and 5 hours of incubation with muscular tissue while no hydrolysis was observed for the subcutaneous tissue. This is explained by the poor permeability characteristics of the extremely lipophilic prodrug, which limits the penetration into the surrounding cells in the tissue.

These poor permeability characteristics of the lipophilic prodrugs limits its contact area with these cells to basically the surface area of the administered oil depot. This surface area is also relevant for the diffusion process which takes place in advance in order to allow intracellular hydrolysis. For a 0.5 mL and 1.0 mL oil depot, these surface areas were respectively 755.4 and 1466.5 mm<sup>2</sup> (see *Chapter 4* and *5*). These numbers are extremely

low compared to the total surface area of erythrocytes, which are cells that are suggested to have a significant contribution in ND hydrolysis (*Chapter 6*). The total surface area of  $4.9 \times 10^{15}$  erythrocytes/mL blood is expected to be  $3.0 \times 10^{15} \text{ mm}^2$  per 5 L blood (the diameter and height of an erythrocyte is respectively 7 and 2  $\mu\text{m}$  (154)). This much larger surface area increases the prodrug rate of membrane diffusion into erythrocytes. Thus, the likelihood for intracellular hydrolysis of prodrugs in erythrocytes is much higher compared to tissue cells due to a larger total surface area of the large number of erythrocytes per mL blood.

It is argued that no significant hydrolysis is expected to occur in interstitial fluid due to the apparent absence of carboxylesterases in human plasma and the poor permeability properties of ND into tissue cells. This means that there is no local conversion of the prodrug to the parent compound. Therefore, it is the prodrug that has to travel to the central circulation. Direct absorption of prodrugs into the central compartment seems very unlikely due to the poor permeability characteristics. Consequently, absorption of these prodrugs must be carried out by the lymphatics system. The migration time from the injection site towards the central compartment will take time. Together with the *hydrolysis lag time* this will contribute to the *overall lag time*. This will be discussed further below.

### Biphasic absorption

The nandrolone pharmacokinetic profile as depicted in *Chapter 3* is characterized by two peak concentrations after a single injection. This suggests a biphasic absorption of nandrolone.

The likely cause of the biphasic pharmacokinetic profile is the presence of BOH. *Chapter 3* shows that the first nandrolone peak at 22 h post-injection coincides with a peak in BOH level, after which both substances show a decline in serum concentration. Basically, this means that the ND partition coefficient between oil and aqueous phase increases because of the presence of BOH in the surrounding aqueous phase. This continues during the release of BOH until full depletion in a few days. During the increase in oil lipophilicity, the molar release rate will decrease, because the more lipophilic ND prefers the oil phase above the aqueous phase. In addition, also the viscosity of the oil depot changes ( $\uparrow$ ) during BOH release, which influences the diffusion coefficient ( $\downarrow$ ) and therefore also the molar release rate ( $\downarrow$ ) of ND.

These types of biphasic absorption profiles from oil depots are described in literature by *Jann et al.* (84). These authors reported in a review that the first peak was thought to be associated with the presence of a certain quantity of parent compound in the formulation, i.e. the substance without the ester moiety. In our clinical study, no additional peaks were obtained during quality control analysis of the investigational medicinal product (IMP). This indicates that no significant amount of parent compound exists in the IMP that may cause the first nandrolone peak.

### Absorption rate constant and the role of the surface area of the oil depot

A logical outcome of an increase in interfacial area between the immiscible oil and aqueous phases is that the molar release rate also will increase. This is a consequence of the assumption that the release is diffusion controlled (see Equation in Figure 3.1 in *Chapter 3*). This is also reported by *Thing et al.* (36) in an *in vitro* model (see Figure 1.6 in *Chapter 1*). The molar release rate and absorption rate constant are not exchangeable however, because the first only plays a role in the mass transfer between the two immiscible liquids, whereas the latter includes also the remaining pathway for absorption. The absorption rate constants ( $k_a$ ) of equal ND oil depots (1 mL, 100 mg/mL) were compared in our literature study (*Chapter 3*). One study injected the depot in the vastus lateralis muscle, two in the gluteal muscle and one in the deltoid muscle. It appeared that the  $k_a$  of nandrolone was the highest when the oil depot was injected in the vastus lateralis, followed by the oil depots injected in the gluteal muscle and deltoid muscle. Until now, an explanation was lacking. This was the reason to study the *in situ* 1) surface area and 2) the disappearance rate of the injected oil depot (1 mL, placebo) in the vastus lateralis and deltoid muscle (*Chapter 5*).

The combined results of *Chapters 4* and *5* show that there are no significant differences between the surface area's of oil depots injected in different muscles. Furthermore, these oil depots disappeared at the same rate from the different injection sites. Thus, the different rates of absorption cannot be explained by the local tissue effects. Consequently, this suggests there are possible *body characteristics* that play a role here. This will be discussed in the next paragraph.

### Contribution of BOH

Benzyl alcohol (BOH), as stated in *Chapter 1*, functions in oil depots as an oil viscosity reducer, prodrug solubility enhancer and local anaesthetic. This commonly used excipient also provides a (temporarily) solubility enhancement to the prodrug in the interstitial fluid. As discussed, a very low portion of the prodrug is hydrolysed in cells near the injection site. It is shown that BOH inhibits carboxylesterases both extra and intracellularly (*Chapter 6*). BOH, as a small molecule, can permeate through the cells near the injection site and therefore also inhibit intracellular carboxylesterases. Clearly, the chance for the released prodrugs to be hydrolysed locally is very low.

During the first 52-hours, BOH exhibits three main effects for drug absorption from oil depots, it:

1. enhances the solubility for prodrugs in the interstitial fluid. The result is that a relatively large amount of prodrug will be released from the oil depot;
2. inhibits the carboxylesterases locally. This lowers the chance of local hydrolysis even more;
3. increases the oil viscosity, which will result in a decrease of the prodrug compound release rate from the oil depot.

Oil depots with BOH were observed to cause a slight formation of a collagen matrix around the site of injection in rats. This in contrast to the injection site whereby the oil depot without BOH was administered. Although it is known that this collagen matrix is formed by activated fibroblasts (124,125), the effect of BOH on fibroblasts remains an aspect for further research.

#### Oil depot disappearance

*Chapter 5* characterized the oil depots in the deltoid and vastus lateralis muscle. It was shown that these oil depots had an equal surface area directly after injection. The histology study in rats showed that fractions of the oil depot remained at the site of injection after 31 days of injection. Unfortunately, the resolution of the MRI scanner was too low to determine these small fractions of the oil depot *in situ* in humans. This means that the oil depot may be emulsified in the interstitial space as suggested in *Chapter 4*; When changing the cut-off voxel intensity value from 0.5 to 0.3 (= if 30% of the voxel contained fat, it was marked as an oil fraction), there appeared to be residual oil present. The results did not elucidate the role of the surface area to the release and absorption parameters of drugs from oil depots. Furthermore, it is still unknown how the oil depot disappears.

It is known that (ingested) fats are transported by chylomicrons and very-low density lipoproteins from the liver towards body tissues (155). It is therefore logical that these transporters could also clear the oil depot from the interstitial space. However, these transporters are absent in interstitial fluid (155), which makes oil clearance via this mechanism impossible from the interstitial space. Thus, it remains open for further research how the oil is cleared from the injection site.

### Role of the immune system

The role of the immune system towards sustained release of compounds from parenteral drug products has been recognized (129). *Darville et al.* studied the effect of macrophage infiltration to drug absorption of suspension injections. Here, clodronate was co-administered to inhibit the recruitment of macrophages towards the injection site. They reported that an infiltration of macrophages from blood towards the injection site caused a significant decrease in  $C_{max}$  of the active substance, but an insignificant altered  $T_{max}$  compared to the group with co-administered clodronate. This was probably caused by phagocytosis of solid particles by macrophages (156). Although we have not specifically focussed on immune responses, histologic examination of tissues after injection of oil depots revealed some similar results: Invasion of lymphocytes, granulocytes and histiocytes were seen at day 1 after an oil depot was injected (*Chapter 5*), which could therefore cause a significant contribution to drug absorption from oil depots.

It is unclear if macrophages also phagocytose small oil droplets like they do with crystals. This could also influence the oil depot disappearance (see paragraph above). If this occurs, this may have a (negative) consequence on the presence of prodrug compounds, which are dissolved in the oil. One could imagine that phagocytosed prodrugs are metabolized inside the macrophages due to the intracellular digestion processes (157,158). This would result in a decreased amount of prodrug and eventually the parent compound (*active substance*) in the central compartment. This may explain the low recoveries of the active substances in all administered oil depots (*Chapter 3*). Moreover, an oil depot with a higher injection volume resulted in a lower active substance recovery when the other conditions remained unchanged (drug load, prodrug and site of injection): a 4 mL injection of ND in the gluteal muscle yielded 45% of nandrolone in contrast to 61% nandrolone with a 1 mL ND injection. This difference can on the one hand be due to a higher amount of BOH in the 4 mL oil depot, as BOH increases the immune response at the site of injection (*Chapter 5*). On the other hand, a higher injection volume may cause more irritation locally and therefore also causes an increased immune response. More research needs to be done to relate this outcome to the involvement of the immune system with regard to drug absorption from oil depots.

### NEW INSIGHTS INTO DRUG ABSORPTION FROM OIL DEPOTS

This dissertation provides new insights into drug absorption from oil depots. Figure 7.1, which was the assumed model before these new findings, is adapted to Figure 7.2. Here, it is shown that the released prodrug (ND) is not hydrolysed locally (*Chapter 6*), but remains unchanged in interstitial fluid. Here, it is logical to assume that the lipophilic prodrug adheres to small proteins (<40 kDa) and subsequently drained with the interstitial fluid into the lymph vessels. Alternatively, it cannot be excluded that small oil droplets might be detached from the main oil depot (*Chapter 4*) and cleared through the lymph. In both ways, ND will end up in the final lymph node to enter the *vena cava superior* to meet blood cells in the central compartment. These blood cells will finally hydrolyse the prodrug compound to nandrolone.

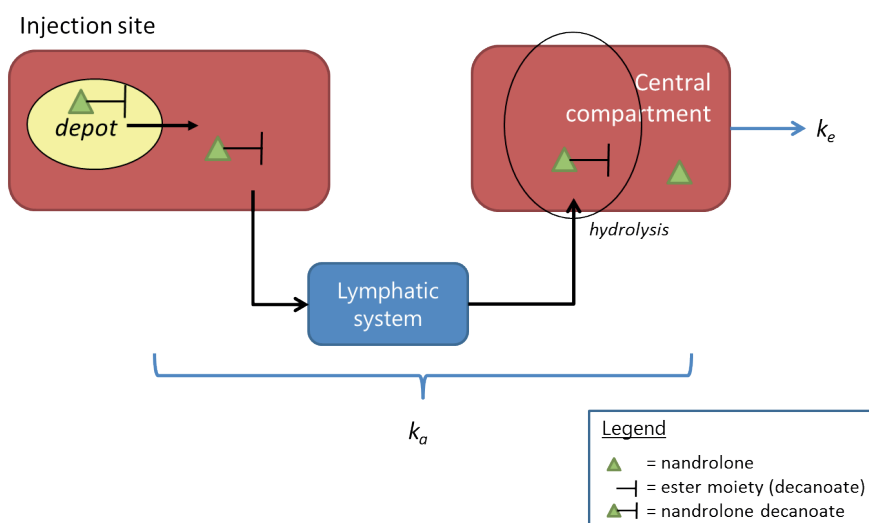


Figure 7.2: Schematic overview of the new insights into drug absorption from oil depots. After release from the oil depot (yellow circle at the injection site), the prodrug is transferred towards the central compartment via the lymphatic system. Here, it will be hydrolysed to the active substance (see circle).  $k_a$  = absorption rate constant;  $k_e$  = elimination rate constant.

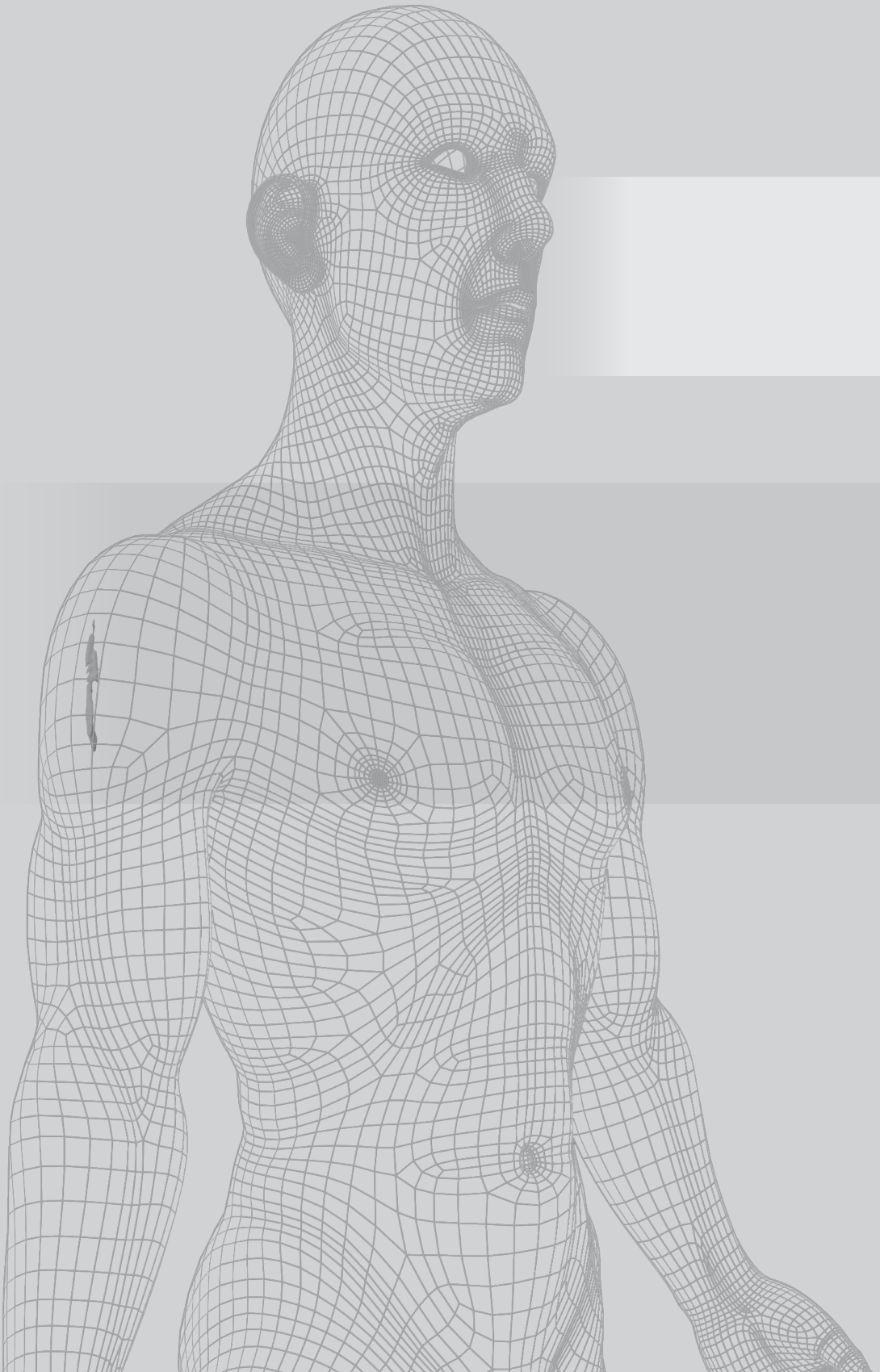
## FUTURE PERSPECTIVES

The open ends of the current research have been indicated above. Both the fate of the oil and the role of the immune system towards drug absorption are still not fully understood. In future research, an option to examine drug release and absorption from an oil depot can be performed with a traceability *in vivo* study. Ideally, 3 tracers would be integrated in the drug product: 1 in the triglyceride structure of the oil components, 1 in the nandrolone molecule and 1 in the decanoic acid moiety. The distinctiveness between these three tracers and between the tissues must obviously be sufficient enough to determine the three compounds separately. The whole process of drug release, hydrolysis and oil digestion could then be followed.

Nowadays, traceability studies can be performed for instance with Single-photon emission computed tomography (SPECT) or PET/MRI-scanners. These imaging techniques use respectively isotopes or fluoride-atoms to visualise compounds *in situ*. Unfortunately, these labeling materials are unsuitable to use in the suggested traceability study, because these materials will alter the physical-chemical properties of either the oil formulation or the prodrug compound. This may change the oil viscosity, drug partition coefficient, spatial distribution in administered tissue or immune response, which may consequently influence the biopharmaceutical aspects of drug absorption from oil depots when these materials are not applied.

## CONCLUSIONS

It is interesting to realize that drug absorption from an oil depot cannot entirely be described by a simple two phase mass transfer model where concentration gradients, diffusion and partition coefficients would enable the calculation of the expected absorption. It is demonstrated in this dissertation that there is a role of the excipient BOH in yielding an initially high absorption. The oil depot forms a continuous phase after injection, but will be dispersed and encapsulated at the injection site after some days. This in turn largely influence the way the prodrug becomes available; after release from the oil depot, it is present in the interstitial fluid which is drained through the lymph into the systemic circulation. Subsequently, the prodrug permeates through the wall of blood cells and is hydrolysed. Both the lymph transport and the cell wall permeation take time which is expressed in a *lag time*. This lag time is different for each injection site: a subcutaneously administered prodrug will enter the systemic circulation via a short path and at a low drainage flow. This results in a short lag time and a slow absorption rate constant of the prodrug. Deeper administered prodrugs (i.e. intramuscular injections) are suggested to be absorbed via a longer path, but at a higher flow, which results in a longer lag time but a higher absorption rate constant of the prodrug.



## Appendix

## References

1. Tausk M. Organon - De geschiedenis van een bijzondere Nederlandse onderneming. Nijmegen: Dekker & van de Vegt; 1978. 510 p.
2. Wood AJJ, Bagatell CJ, Bremner WJ. Androgens in Men — Uses and Abuses. *N Engl J Med*. 1996 Mar 14;334(11):707–15.
3. Overbeek GA, de Visser J. NOR-ANDROSTENOLONEPHENYLPROPIONATE, A NEW POTENT ANABOLIC ESTER. *Eur J Endocrinol*. 1957 Feb 1;24(2):209–19.
4. Van Der Vies J. On the Mechanism of Action of Nandrolone Phenylpropionate and Nandrolone Decanoate in Rats. *Acta Endocrinol (Copenh)*. 1965;49(2):271–82.
5. Geusens P. Nandrolone decanoate: Pharmacological properties and therapeutic use in osteoporosis. *Clin Rheumatol*. 1995 Sep;14(S3):32–9.
6. Wu FCW. Endocrine aspects of anabolic steroids. *Clin Chem*. 1997;43(7):1289–92.
7. Van Der Vies J. Implications of basic pharmacology in the therapy with esters of nandrolone. *Acta Endocrinol Suppl (Copenh)*. 1985;271:38–44.
8. Stubbe, Chorus, Frank, Hon D, Schermers, Heijden van der. *Prestatiebevorderende middelen bij fitnessbeoefenaars*. 2009.
9. Dobs AS, Hoover DR, Chen MC, Allen R. Pharmacokinetic characteristics, efficacy, and safety of buccal testosterone in hypogonadal males: A pilot study. *J Clin Endocrinol Metab*. 1998;83(1):33–9.
10. Kim S, Snipes W, Hodgen GD, Anderson F. Pharmacokinetics of a single dose of Buccal testosterone. *Contraception*. 1995 Nov;52(5):313–6.
11. Slater CC, Souter I, Zhang C, Guan C, Stanczyk FZ, Mishell DR. Pharmacokinetics of testosterone after percutaneous gel or buccal administration. *Fertil Steril*. 2001;76(1):32–7.
12. van Rooij K, Bloemers J, de Leede L, Goldstein I, Lentjes E, Koppeschaar H, et al. Pharmacokinetics of three doses of sublingual testosterone in healthy premenopausal women. *Psychoneuroendocrinology*. Elsevier Ltd; 2012 Jun;37(6):773–81.
13. Morgentaler A, Dobs AS, Kaufman JM, Miner MM, Shabsigh R, Swerdloff RS, et al. Long Acting Testosterone Undecanoate Therapy in Men With Hypogonadism: Results of a Pharmacokinetic Clinical Study. *J Urol*. American Urological Association; 2008 Dec;180(6):2307–13.
14. Geneesmiddel Informatie Centrum van de KNMP. *Informatorium Medicamentorum 2016*. Den Haag: Koninklijke Nederlandse Maatschappij ter bevordering der Pharmacie; 2016.
15. Anatsol decanoate - Summary of Product Characteristics (SPC). [cited 2016 Jul 1]. Available from: <http://db.cbg-meb.nl/IB-teksten/h06170.pdf>
16. Haldol decanoas - Summary of Product Characteristics (SPC). [cited 2016 Jul 1]. Available from: <http://db.cbg-meb.nl/IB-teksten/h08994.pdf>
17. Impromen decanoas - Summary of Product Characteristics (SPC). [cited 2016 Jul 1]. Available from: <http://db.cbg-meb.nl/IB-teksten/h10194.pdf>
18. Cisordinol Depot - Summary of Product Characteristics (SPC). [cited 2016 Jul 1]. Available from: <http://db.cbg-meb.nl/IB-teksten/h07288.pdf>
19. Fluaxol Depot - Summary of Product Characteristics (SPC). [cited 2016 Jul 1]. p. 1–11. Available from:

- <http://db.cbg-meb.nl/IB-teksten/h07228.pdf>
20. Deca-Durabolin - Summary of Product Characteristics (SPC). [cited 2016 Jul 1]. Available from: <http://db.cbg-meb.nl/IB-teksten/h00126.pdf>
  21. Faslodex - Summary of Product Characteristics (SPC). [cited 2016 Jul 1]. Available from: [http://www.ema.europa.eu/docs/nl\\_NL/document\\_library/EPAR\\_-\\_Product\\_Information/human/000540/WC500021174.pdf](http://www.ema.europa.eu/docs/nl_NL/document_library/EPAR_-_Product_Information/human/000540/WC500021174.pdf)
  22. Androcur Depot - Summary of Product Characteristics (SPC). [cited 2016 Jul 1]. Available from: <http://db.cbg-meb.nl/IB-teksten/h07529.pdf>
  23. Nebido - Summary of Product Characteristics (SPC). [cited 2016 Jul 1]. Available from: <http://db.cbg-meb.nl/IB-teksten/h30794.pdf>
  24. Sustanon - Summary of Product Characteristics (SPC). [cited 2016 Jul 1]. Available from: <http://db.cbg-meb.nl/IB-teksten/h00027.pdf>
  25. Artecef - Summary of Product Characteristics (SPC). [cited 2016 Jul 1]. Available from: <http://db.cbg-meb.nl/IB-teksten/h24881.pdf>
  26. Rowe RCR, Sheskey PJS, Cook W. Handbook Pharmaceutical Excipients, Sixth Edition. Seventh ed. London: Pharmaceutical Press; 2009. 1064 p.
  27. Rodger MA, King L. Drawing up and administering intramuscular injections: a review of the literature. *J Adv Nurs*. 2000 Mar;31(3):574–82.
  28. Mathaes R, Koulov A, Joerg S, Mahler H-C. Subcutaneous Injection Volume of Biopharmaceuticals—Pushing the Boundaries. *J Pharm Sci*. Elsevier Ltd; 2016 Aug;105(8):2255–9.
  29. Kadir F, Seijssener CBJ, Zuidema J, Zuideman J. Influence of the injection volume on the release pattern of intramuscularly administered propranolol to rats. *Int J Pharm*. 1992;81(2–3):193–8.
  30. Minto C, Howe C, Wishart S, Conway A, Handelsman D. Pharmacokinetics and pharmacodynamics of nandrolone esters in oil vehicle: effects of ester, injection site and injection volume. *J Pharmacol Exp Ther*. 1997;281(1):93–102.
  31. Ballard BE. Biopharmaceutical Considerations in Subcutaneous and Intramuscular Drug Administration. *J Pharm Sci*. Elsevier Masson SAS; 1968 Mar;57(3):357–78.
  32. Wijnand HP, Bosch AMG, Donker CW. Pharmacokinetic parameters of nandrolone (19-nortestosterone) after intramuscular administration of nandrolone decanoate (Deca-Durabolin(R)) to healthy volunteers. *Eur J Endocrinol*. 1985 Dec 1;110(3 Suppl):S19–30.
  33. Bagchus WM, Smeets JMW, Verheul HAM, De Jager-Van Der Veen SM, Port A, Geurts TBP. Pharmacokinetic evaluation of three different intramuscular doses of nandrolone decanoate: Analysis of serum and urine samples in healthy men. *J Clin Endocrinol Metab*. 2005 May;90(5):2624–30.
  34. Charman WN, Stella VJ. Lymphatic transport of Drugs. Florida: CRC Press; 1992. 352 p.
  35. Larsen SW, Østergaard J, Friberg-Johansen H, Jessen MNB, Larsen C. In vitro assessment of drug release rates from oil depot formulations intended for intra-articular administration. *Eur J Pharm Sci*. 2006 Dec;29(5):348–54.
  36. Thing M, Larsen C, Østergaard J, Jensen H, Larsen SW. In vitro release from oil injectables for intra-articular administration: Importance of interfacial area, diffusivity and partitioning. *Eur J Pharm Sci*.

- Elsevier B.V.; 2012 Feb 14;45(3):351–7.
37. Larsen SW, Thomsen AE, Rinvar E, Friis GJ, Larsen C, Weng Larsen S, et al. Effect of drug lipophilicity on in vitro release rate from oil vehicles using nicotinic acid esters as model prodrug derivatives. *Int J Pharm.* 2001;216(1–2):83–93.
  38. Larsen SW, Larsen C. Critical Factors Influencing the In Vivo Performance of Long-acting Lipophilic Solutions—Impact on In Vitro Release Method Design. *AAPS J.* 2009 Dec 6;11(4):762–70.
  39. Haan F De. Transport rate constants and transport rate parameters in various organic solvent—water systems. *Int J Pharm.* 1982;13:75–87.
  40. Tanaka T, Kobayashi H, Okumura K, Muranishi S, Sezaki H. Intramuscular absorption of drugs from oily solutions in the rat. *Chem Pharm Bull (Tokyo).* 1974;22(6):1275–84.
  41. SHAFFER LW. THE FATE OF INTRAGLUTEAL INJECTIONS. *Arch Dermatol.* 1929 Mar;19(3):347.
  42. Zuidema J, Kadir F, Titulaer H a C, Oussoren C. Release and absorption rates of intramuscularly and subcutaneously injected pharmaceuticals (II). *Int J Pharm.* 1994;105(3):189–207.
  43. Charman WN, Stella VJ. Transport of lipophilic molecules by the intestinal lymphatic system. *Adv Drug Deliv Rev.* 1991 Jul;7(1):1–14.
  44. Kadir F, Zuidema J, Pijpers A, Vulto A, Verheijden JHM. Drug lipophilicity and release pattern of some beta-blocking agents after intra-adipose injection in pigs. *Int J Pharm.* 1990 Oct;64(2–3):171–80.
  45. Garrett ER. The Bateman Function Revisited: A Critical Reevaluation of the Quantitative Expressions to Characterize Concentrations in the One Compartment Body Model as a Function of Time with First-Order Invasion and First-Order Elimination. *J Pharmacokinet Biopharm.* 1994;22(2):103–28.
  46. Rowland M, Tozer T. *Clinical Pharmacokinetics Concepts and Applications.* 3rd editio. Pennsylvania: Williams & Wilkins; 1995. 601 p.
  47. Zuidema J, Pieters F a. JM, Duchateau GSMJE. Release and absorption rate aspects of intramuscularly injected pharmaceuticals. *Int J Pharm.* 1988;47(1–3):1–12.
  48. Larsen C, Larsen SW, Jensen H, Yaghmur A, Ostergaard J. Role of in vitro release models in formulation development and quality control of parenteral depots. *Expert Opin Drug Deliv.* 2009;6(12):1283–95.
  49. Matsunaga Y, Nambu K, Oh-E Y, Miyazaki H, Hashimoto M. Absorption of intramuscularly administered [<sup>14</sup>C]haloperidol decanoate in rats. *Eur J Drug Metab Pharmacokinet.* 1987 Jul;12(3):175–81.
  50. van Weringh G, Komen BJ, Thieme RE, van der Hoeven RTM, Vos T. Comparative bioavailability study of two haloperidol decanoate containing products. *Pharm World Sci.* 1994;16(6):343–7.
  51. Taylor MJ, Tanna S, Sahota T. In vivo study of a polymeric glucose-sensitive insulin delivery system using a rat model. *J Pharm Sci.* 2010;99(10):4215–27.
  52. Croshaw B. Preservatives for cosmetics and toiletries. *J Soc Cosmet Chem.* 1977;28(1):3–16.
  53. Seddon KR, Stark A. Selective catalytic oxidation of benzyl alcohol and alkylbenzenes in ionic liquids. *Green Chem.* 2002 Apr 16;4(2):119–23.
  54. Final Report on the Safety Assessment of Benzyl Alcohol, Benzoic Acid, and Sodium Benzoate. *Int J Toxicol.* 2001 Jan 3;20(4):23–50.
  55. Gu L, Wang X, Zhang Y, Jiang Y, Lu H, Bi K, et al. Determination of 12 potential nephrotoxicity biomarkers in rat serum and urine by liquid chromatography with mass spectrometry and its application to renal

- failure induced by Semen Strychni. *J Sep Sci.* 2014 May;37(9–10):1058–66.
56. Warth AD. Effect of Benzoic Acid on Growth Yield of Yeasts Differing in Their Resistance to Preservatives. *Appl Environ Microbiol.* 1988;54(8):2091–5.
57. Hazan R, Levine A, Abeliovich H. Benzoic Acid, a Weak Organic Acid Food Preservative, Exerts Specific Effects on Intracellular Membrane Trafficking Pathways in *Saccharomyces cerevisiae* Benzoic Acid, a Weak Organic Acid Food Preservative, Exerts Specific Effects on Intracellular Membr. *Appl Environ Microbiol.* 2004;70(8):4449–57.
58. Tan HSI, Manning MA, Hahn M-K, Tan HGH, Kotagal UR. Determination of benzyl alcohol and its metabolite in plasma by reversed-phase high-performance liquid chromatography. *J Chromatogr B Biomed Sci Appl.* 1991 Jul 17;568(1):145–55.
59. ICH Expert Working Group. Validation of analytical procedures: text and methodology, Q2 (R1). 2005;1994(November 1996).
60. Committee for Medicinal Products for Human Use. Guideline on bioanalytical method validation. EMEA/CHMP/EWP/192217/2009 Rev. 1 Corr. 2\*\*. 2012;44(July 2011):1–23.
61. Penner N, Ramanathan R, Zgoda Pols J, Chowdhury S. Quantitative determination of hippuric and benzoic acids in urine by LC-MS/MS using surrogate standards. *J Pharm Biomed Anal.* Elsevier B.V.; 2010 Aug 1;52(4):534–43.
62. Pan Z, Wang L, Mo W, Wang C, Hu W, Zhang J. Determination of benzoic acid in soft drinks by gas chromatography with on-line pyrolytic methylation technique. *Anal Chim Acta.* 2005 Jul;545(2):218–23.
63. Dong C, Mei Y, Chen L. Simultaneous determination of sorbic and benzoic acids in food dressing by headspace solid-phase microextraction and gas chromatography. *J Chromatogr A.* 2006 Jun 2;1117(1):109–14.
64. Hewala II. Gas-liquid chromatographic and difference spectrophotometric techniques for the determination of benzaldehyde in benzyl alcohol. *J Pharm Biomed Anal.* 1994;12(1):73–9.
65. Sudareva NN, Chubarova E V. Time-dependent conversion of benzyl alcohol to benzaldehyde and benzoic acid in aqueous solutions. *J Pharm Biomed Anal.* 2006 Jun 16;41(4):1380–5.
66. Pérez-Lozano P, García-Montoya E, Orriols a., Miñarro M, Ticó JR, Suñé-Negre JM. A new validated method for the simultaneous determination of benzocaine, propylparaben and benzyl alcohol in a bioadhesive gel by HPLC. *J Pharm Biomed Anal.* 2005;39(5):920–7.
67. Shah VP, Midha KK, Dighe S, McGilveray IJ, Skelly JP, Yacobi A, et al. Analytical methods validation: Bioavailability, bioequivalence, and pharmacokinetic studies. *J Pharm Sci.* 1992 Mar;81(3):309–12.
68. Dasgupta A, Humphrey PE. Gas chromatographic-mass spectrometric identification and quantitation of benzyl alcohol in serum after derivatization with perfluorooctanoyl chloride: A new derivative. *J Chromatogr B Biomed Appl.* 1998;708(1–2):299–303.
69. Gillberg M, Akerstedt T. Body temperature and sleep at different times of day. *Sleep.* 1982;5(4):378–88.
70. Roberts MS, Magnusson BM, Burczynski FJ, Weiss M. Enterohepatic circulation: physiological, pharmacokinetic and clinical implications. *Clin Pharmacokinet.* 2002;41(10):751–90.
71. Brayfield A. *Martindale: The Complete Drug Reference.* 38th ed. London: Pharmaceutical Press; 2014. 4688 p.

72. Hall CM, Milligan DW a, Berrington J. Probable adverse reaction to a pharmaceutical excipient. *Arch Dis Child Fetal Neonatal Ed.* 2004 Mar 1;89(2):F184.
73. Pereira-Caro G, Borges G, van der Hooff J, Clifford MN, Del Rio D, Lean ME, et al. Orange juice (poly) phenols are highly bioavailable in humans. *Am J Clin Nutr.* 2014 Nov;100(5):1378–84.
74. Woiwode W, Wodarz R, Drysch K, Weichardt H. Metabolism of toluene in man: gas-chromatographic determination of o-, m- and p-cresol in urine. *Arch Toxicol.* 1979;43(2):93–8.
75. Bray HG, Thorpe WV, White K. Kinetic studies of the metabolism of foreign organic compounds; the formation of benzoic acid from benzamide toluene, benzyl alcohol and benzaldehyde and its conjugation with glycine and glucuronic acid in the rabbit. *Biochem J.* 1951;48(1):88–96.
76. European Commission. Opinion of the Scientific Committee on Food on Benzyl alcohol Opinion of the Scientific Committee on Food on Benzyl alcohol. 2002;(September):1–15.
77. Ronald A, Docherty D, Broom J, Chambers W. Subarachnoid local anesthetic block does not affect morphine absorption from paired intramuscular and subcutaneous injection sites in the elderly patient. *Anesth Analg.* 1993;76(4):778–82.
78. Vukovich R a, Brannick LJ, Sugerma a a, Neiss ES. Sex differences in the intramuscular absorption and bioavailability of cephadrine. *Clin Pharmacol Ther.* 1975 Aug 1 [cited 2014 Feb 27];18(2):215–20. Available from: <http://europepmc.org/abstract/MED/233954>
79. Soni SM, Wiles D, Schiff a. a., Bamrah JS. Plasma levels of fluphenazine decanoate: Effects of site of injection, massage and muscle activity. *Br J Psychiatry.* 1988;153(SEP):382–4.
80. Wagner JG. Application of the Wagner-Nelson absorption method to the two-compartment open model. *J Pharmacokinet Biopharm.* 1974;2(6):469–86.
81. Kudo S, Ishizaki T. Pharmacokinetics of haloperidol: an update. *Clin Pharmacokinet.* 1999;37(6):435–56.
82. White CM, Ferraro-Borgida MJ, Moyna NM, McGill CC, Ahlberg a W, Thompson PD, et al. The effect of pharmacokinetically guided acute intravenous testosterone administration on electrocardiographic and blood pressure variables. *J Clin Pharmacol.* 1999;39(10):1038–43.
83. Yáñez JA, Remsberg CM, Sayre CL, Forrest ML, Davies NM. Flip-flop pharmacokinetics – delivering a reversal of disposition: challenges and opportunities during drug development. *Ther Deliv.* 2011 May;2(5):643–72.
84. Jann MW, Ereshefsky L, Saklad SR. Clinical pharmacokinetics of the depot antipsychotics. *Clin Pharmacokinet.* 1985;10(4):315–33.
85. Moffat AC, Osselton MD, Widdop B, Watts J. Clarke's analysis of drugs and poisons. fourth edi. London: Pharmaceutical Press; 2003. 2736 p.
86. ChemSpider. 2015. Available from: <http://www.chemspider.com/>
87. O'Neil MJ, Heckelman PE, Koch CB, Roman KJ. The Merck Index: An Encyclopedia of Chemicals. Fourteenth. New Jersey: Merck & Co., Inc; 2006.
88. Van Der Vies J. Model studies in vitro with long-acting hormonal preparations. *Acta Endocrinol (Copenh).* 1970 Aug;64(4):656–69.
89. Olszewski W. Peripheral lymph: formation and immune function. CRC Press; 1985. 167 p. Available from: <http://books.google.com/books?id=cfRqAAAAMAAJ&pgis=1>

90. O'Hagan D, Christy N, Davis S. Particulates and lymphatic drug delivery. In: *Lymphatic Transport of Drugs*. CRC Press; 1992. p. 352.
91. Swartz M a., Fleury ME. Interstitial Flow and Its Effects in Soft Tissues. *Annu Rev Biomed Eng*. 2007 Jan ;9(1):229–56.
92. Porter CJH, Trevaskis NL, Charman WN. Lipids and lipid-based formulations: optimizing the oral delivery of lipophilic drugs. *Nat Rev Drug Discov*. 2007 Mar;6(3):231–48.
93. Porter CJH, Charman S a. Lymphatic transport of proteins after subcutaneous administration. *J Pharm Sci*. 2000 Mar;89(3):297–310.
94. Romagnoli E, Mascia ML, Cipriani C, Fassino V, Mazzei F, D'Erasmus E, et al. Short and long-term variations in serum calcitropic hormones after a single very large dose of ergocalciferol (vitamin D2) or cholecalciferol (vitamin D3) in the elderly. *J Clin Endocrinol Metab*. 2008 Aug ;93(8):3015–20.
95. Andrés A, Rosés M, Ràfols C, Bosch E, Espinosa S, Segarra V, et al. Setup and validation of shake-flask procedures for the determination of partition coefficients (logD) from low drug amounts. *Eur J Pharm Sci*. 2015 May 9 ;76:181–91.
96. Evans EF, Proctor JD, Fratkin MJ, Velandia J, Wasserman a J. Blood flow in muscle groups and drug absorption. *Clin Pharmacol Ther*. 1975;17(1):44–7.
97. Olszewski WL, Engeset a. Intrinsic contractility of prenodal lymph vessels and lymph flow in human leg. *Am J Physiol*. 1980;239(6):H775–83.
98. Bach C, Lewis GP. Lymph flow and lymph protein concentration in the skin and muscle of the rabbit hind limb. *J Physiol*. 1973;235(2):477–92.
99. Renkin E, Wiig H. Limits to steady-state lymph flow rates derived from plasma-to-tissue uptake measurements. *Microvasc Res*. 1994;47(3):318–28.
100. Havas E, Parviainen T, Vuorela J, Toivanen J, Nikula T, Vihko V. Lymph flow dynamics in exercising human skeletal muscle as detected by scintigraphy. *J Physiol*. 1997 Oct 1;504(1):233–9.
101. Ikomi F, Hunt J, Hanna G, Schmid-schönbein GW, Szuba A, Shin WS, et al. Interstitial fluid , plasma protein , colloid , and leukocyte uptake into initial lymphatics Interstitial fluid , plasma protein , colloid , and leukocyte uptake into initial lymphatics. 2014;2060–7.
102. Uchida T, Suzuki T, Sakurai H, Tsutsumi C, Den R, Mimura M, et al. Ten year outcomes of outpatients with schizophrenia on conventional depot antipsychotics. *Int Clin Psychopharmacol*. 2013 Sep;28(5):261–6.
103. Novakovic V, Adel T, Peselow E, Lindenmayer J-P. Long-Acting Injectable Antipsychotics and the Development of Postinjection Delirium/Sedation Syndrome (PDSS). *Clin Neuropharmacol*. 2013 Jan;36(2):59–62.
104. Covell NH, McEvoy JP, Schooler NR, Stroup TS, Jackson CT, Rojas IA, et al. Effectiveness of Switching From Long-Acting Injectable Fluphenazine or Haloperidol Decanoate to Long-Acting Injectable Risperidone Microspheres. *J Clin Psychiatry*. Physicians Postgraduate Press, Inc.; 2012 May 15;73(5):669–75.
105. Edelstein D, Basaria S. Testosterone undecanoate in the treatment of male hypogonadism. *Expert Opin Pharmacother*. Taylor & Francis; 2010 Aug 19;11(12):2095–106.
106. Prettyman J. Subcutaneous or intramuscular? Confronting a parenteral administration dilemma. *MEDSURG Nurs*. 2005;14(2):93–9.

107. Düsterberg B, Nishino Y. Pharmacokinetic and pharmacological features of oestradiol valerate. *Maturitas*. 1982 Dec;4(4):315–24.
108. Shaik IH, Bastian JR, Zhao Y, Caritis SN, Venkataramanan R. Route of administration and formulation dependent pharmacokinetics of 17-hydroxyprogesterone caproate in rats. *Xenobiotica*. 2015;8254(October):1–6.
109. Luo JP, Hubbard JW, Midha KK. Studies on the mechanism of absorption of depot neuroleptics: fluphenazine decanoate in sesame oil. *Pharm Res*. 1997;14(8):1079–84.
110. Larsen SW, Rinvar E, Svendsen O, Lykkesfeldt J, Friis GJ, Larsen C. Determination of the disappearance rate of iodine-125 labelled oils from the injection site after intramuscular and subcutaneous administration to pigs. *Int J Pharm*. 2001 Nov 6;230(1–2):67–75.
111. Nelson KG, Shah AC. Convective diffusion model for a transport-controlled dissolution rate process. *J Pharm Sci*. 1975 Apr;64(4):610–4.
112. Philips Medical Systems. Basic principles of MR imaging. Philips Medical Systems; 2008. 138 p.
113. Ritter F, Boskamp T, Homeyer A, Laue H, Schwier M, Link F, et al. Medical Image Analysis. *IEEE Pulse*. 2011 Nov;2(6):60–70.
114. Kuijf HJ. Image processing techniques for quantification and assessment of brain MRI. Utrecht University, the Netherlands; 2013.
115. Querleux B, Cornillon C, Jolivet O, Bittoun J. Anatomy and physiology of subcutaneous adipose tissue by in vivo magnetic resonance imaging and spectroscopy: Relationships with sex and presence of cellulite. *Ski Res Technol*. 2002 May;8(2):118–24.
116. Ren J, Dimitrov I, Sherry A D, Malloy CR. Composition of adipose tissue and marrow fat in humans by <sup>1</sup>H NMR at 7 Tesla. *J Lipid Res*. 2008 Mar 27;49(9):2055–62.
117. Dixon WT. Simple proton spectroscopic imaging. *Radiology*. 1984;153(1):189–94.
118. Hu HH, Kim H-W, Nayak KS, Goran MI. Comparison of Fat–Water MRI and Single-voxel MRS in the Assessment of Hepatic and Pancreatic Fat Fractions in Humans. *Obesity*. Nature Publishing Group; 2010 Apr 15;18(4):841–7.
119. Ma J. Dixon techniques for water and fat imaging. *J Magn Reson Imaging*. 2008;28(3):543–58.
120. Koivisto VA, Felig P. Effects of Leg Exercise on Insulin Absorption in Diabetic Patients. *N Engl J Med*. 1978 Jan 12;298(2):79–83.
121. Frid A, Ostman J, Linde B, Background C. Hypoglycemia Risk During Exercise After Intramuscular Injection of Insulin in Thigh in IDDM. *Diabetes Care*. 1990 May 1;13(5):473–7.
122. Berger M, Cuppers HJ, Hegner H, Jorgens V, Berchtold P. Absorption Kinetics and Biologic Effects of Subcutaneously Injected Insulin Preparations. *Diabetes Care*. 1982 Mar 1;5(2):77–91.
123. Titulaer H a, Eling WM, Zuidema J. Pharmacokinetic and pharmacodynamic aspects of artelinic acid in rodents. *J Pharm Pharmacol*. 1993 Sep;45(9):830–5.
124. KJAeR M. Role of Extracellular Matrix in Adaptation of Tendon and Skeletal Muscle to Mechanical Loading. *Physiol Rev*. 2004 Apr 1;84(2):649–98.
125. Diegelmann RF, Cohen IK, McCoy BJ. Growth kinetics and collagen synthesis of normal skin, normal scar and keloid fibroblasts in vitro. *J Cell Physiol*. 1979 Feb;98(2):341–6.

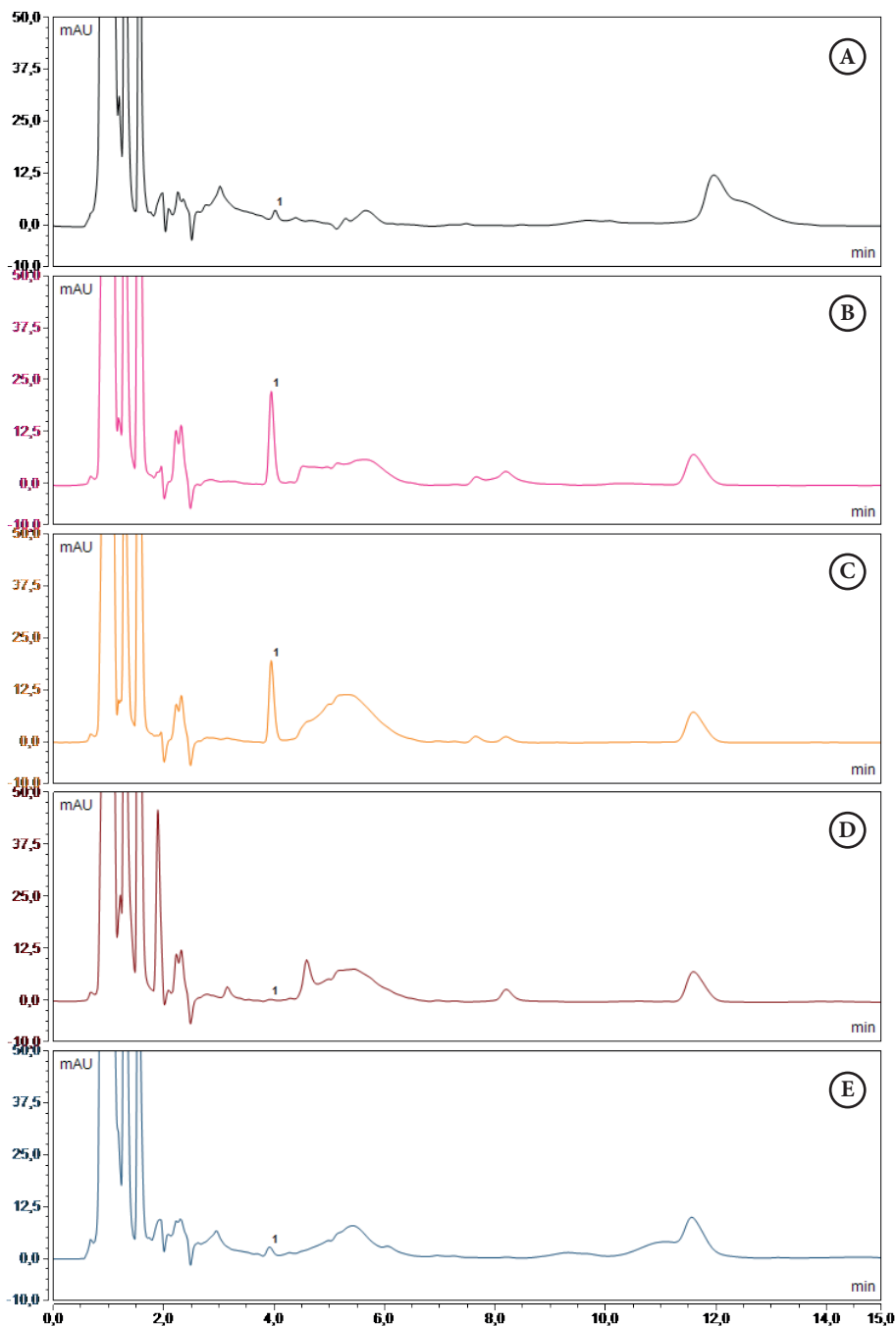
126. Haralambie G. Neuromuscular irritability and serum creatine phosphate kinase in athletes in training. *Int Zeitschrift für Angew Physiol Einschl Arbeitsphysiologie*. 1973;31(4):279–88.
127. Uren RF, Howman-Giles RB, Thompson JF, Roberts J, Bernard E. Variability of cutaneous lymphatic flow rates in melanoma patients. *Melanoma Res*. 1998 Jun;8(3):279–82.
128. Uren RF. Lymphatic Drainage of the Skin. *Ann Surg Oncol*. 2004 Mar 1;11(3\_suppl):179S–185S.
129. Darville N, van Heerden M, Mariën D, De Meulder M, Rossenu S, Vermeulen A, et al. The effect of macrophage and angiogenesis inhibition on the drug release and absorption from an intramuscular sustained-release paliperidone palmitate suspension. *J Control Release*. Elsevier B.V.; 2016;230:95–108.
130. Stanton AWB, Modi S, Bennett Britton TM, Purushotham AD, Peters a. M, Levick JR, et al. Lymphatic drainage in the muscle and subcutis of the arm after breast cancer treatment. *Breast Cancer Res Treat*. 2009 Oct 4;117(3):549–57.
131. Modi S, Stanton AWB, Mortimer PS, Levick JR. Clinical Assessment of Human Lymph Flow Using Removal Rate Constants of Interstitial Macromolecules: A Critical Review of Lymphoscintigraphy. *Lymphat Res Biol*. 2007 Nov;5(3):183–202.
132. Frisoli A, Chaves PHM, Pinheiro MM, Szejnfeld VL. The Effect of Nandrolone Decanoate on Bone Mineral Density, Muscle Mass, and Hemoglobin Levels in Elderly Women With Osteoporosis: A Double-Blind, Randomized, Placebo-Controlled Clinical Trial. *Journals Gerontol Ser A Biol Sci Med Sci*. 2005 May 1;60(5):648–53.
133. Notelovitz M. Androgen effects on bone and muscle. *Fertil Steril*. 2002 Apr;77(4):34–41.
134. Erdsieck RJ, Pols HAP, van Kuijk C, Birkenhäger-Frenkel DH, Zeelenberg J, Kooy PPM, et al. Course of bone mass during and after hormonal replacement therapy with and without addition of nandrolone decanoate. *J Bone Miner Res*. 1994 Dec 3;9(2):277–83.
135. Crawford B a L, Liu PY, Kean MT, Bleasel JF, Handelsman DJ. Randomized placebo-controlled trial of androgen effects on muscle and bone in men requiring long-term systemic glucocorticoid treatment. *J Clin Endocrinol Metab*. 2003;88(7):3167–76.
136. Jewell C, Ackermann C, Payne NA, Fate G, Voorman R, Williams FM. Specificity of procaine and ester hydrolysis by human, minipig, and rat skin and liver. *Drug Metab Dispos*. 2007;35(11):2015–22.
137. Prusakiewicz JJ, Ackermann C, Voorman R. Comparison of skin esterase activities from different species. *Pharm Res*. 2006 Jul ;23(7):1517–24.
138. Li B, Sedlacek M, Manoharan I, Boopathy R, Duysen EG, Masson P, et al. Butyrylcholinesterase, paraoxonase, and albumin esterase, but not carboxylesterase, are present in human plasma. *Biochem Pharmacol*. 2005;70(11):1673–84.
139. Imai T, Ohura K. The role of intestinal carboxylesterase in the oral absorption of prodrugs. *Curr Drug Metab*. 2010;11(9):793–805.
140. Nambu K, Miyazaki H, Nakanishi Y, Oh-e Y, Matsunaga Y, Hashimoto M. Enzymatic hydrolysis of haloperidol decanoate and its inhibition by proteins. *Biochem Pharmacol*. 1987 May 15;36(10):1715–22.
141. Oh-E Y, Miyazaki H, Matsunaga Y, Nambu K, Kobayashi N, Hashimoto M. Hydrolysis of haloperidol decanoate in vitro by cultured cells. *Eur J Drug Metab Pharmacokinet*. 1987 Jul;12(3):183–8.
142. Hatfield MJ, Potter PM. Carboxylesterase inhibitors. *Expert Opin Ther Patents*. 2011;21(8):1159–71.

143. Wiig H, Swartz M a. Interstitial Fluid and Lymph Formation and Transport: Physiological Regulation and Roles in Inflammation and Cancer. *Physiol Rev.* 2012 Jul 1;92(3):1005–60.
144. Rudakova E V., Boltneva NP, Makhaeva GF. Comparative Analysis of Esterase Activities of Human, Mouse, and Rat Blood. *Bull Exp Biol Med.* 2011 Nov 17;152(1):73–5.
145. Quon CY, Stampfli HF. Biochemical properties of blood esmolol esterase. *Drug Metab Dispos.* 1985 Jul 1;13(4):420–4.
146. Lerner SP, Schoenberg M, Sternberg C. *Textbook of Bladder Cancer.* CRC Press; 2006. 816 p.
147. Changjun Liu, Dongwoo Sheen, Kama Huang. A hybrid numerical method to compute erythrocyte TMP in low-frequency electric fields. *IEEE Trans Nanobioscience.* 2003 Jun;2(2):104–9.
148. Scheuplein RJ, Blank IH, Brauner GJ, Macfarlane DJ. Percutaneous Absorption of Steroids\*. *J Invest Dermatol.* 1969 Jan;52(1):63–70.
149. Livingston JN, Lerea KM, Bolinder J, Kager L, Backman L, Arner P. Binding and molecular weight properties of the insulin receptor from omental and subcutaneous adipocytes in human obesity. *Diabetologia.* 1984 Oct;27(4):447–53.
150. Calvillo L, Latini R, Kajstura J, Leri A, Anversa P, Ghezzi P, et al. Recombinant human erythropoietin protects the myocardium from ischemia-reperfusion injury and promotes beneficial remodeling. *Proc Natl Acad Sci.* 2003 Apr 15;100(8):4802–6.
151. Smith U, Sjöström L, Björnorp P. Comparison of two methods for determining human adipose cell size. *J Lipid Res.* 1972;13:822–4.
152. Pcaathol JC, Slavin G. diameters using interactive computer-aided. 1982;1268–71.
153. Harada T, Nakagawa Y, Wadkins RM, Potter PM, Wheelock CE. Comparison of benzil and trifluoromethyl ketone (TFK)-mediated carboxylesterase inhibition using classical and 3D-quantitative structure-activity relationship analysis. *Bioorganic Med Chem.* Elsevier Ltd; 2009;17(1):149–64.
154. Zhao Y, Sun X, Zhang G, Trewyn BG, Slowing II, Lin VS-Y. Interaction of Mesoporous Silica Nanoparticles with Human Red Blood Cell Membranes: Size and Surface Effects. *ACS Nano.* 2011 Feb 22;5(2):1366–75.
155. Randolph GJ, Miller NE. Lymphatic transport of high-density lipoproteins and chylomicrons. *J Clin Invest.* 2014;124(3):929–35.
156. Darville N, van Heerden M, Erkens T, De Jonghe S, Vynckier A, De Meulder M, et al. Modeling the Time Course of the Tissue Responses to Intramuscular Long-acting Paliperidone Palmitate Nano-/Microcrystals and Polystyrene Microspheres in the Rat. *Toxicol Pathol.* 2016;44(2):189–210.
157. Allison AC. AN EXAMINATION OF THE CYTOTOXIC EFFECTS OF SILICA ON MACROPHAGES. *J Exp Med.* 1966 Aug 1;124(2):141–54.
158. Gordon S. INDUCTION OF MACROPHAGE PLASMINOGEN ACTIVATOR BY ENDOTOXIN STIMULATION AND PHAGOCYTOSIS: Evidence for A Two-Stage Process. *J Exp Med.* 1974 Oct 1;140(4):995–1010.

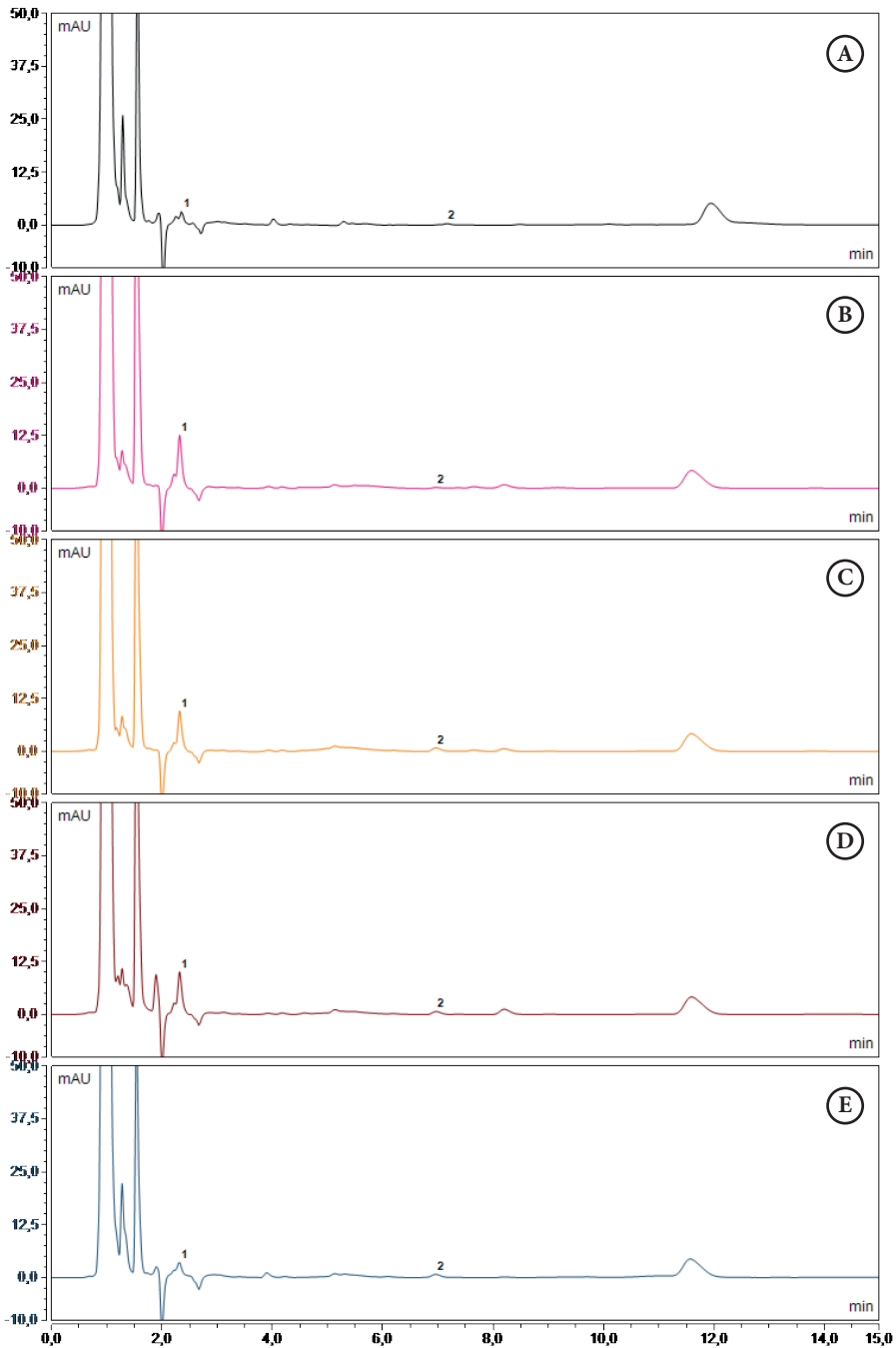
---

## Supplementary data Chapter 3

A



Representative chromatograms. A = blank newborn calf serum; B = serum sample of a random volunteer at t = 0 min; C = serum sample of a random volunteer at t = 22 min; D = serum sample of a random volunteer at t = 96 min; E = newborn calf serum spiked with benzyl alcohol at a concentration of 0.1 µg/mL (Limit of Quantitation). All detected at  $\lambda = 207$  nm. 1 = benzyl alcohol



Representative chromatograms. A = blank newborn calf serum; B = serum sample of a random volunteer at  $t = 0$  min; C = serum sample of a random volunteer at  $t = 22$  min; D = serum sample of a random volunteer at  $t = 96$  min; E = newborn calf serum spiked with hippuric acid (1) and benzoic acid (2) at a concentration of  $0.1 \mu\text{g/mL}$  (Limit of Quantitation). All detected at  $\lambda = 230 \text{ nm}$ . 1 = hippuric acid; 2 = benzoic acid



## Summary

Sustained delivery formulations are used in order to prolong the pharmacological activity of a drug. A commonly used parenteral sustained delivery formulation is an *oil depot* which consists of a solution of lipophilic molecules in a vegetable oil. These are normally administered either intramuscularly (i.m.) or subcutaneously (s.c.).

The idea of the formulation approach is that a substance that is far better soluble in oil than in water tends to stay in the oil phase. The exact mechanism of drug absorption from these formulations is not fully understood however. The aim of this dissertation was to obtain more understanding about the way a drug is absorbed from an oil depot into the human body.

**Chapter 1** introduces the diverse aspects that may be relevant. It is generally assumed that the drug release from the oil is mainly determined by the substance's partition coefficient, i.e. the ratio between lipid and aqueous solubilities of the drug. In the human body, the aqueous phase is represented by the interstitial fluid, which is located between cell tissue at the site of injection. Logically, the higher the affinity for oil, the lower the tendency a drug will have to leave the oil phase. Consequently, a more pronounced sustained compound release is obtained by an increase of the drugs lipophilicity (i.e. higher partition coefficient). A drug can be made more lipophilic through esterification of the molecule with a fatty acid. This esterified compound is inactive as such and is therefore referred to as *prodrug*. After release from the oil it is activated by hydrolysis, resulting in the so-called *parent compound* or *active substance*, which is responsible for the pharmacological effect. The papers that have been published until now can be distinguished into two different focus points: On the one hand, *in vitro* models examined the prodrug release from the oil depot, which is basically nothing else than a diffusion process through an interface. On the other hand, other studies focused mainly on the pharmacokinetic profiles, i.e. the plasma concentrations of the parent compound. Clearly, the appearance of the parent compound in the blood stream must be considered as a result of a sequence of steps including release out of the oil, hydrolysis of the prodrug and transport to the central circulation. These steps, i.e. the exact fate of the prodrug once released from the oil depot has remained relatively uninvestigated. Therefore, the specific aim of this dissertation is to assess what happens with the prodrug once it is released out of the oil depot.

The partition coefficient of a prodrug can be influenced by some of the pharmaceutical excipients used in oil depots. As a consequence, this might also alter the prodrug release rate from the oil depot. Until now, no studies have examined the influence of excipients in oil depots on the absorption kinetics of the active substance. The effect of the excipient benzyl alcohol is of great interest, because it is processed in nearly all oil depots. As the main function of benzyl alcohol in oil depots is to enhance the solubility of the processed lipophilic prodrugs, there is a rationale to study its influence on drug release.

In **Chapter 2**, a bioassay was developed to measure serum levels of benzyl alcohol and its metabolites benzoic acid and hippuric acid. Using this analytical method, the pharmacokinetic

profiles of benzyl alcohol and its metabolites in healthy volunteers were assessed. The volunteers were subcutaneously injected with an oil depot that contained 10% benzyl alcohol, nandrolone decanoate and cholecalciferol. Benzyl alcohol was immediately detected in blood after injection. The pharmacokinetic profile revealed that benzyl alcohol was fully depleted from the oil depot within 52 hours after injection. It is argued that this depletion may alter the solubility of the lipophilic prodrugs in the oil. Consequently, the partition coefficient and hence the release rate may change rapidly in the first days after injection, but will remain constant hereafter.

**Chapter 3** describes the plasma profiles of nandrolone after subcutaneous administration of an oil depot containing nandrolone decanoate. The data were obtained from the same clinical study as described in Chapter 2. Pharmacokinetic profiles of nandrolone and benzyl alcohol were compared with each other. Benzyl alcohol was absorbed much more rapidly than nandrolone: it was measured in the central compartment immediately after injection, while nandrolone was recovered in blood after a lag time. This lag time is the total time delay between the moment of administration and the systemic appearance of the active substance. The lag time was estimated to be approximately 8 hours. In literature this lag time has also been measured, but it has never been reported explicitly.

The absorption of nandrolone appeared to be enhanced by the presence of benzyl alcohol. This is most likely an effect of altered oil viscosity and partition coefficient of nandrolone decanoate as suggested in Chapter 2. Literature review revealed that the absorption rate constant (= velocity in which a molecule is absorbed into the central compartment) of active substances is indeed determined by the partition coefficient of the solubilized prodrug. This absorption rate constant was demonstrated however not only to be determined by the physico-chemical properties of the oil formulation but also by the tissue properties. When the same nandrolone decanoate depot injection was administered in different muscles, it was shown that the absorption rate constant varied between these muscles.

Chapter 3 provides a mass transfer model, which suggests that not only the partition coefficient, but also the surface area of the oil-water interface is a relevant parameter for the drug release from an oil depot. Logically, a larger surface area will exhibit a higher drug release rate. Although the *in vivo* shape of an oil depot is often assumed to be spherical, it has never been established until now.

In **Chapter 4**, the *in situ* shape and surface area of oil depots were determined using magnetic resonance imaging (MRI). For this purpose, an imaging and quantification method was developed and tested to be suitable for clinical use. Four healthy male volunteers were injected with a 0.5 mL placebo oil in the *biceps branchii*. Instead of a spherical shape, the oil depot was visualized as a thin and oblong shape which seems to be squeezed by the muscle fibres. The mean ( $\pm$ RSD) surface area and volume of the oil measured directly after

injection were respectively  $755.4 (\pm 26.5) \text{ mm}^2$  and  $520.1 (\pm 24.6) \text{ mm}^3$ . Furthermore, the oil disappearance from the injection site was shown to be variable between the four volunteers. In all subjects, no oil was detected anymore after 14 days. This is surprising, since a prolonged pharmacokinetic profile of drugs during 2-4 weeks has been shown (Chapter 1 and 3), which suggests that there is still an oil depot present. It is argued that this discrepancy may be caused by a limitation in sensitivity of the MRI technique. Since small particles cannot be detected, it is well possible that the oil is dispersed into small sized droplets which are not detected.

In **Chapter 5**, we studied the *in situ* surface areas and disappearance rates of oil depots administered in *deltoid* and *vastus lateralis* muscle. These muscles were chosen because different nandrolone absorption rate constants were obtained in clinical studies (Chapter 3), whereas identical oil depots were administered. Again 4 healthy male volunteers were enrolled in a clinical study. These volunteers received a 1.0 mL placebo oil depot in both muscles. All oil depots were equal in volume and surface area directly after injection. This phenomenon was further explored in animals. A study in rats was conducted to microscopically examine the oil immediately after injection and after 31 days. All rats were injected with a 0.1 mL oil depot, with or without benzyl alcohol. The injected oil depots were still microscopically visible as small, separate droplets after 31 days. This led to the conclusion that MRI is obviously not always able to detect the oil, which must be a consequence of the degree to which the oil is dispersed in the tissue; Oil depots with benzyl alcohol were observed to cause a slight formation of collagen matrix around the site of injection. This in contrast to the injection site where the oil depot without benzyl alcohol was administered.

The combined results of **Chapters 4** and **5** show that there are no significant differences between the surface area's of oil depots injected in different muscles. Furthermore, these oil depots disappeared at the same rate from the different injection sites. Thus, the different rates of absorption cannot be explained by the local tissue effects. Consequently, this suggests there are possible body characteristics that play a role here; the collagen formation (as seen in the study in rats) around the separate droplets forms some encapsulation of the oil fractions. This includes all separate droplets and apparently acts as a continuous phase oil depot. The drug release rate is determined by the outer-layer of the assembly of small droplets. Consequently, the droplets in the centre of the encapsulated oil depot have minor contribution to the drug release rate due to a lack of sink conditions. After release from the oil depot, drug absorption from the injection site into the systemic circulation can occur directly via venous blood or indirectly via the lymphatic system. Due to its lipophilic character, it is very likely that a released prodrug is transported via the lymphatic system to the systemic circulation. As will be seen later, prodrug hydrolysis will only occur in blood. Therefore, it is likely that the differences in absorption rate constants are caused by differences in lymphatic transport.

**Chapter 6** investigates where hydrolysis of the prodrug into the parent compound occurs. Hydrolysis is the process in which the ester bond in the prodrug is cleaved into the active (parent) substance and a fatty acid. Hydrolysis can either occur spontaneously in water (chemical hydrolysis) or via carboxylesterases (enzymatic process). Nandrolone decanoate was used again as a model compound. In the literature it is suggested that hydrolysis of nandrolone decanoate occurs in human serum. Until now, the rate of hydrolysis of nandrolone decanoate has hardly been studied in human serum or in any other biological environment.

It was shown that carboxylesterases are absent in human serum and plasma, as the nandrolone decanoate did not hydrolyse to nandrolone. Moreover, the prodrug remained intact during 5 hours of incubation at 37°C, which indicates that chemical hydrolysis of nandrolone decanoate did not occur in this media. The appearance of nandrolone was only observed in human whole blood after an average lag time of  $34.9 \pm 2.5$  minutes. Noticeable was the absence of Michaelis-Menten behaviour, in contrast to the control experiments where carboxylesterases were added to the samples. The results suggest that the carboxylesterases, involved in nandrolone decanoate hydrolysis, must be present in the blood cells since the distinction between whole blood and plasma is the presence of cells. Hydrolysis can occur either on the blood cell membrane, or occurs intracellularly. Because a lag time of nandrolone appearance was noticed, carboxylesterase activity on the cell membrane is apparently not very pronounced. Otherwise, the nandrolone recovery should be seen instantaneously. It can therefore be concluded that hydrolysis occurs intracellularly.

Other cells that may contain carboxylesterases are muscular or subcutaneous cells that are situated around the oil depot. It is imaginable that the prodrug is absorbed by such tissue cells after its release from the oil depot. The hydrolysis study in this chapter was therefore expanded to examine if nandrolone decanoate hydrolysis could be detected with muscular and subcutaneous tissues from pigs. It was found that the contribution to the total nandrolone recovery can be neglected: Only a small fraction of nandrolone appeared after 5 hours of incubation with muscular tissue, while no hydrolysis was observed for the subcutaneous tissue. This is explained by the poor permeability characteristics of the extremely lipophilic prodrug, which limits the penetration into the surrounding cells in the tissue. Of course this also applies for the blood cells. However, blood cells expose a large surface area ( $3.0 \times 10^{15}$  mm<sup>2</sup> per 5 L blood) compared to the surface area of the surrounding cells that equals the *in situ* surface area of oil depots (1.0 mL oil depot has an area of 1466.5 mm<sup>2</sup>). The much larger surface area of blood cells increases the membrane diffusion rate of prodrugs into erythrocytes. Thus, the intracellular hydrolysis of prodrugs in erythrocytes is much higher compared to tissue cells due to a larger total surface area of the large number of erythrocytes in blood. The results in this chapter demonstrate that the carboxylesterases, responsible for nandrolone decanoate hydrolysis, are located intracellularly in blood cells.

**Chapter 7** discusses the results described in this thesis and provides scientific proposals for future research. The findings yield new insights into drug absorption from oil depots. This oil depot forms a continuous phase after injection, but will be dispersed and encapsulated at the injection site after some days. The absorption of drugs starts with the prodrug release from the oil depot. The prodrug is then present in the interstitial fluid which is slowly drained through the lymph into the systemic circulation. Subsequently, the prodrug permeates through the membrane of blood cells and is hydrolysed to the active substance. Both the slow lymph transport and the cell membrane permeation take time which is expressed in a lag time. This *lag time* is different for each injection site: a subcutaneously administered prodrug is thought to enter the systemic circulation via a short path and at a low drainage flow. This results in a short lag time and a slow absorption rate constant of the prodrug. Deeper administered prodrugs (i.e. intramuscular injections) are suggested to be absorbed via a longer path, but at a higher flow, which results in a longer lag time but a higher absorption rate constant of the prodrug.

## Begrippenlijst

**Ester:** Een chemische verbinding van een alcohol met een (carbon) zuur. De samenstelling bestaat vaak uit een geneesmiddel en een onschadelijke stof. Het proces om een esterverbinding te verkrijgen noemt men *verestering*. In de farmaceutische wereld is verestering noodzakelijk om het inactieve molecuul in het lichaam te krijgen en pas na hydrolyse te activeren op de plek waar het nodig is.

**Farmacokinetiek:** Een weerspiegeling van de hoeveelheid geneesmiddel in het bloed als functie van tijd. Hierbij zijn geneesmiddelopname en –uitscheiding van belang.

**Hydrolyse:** Het proces waarbij de esterverbinding uit elkaar valt in een geneesmiddel en een onschadelijke stof. Dit gebeurt vaak spontaan in water, maar het kan ook versneld gebeuren als er enzymen bij betrokken zijn.

**Lipofiel:** Een karaktereigenschap van een stof die liever oplost in een vette omgeving (zoals olie) dan in water.

**Michaelis-Menten gedrag:** Het gedrag dat stoffen vertonen als ze een reactie aangaan met enzymen, zoals in het hydrolyseproces.

**Parenteraal:** Alle toedienroutes van een geneesmiddel die niet via de mond gaan. Meestal synoniem voor een injectie.

**Partiticoëfficiënt:** De verdeling van een stof tussen een olieachtige vloeistof en water. Een stof met een hoge partiticoëfficiënt lost dus relatief makkelijker op in een olieachtige vloeistof dan in water. Een stof met een lage partiticoëfficiënt lost beter op in water dan in olieachtige vloeistoffen.

## Samenvatting

Vertraagde afgifte formuleringen worden gebruikt ter verkrijging van een verlengde farmacologische werking van geneesmiddelen. Een veelgebruikt parenteraal preparaat is een *oliedepot*, welke bestaat uit een olieoplossing van lipofiele moleculen. Deze olieoplossing worden in de spier (intramusculair, i.m.) of onder de huid (subcutaan, s.c.) geïnjecteerd.

Een molecuul dat veel beter oplost in olie dan in water, blijft liever in de olie-fase en heeft een geringe neiging om naar de waterfase te diffunderen. Dat is het idee van deze formuleringsbenadering. Het exacte mechanisme van geneesmiddelabsorptie uit deze formuleringen is helaas nog niet volledig bekend. Het doel van dit proefschrift is daarom om een beter begrip te krijgen hoe geneesmiddelen vanuit oliedepots geabsorbeerd worden in het menselijk lichaam. **Hoofdstuk 1** introduceert de verschillende aspecten die hierbij relevant kunnen zijn. In het algemeen wordt aangenomen dat geneesmiddelafgifte uit oliedepots voornamelijk bepaald wordt door de partiticoëfficiënt van de stof. Deze coëfficiënt geeft de verhouding van oplosbaarheid in olie- en waterfase weer. In het menselijk lichaam wordt met de waterfase de interstitiële vloeistof bedoeld die zich tussen de weefsels op de injectieplek bevindt. Wanneer de affiniteit van de stof hoger is voor de olie, treedt de stof logischerwijs minder snel uit de olie. Hierdoor wordt een duidelijker verlengde geneesmiddelafgifte verkregen door de stof lipofiel te maken (oftewel de partiticoëfficiënt te verhogen). Een geneesmiddel kan lipofiel worden gemaakt door het molecuul te veresteren met een vetzuur. Deze veresterde verbinding is als zodanig inactief en wordt de *prodrug* genoemd. Het is deze stof die afgegeven wordt door het oliedepot. Activatie van de prodrug geschiedt door hydrolyse. Hydrolyse is het proces waarbij de esterverbinding in de prodrug uit elkaar valt. De resulterende verbinding wordt de *moederverbinding* of de *werkzame stof* genoemd, de stof die verantwoordelijk is voor het farmacologisch effect. Onderzoeken die tot nu toe zijn gepubliceerd, hebben zich gericht op de eerste en op de laatste stap van het absorptieproces: Aan de ene kant bestudeerde men *in vitro* (letterlijk: in glas; in het laboratorium) de prodrug-afgifte uit het oliedepot. In feite omvat dit eigenlijk alleen maar het diffusieproces door het grensvlak. Aan de andere kant hebben studies de focus gelegd op de farmacokinetische profielen. Deze profielen tonen het verloop van de concentratie van de moederverbinding in het bloed. De tussenliggende stappen hebben minder aandacht gekregen. Hierbij kan worden gedacht aan het verdwijnen van de olie zelf, de plaats en snelheid van hydrolyse van de prodrug en de wijze van transport naar het bloed. Wat er gebeurt tussen het moment van de prodrug-afgifte en de absorptie van de werkzame stof in het bloed is nog relatief onbekend. Daarom was het specifieke doel van dit proefschrift het onderzoek naar wat er gebeurt met de prodrug wanneer deze is afgegeven uit het oliedepot.

De partiticoëfficiënt van de prodrug kan worden beïnvloed door de aanwezigheid van hulpstoffen in het oliedepot. Deze kan een directe invloed hebben op de prodrug-afgifte uit het oliedepot. Tot nu toe zijn er geen studies die de invloed van hulpstoffen hebben bestudeerd

op de absorptiekinetiek van de werkzame stof. Hierbij is met name benzylalcohol van belang, aangezien deze hulpstof in bijna ieder oliedepot is verwerkt. Benzylalcohol wordt verwerkt in oliedepots om de oplosbaarheid van lipofiele prodrugverbindingen te verhogen. Daarmee is het aannemelijk dat deze hulpstof de geneesmiddelafgifte kan beïnvloeden.

**Hoofdstuk 2** beschrijft een bioanalyse die ontwikkeld is om benzylalcohol en zijn metabolieten benzoëzuur en hippuurzuur in serum te bepalen. Door gebruik te maken van deze bioanalyse werd het farmacokinetisch profiel van benzylalcohol en zijn metabolieten in gezonde vrijwilligers bepaald. In een klinische studie kregen vrijwilligers een subcutane injectie met een oliedepot dat 10% benzylalcohol, nandrolondecanoaat (de veresterde vorm van nandrolon, een spierversterker) en cholecalciferol (vitamine D3) bevatte. Benzylalcohol verscheen meteen na injectie in het bloed. Het farmacokinetisch profiel toonde aan dat binnen 52 uur na injectie alle benzylalcohol uit het oliedepot was afgegeven. Verondersteld kan worden dat door deze volledige depletie de oplosbaarheid van de prodrug in de olie verandert. De verandering in de partiticoëfficiënt kan van invloed zijn op de afgifte van de lipofiele prodrug.

**Hoofdstuk 3** beschrijft de plasmaconcentraties van nandrolon na een subcutaan toegediend oliedepot met nandrolondecanoaat. De data werden verkregen uit dezelfde klinische studie als beschreven in Hoofdstuk 2. De farmacokinetische profielen van nandrolon en benzylalcohol werden met elkaar en met literatuur data vergeleken. Benzylalcohol werd veel sneller geabsorbeerd dan nandrolon: benzylalcohol was meteen na injectie in het bloed aantoonbaar, terwijl nandrolon pas na een zekere tijd in de circulatie verscheen. Deze uitgestelde tijd (*lag time*) was in deze studie voor nandrolon ongeveer 8 uur. Nauwkeurig bestuderen van de literatuurdata laat zien dat dezelfde fenomenen van uitgestelde verschijning in de bloedbaan algemeen plaatsvinden. Tot op heden is dit nooit als zodanig gerapporteerd.

De absorptiesnelheid van nandrolon bleek hoger te zijn in aanwezigheid van benzylalcohol. Het is voor de hand liggend te veronderstellen dat dit het effect is van de snel veranderende concentratie van benzylalcohol in het oliedepot. Met de afgifte van benzylalcohol uit het oliedepot veranderen zowel de olieviscositeit als partiticoëfficiënt voor nandrolondecanoaat.

Dit hoofdstuk gaat verder in op de fundamentele mechanismen voor geneesmiddelabsorptie uit oliedepots. De snelheid van geneesmiddelabsorptie wordt uitgedrukt in de absorptiesnelheidsconstante. Hoe hoger deze constante, hoe sneller de werkzame stof in het bloed terecht komt. Ons onderzoek heeft aangetoond dat de absorptiesnelheidsconstante van werkzame stoffen is gerelateerd aan de partiticoëfficiënt van prodrugs in de oliedepots. De absorptiesnelheidsconstante lijkt niet alleen beïnvloed door de fysisch-chemische eigenschappen van de formulering, maar ook door de anatomische en/of fysiologische omgeving waarin de formulering is ingespoten. In ons onderzoek hebben we aangetoond dat de absorptiesnelheidsconstante van nandrolon niet constant is, maar varieert tussen drie verschillende spieren.

Met de gevonden resultaten wordt een massatransport model voorgesteld dat in hoge mate is gebaseerd op fysisch chemische overwegingen. Naast de partiticoëfficiënt geldt het grensvlak tussen olie en water als een relevante parameter voor prodrug-afgifte uit oliedepots. Een groter oppervlak zorgt logischerwijs voor een hogere afgiftesnelheid. Hoewel de vorm en oppervlakte van de oliedepots na injectie vaak als sferisch worden verondersteld, is er voor zover ons bekend tot dusverre geen uitgebreid onderzoek naar gedaan.

De vorm en oppervlakte van oliedepots werden *in situ* (letterlijk: ter plaatse; in de spier) bepaald met behulp van magnetic resonance imaging (MRI) (**Hoofdstuk 4**). Specifiek voor dit doel werd er een kwantitatieve beeldbepalingsmethode ontwikkeld, welke ook geschikt was voor gebruik in klinisch onderzoek. Vier gezonde, mannelijke vrijwilligers kregen vervolgens een 0,5 mL placebo oliedepot in de bovenarmspier (*biceps brachii*) geïnjecteerd. De eerder veronderstelde sferische vorm werd niet teruggevonden na de intramusculaire injectie. In plaats hiervan werd het oliedepot als een dunne en langwerpige vorm gevisualiseerd, waarbij het erop lijkt dat de vloeistof tussen de vezels van de spieren is gedrukt. Het oppervlak en volume van het oliedepot na injectie waren respectievelijk gemiddeld ( $\pm$  relatieve standaarddeviatie)  $755,4 (\pm 26,5)$  mm<sup>2</sup> en  $520,1 (\pm 24,6)$  mm<sup>3</sup>. Verder werd aangetoond dat de verdwijning van het oliedepot van de plaats van injectie erg varieerde tussen de vier vrijwilligers. In alle gevallen was de olie niet meer detecteerbaar binnen 14 dagen. Dit is verrassend aangezien de gemeten geneesmiddelfgifte tussen de 2 en 4 weken aanhoudt (Hoofdstuk 1 en 3). De discrepantie suggereert dat er wel degelijk nog een depot op de injectieplaats aanwezig kan zijn, maar dat dit niet aangetoond kan worden door een beperkte gevoeligheid van de MRI-techniek. Aangezien kleine oliedruppels met MRI niet kunnen worden gedetecteerd, is het mogelijk dat de olie is gedispergeerd in kleine, niet-detecteerbare oliedruppels.

In **Hoofdstuk 5** onderzochten we de *in situ* oppervlaktes en verdwijningssnelheden van oliedepots in de schouder- en dijbeenspier. Deze spieren werden gekozen vanwege de verschillende absorptiesnelheidsconstanten van actieve stoffen (zie Hoofdstuk 3). Opnieuw werden er vier gezonde, mannelijke vrijwilligers geïncludeerd in een klinisch onderzoek. Elke vrijwilliger kreeg een 1,0 mL placebo oliedepot gespoten in elk van de twee genoemde spieren. Alle oliedepots hadden direct na injectie hetzelfde oppervlak en volume. Verrassend genoeg verdwenen alle oliedepots in alle vrijwilligers binnen één week. Dit fenomeen werd verder bestudeerd in dieren. Een rattenstudie werd uitgevoerd om het oliedepot onder de microscoop te bestuderen. Iedere rat kreeg twee dezelfde 0,1 mL injecties, waarbij er oliedepots met en zonder benzylalcohol werden ingespoten. De oliedepots werden direct en na 31 dagen bestudeerd. De geïnjecteerde olie was in alle ratten na 31 dagen nog zichtbaar als kleine, separate druppels. De formuleringen met benzylalcohol veroorzaakten een lichte vorming van collageen op de injectieplek. Dit was niet waarneembaar bij de injectieplekken waarbij oliedepots zonder benzylalcohol waren gespoten.

De gecombineerde resultaten uit **Hoofdstukken 4** en **5** tonen aan dat er geen significant verschil is tussen de verdwijningssnelheden van oliedepots die zijn geïnjecteerd in verschillende

spieren. Dit geeft dit aan dat de verschillende absorptiesnelheidsconstanten een fysiologische oorzaak hebben. Het collageen (zoals gezien in de rattenstudie) rond de afzonderlijke oliedruppels vormen een inkapseling van deze oliefracties, dat met MRI schijnbaar een geheel is. De geneesmiddelafrgifte wordt bepaald door de buitenste laag van deze separate druppels. In het midden van de inkapseling hebben de oliefracties een lagere bijdrage aan de geneesmiddelafrgifte, omdat er minder waterfase beschikbaar is voor de prodrug om in op te lossen (de zogenoemde *sinkcondities* zijn er niet). Na afgifte uit het oliedepot begint het proces van geneesmiddelabsorptie vanuit de plaats van injectie. Het transport naar de systemische circulatie kan direct via afvoerend bloed of indirect via het lymfatisch systeem plaatsvinden. Dankzij het lipofiel karakter is het aannemelijk dat de afgegeven prodrugverbinding via het lymfatisch systeem in het bloed wordt opgenomen, omdat lipofiele verbindingen met een partitiecöëfficiënt hoger dan 5 niet door bloedvatwanden kunnen diffunderen. Zoals later zal blijken, vindt hydrolyse van de prodrug alleen in bloed plaats. Hieruit kan worden geconcludeerd dat het er sterk op lijkt dat het lymfatische transport de oorzaak is voor de absorptiesnelheidsverschillen.

**Hoofdstuk 6** beschrijft de locaties in het lichaam waar de prodrugverbinding gehydrolyseerd kan worden naar de moederverbinding. Hydrolyse is het proces waarbij de esterverbinding in de prodrug uit elkaar valt. Dit resulteert in de werkzame stof en een vetzuurstaart. Hydrolyse kan optreden hetzij spontaan in water (chemische hydrolyse), hetzij via carboxylesterases (enzymatische hydrolyse). Eén van de oudste prodrugverbindingen in oliedepots, nandrolondecanoaat, is in dit hoofdstuk als modelstof gebruikt. In de literatuur is gesuggereerd dat hydrolyse van deze prodrug in humaan serum kan plaatsvinden. Tot nu toe is de snelheid waarmee dit gebeurt niet bekend.

Dit hoofdstuk beschrijft dat carboxylesterases in humaan serum en plasma afwezig zijn. Bovendien bleef de prodrugverbinding intact tijdens incubatie van 5 uur bij 37°C, aangezien nandrolondecanoaat niet hydrolyseerde in deze media. Dit toont ook aan dat chemische hydrolyse van nandrolondecanoaat niet optrad in deze media. De hydrolyse trad alleen op in humaan volbloed: nandrolon verscheen na een gemiddelde tijd van  $34,9 \pm 2,5$  minuten in dit medium. Opvallend was de afwezigheid van Michaelis-Menten gedrag, dat wel werd gezien in controle experimenten met toegevoegde carboxylesterases. De resultaten suggereren dat carboxylesterases alleen aanwezig zijn in humaan volbloed, aangezien er in dit medium wel hydrolyse van nandrolondecanoaat optrad. Het grote verschil tussen volbloed en bloedplasma zijn (rode) bloedcellen. Hydrolyse kan optreden aan het bloedceloppervlak of in de bloedcel. Aangezien er een vertragingstijd bij de vorming van nandrolon geldt, is de aanwezigheid van carboxylesterases aan het oppervlak niet aannemelijk. In dat geval zou de verschijning van nandrolon immers direct meetbaar moeten zijn. Er kan daarom worden geconcludeerd dat hydrolyse intracellulair plaatsvindt.

Andere cellen die mogelijk carboxylesterases bevatten zijn de spier- en subcutaanellen

rondom het geïnjecteerde oliedepot. Er kan worden aangenomen dat een prodrugverbinding (zoals nandrolondecanoaat) ook kan worden geabsorbeerd door deze weefselcellen. De studie in dit hoofdstuk werd daarom uitgebreid met een nandrolondecanoaat hydrolysebepalingen in spier en subcutaan weefsel van varkens. De resultaten lieten zien dat de hydrolysebijdrage van deze weefsels verwaarloosbaar is. Slechts een kleine hoeveelheid nandrolon verscheen na incubatie van 5 uur met spierweefsel, terwijl er geen nandrolon verscheen bij de incubatie met subcutaanweefsel. Dit kan worden verklaard door de slechte permeabiliteit van de extreem lipofiele prodrugverbindingen, die de penetratie van de stof in de omliggende weefsels limiteert. Dit geldt ook voor bloedcellen, maar deze hebben een veel groter totaal oppervlak ( $3.0 \times 10^{15}$  mm<sup>2</sup> per 5 L bloed) in vergelijking tot het oppervlak van de omliggende cellen die in contact staan met een geïnjecteerd oliedepot (1,0 mL oliedepot heeft een oppervlak van 1466,5 mm<sup>2</sup>). Het groter oppervlak van bloedcellen verhoogt de stofstroom van prodrugverbindingen door de celmembranen. De kans dat er hydrolyse plaatsvindt in rode bloedcellen is dus veel groter dan dat dit gebeurt in weefselcellen rondom het oliedepot. De resultaten in dit hoofdstuk tonen aan dat carboxylesterases, verantwoordelijk voor hydrolyse van nandrolondecanoaat, zich intracellulair bevinden. Natuurlijk gelden de gevonden resultaten niet alleen voor onze modelstof, maar ook voor andere veresterde prodrugverbindingen verwerkt in oliedepots.

**Hoofdstuk 7** is een algemene discussie van alle resultaten van de voorgaande hoofdstukken. Daarnaast biedt dit hoofdstuk wetenschappelijke voorstellen voor vervolgonderzoeken. De resultaten in deze algemene discussie geven nieuwe inzichten van geneesmiddelabsorptie vanuit oliedepots. Direct na injectie van de olievloeistof vormt het oliedepot een aaneengesloten geheel. Na een paar dagen wordt de olie op de plaats van injectie gedispergeerd en ingekapseld. De absorptie van geneesmiddelen begint met prodrug-afgifte uit het oliedepot. De prodrugverbinding is dan aanwezig in de interstitiële vloeistof, welke langzaam wordt afgevoerd via het lymfatisch systeem naar de systemische circulatie. Vervolgens diffundeert de prodrugverbinding door het membraan van bloedcellen waar het wordt gehydrolyseerd naar de werkzame stof. Zowel het lymfatisch transport als de diffusie door het celmembraan zijn traag en kosten tijd. Deze tijdsperiodes worden aangeduid door een vertragingstijd. Deze vertragingstijd is verschillend voor elke injectieplaats: een subcutaan toegediende prodrug bereikt blijkbaar het bloed via een korte, maar trage weg. Dit resulteert in een korte vertragingstijd en een trage absorptiesnelheid van de prodrug in het bloed. Wanneer een oliedepot dieper wordt ingespoten (een injectie in de spier) zal de absorptie via een langere, maar snelle weg worden geabsorbeerd. Dit heeft als gevolg dat de vertragingstijd langer is en de absorptiesnelheid hoger.



---

## List of coauthors

*Affiliations at the time the research was conducted.*

*Presented in alphabetic order.*

### **Dr Paul Baron**

Image Sciences Institute, University Medical Center Utrecht, Utrecht, the Netherlands

### **Dr Wilbert Bartels**

Image Sciences Institute, University Medical Center Utrecht, Utrecht, the Netherlands

### **Merel Bout, BSc**

Department of Clinical Pharmacy, Division of Laboratory Medicine & Pharmacy, University Medical Center Utrecht, Utrecht, the Netherlands

### **Mohsin El Amrani, MSc**

Department of Clinical Pharmacy, Division of Laboratory Medicine & Pharmacy, University Medical Center Utrecht, Utrecht, the Netherlands

### **Dr Christien Oussoren**

Department of Pharmaceutical Sciences, Division of Pharmaceutics, Pharmaceutical Technology & Biopharmaceutics, Utrecht University, Utrecht, the Netherlands

### **Dr Eveline de Rijk**

Charles River Laboratories, Den Bosch, the Netherlands

### **Dr Peter Schot**

OrgaNext Research BV, Arnhem, the Netherlands

### **Prof. dr Herman Vromans**

Department of Pharmaceutical Sciences, Division of Pharmaceutics, Pharmaceutical Technology & Biopharmaceutics, Utrecht University, Utrecht, the Netherlands

&

Department of Clinical Pharmacy, Division of Laboratory Medicine & Pharmacy, University Medical Center Utrecht, Utrecht, the Netherlands



---

## List of publications

### PUBLICATIONS RELATED TO THIS DISSERTATION

#### **Where Does Hydrolysis Of Nandrolone Decanoate Occur In The Human Body After Release From An Oil Depot?**

- Kalicharan RW, Bout MR, Oussoren C, Vromans H.
- International Journal of Pharmaceutics. 2016: 515 (1-2), p721-728.

#### **Spatial Distribution Of Oil Depots Monitored In Human Muscle Using MRI.**

- Kalicharan RW, Baron P, Oussoren C, Bartels LW, Vromans H.
- International Journal of Pharmaceutics. 2016: 505 (1-2), p52-60.

#### **Pharmacokinetics In Elderly Women Of Benzyl Alcohol From An Oil Depot.**

- Kalicharan RW, El Amrani M, Schot P, Vromans H.
- Journal of Pharmaceutical Sciences. 2016: 105 (4), p1519-1525.

#### **Fundamental Understanding Of Drug Absorption From A Parenteral Oil Depot.**

- Kalicharan RW, Schot P, Vromans H.
- European Journal of Pharmaceutical Sciences. 2016: 83, p19-27

### OTHER PUBLICATIONS

#### **Extemporaneously Prepared Ciarithromycin Ophthalmic Formulations Tested In Vitro On The Growth Inhibition Of *Moraxella Catarrhalis*.**

*Magistraal Bereide Claritromycine Oogpreparaten In Vitro Getest Op Groeiremming Bij *Moraxella Catarrhalis*.*

- Kalicharan RW, Langenhorst JB, Tosun G, Lalmohamed A, Vromans H.
- Pharmaceutisch Weekblad. 2015: 150 (50), p254-259.

#### **Mechanism Of Release Of Tobramycin, Colistin And Nystatin From A Mouth Paste Applied To Selectively Decontaminate The Oral Cavity.**

*Afgiftemechanisme Van Tobramycine, Colistine En Nystatine Uit Mondpasta Voor Selectieve Decontaminatie Van De Mondholte.*

- Akbarali S, Kalicharan RW, Vromans, H.
- Pharmaceutisch Weekblad. 2016: 151 (3), p34-38.

**Drug Release From An Oromucosal Paste For The Selective Decontamination Of The Oropharynx (In ICU Patients And Healthy Volunteers).**

- Rood J, Nawzad H, Kalicharan RW, Van Steenberg M, Vromans H.
- European Journal of Pharmaceutical Sciences. 2015: 73, p88-92.

PODIUM PRESENTATIONS

**Fundamental Understanding Of Drug Absorption From A Parenteral Oil Depot.**

- 10th World Meeting on Pharmaceutics, Biopharmaceutics and Pharmaceutical Technology, 2016. *Glasgow, United Kingdom*
- Farmalab symposium, UMC Utrecht, 2016. *Utrecht, the Netherlands*

**Oil Depots: Visualization By MRI Of The Fate Of The Depot After Injection.**

- Dutch Medicines Days (FIGON), 2015. *Ede, the Netherlands*

**Parenteral Depot Oil Formulations: New Insights Into Drug Release Mechanism.**

- Farmalab symposium, UMC Utrecht, 2014. *Utrecht, the Netherlands*
- Biopharmacy day, 2013. *Ghent, Belgium*

POSTER PRESENTATIONS

**Role of nandrolone decanoate hydrolysis to the overall lag time in nandrolone absorption.**

- Biopharmacy day, 2016. *Utrecht, the Netherlands*

**A pharmacokinetic study of benzyl alcohol from an oil depot injection.**

- Dutch Medicines Days (FIGON), 2015. *Ede, the Netherlands*
- Surinamedag, 2015. *Amsterdam, the Netherlands*
- Biopharmacy day, 2015. *Leuven, Belgium*

**Development of a MRI visualization method to study oil depots in vivo.**

- Biopharmacy day, 2015. *Leuven, Belgium*

**Oily parenteral depot formulations: Critical parameters on drug release.**

- Ziekenhuisfarmaciedagen, 2014. *Rotterdam, the Netherlands*
- Dutch Medicines Days (FIGON), 2013. *Ede, the Netherlands*

**Benzyl alcohol increases the release rate of drugs from oil depots.**

- Surinamedag, 2015. *Amsterdam, the Netherlands*
- Ziekenhuisfarmaciedagen, 2014. *Rotterdam, the Netherlands*